General Disclaimer

One or more of the Following Statements may affect this Document

- This document has been reproduced from the best copy furnished by the organizational source. It is being released in the interest of making available as much information as possible.

- This document may contain data, which exceeds the sheet parameters. It was furnished in this condition by the organizational source and is the best copy available.

- This document may contain tone-on-tone or color graphs, charts and/or pictures, which have been reproduced in black and white.

- This document is paginated as submitted by the original source.

- Portions of this document are not fully legible due to the historical nature of some of the material. However, it is the best reproduction available from the original submission.

BTS40-85-01/rb
1036

31 July 1985

MAGNETIC PROBING OF THE SOLAR INTERIOR
FINAL REPORT COVERING THE PERIOD
1 JANUARY 1983 THROUGH 31 JULY 1985

NASA GRANT # NAGW-404
OFFICE OF SPACE SCIENCE AND APPLICATIONS
INNOVATIVE RESEARCH PROGRAM
TECHNICAL OFFICER: DR. JEFFREY D. ROSENDHAL
CODE E, NASA HEADQUARTERS

PRINCIPAL INVESTIGATOR
Professor Edward R. Benton
Campus Box 391
Department of Astrophysical, Planetary,
and Atmospheric Sciences
University of Colorado
Boulder, Colorado 80309
(303) 492-7988

CO-INVESTIGATOR
Mr. Ronald H. Estes
Business and Technological Systems, Inc.
Aerospace Building, Suite 440
10210 Greenbelt Road
Seabrook, Maryland 20706
(301) 794-8800

OUTLINE

ACKNOWLEDGEMENTS

I. INTRODUCTION

II. A THEORY FOR THE SUBPHOTOSPHERIC SOLAR MAGNETIC FIELD

III. IMPLEMENTATION OF THE THEORY

IV. CONCLUSIONS

V. REFERENCES

APPENDIX: SOLAR MAGNETIC FIELD MODELS FROM PHOTOSPHERIC MEASUREMENTS

ACKNOWLEDGEMENTS

Some of the theoretical work undertaken during this project was accomplished while the Principal Investigator was on sabbatical leave from the University of Colorado as a Scientific Visitor at the High Altitude Observatory of the National Center for Atmospheric Research, Boulder, Colorado (January to July, 1984). He is indebted especially to Drs. Robert M. MacQueen, Peter A. Gilman and Gordon N. Newkirk of that organization for financial support, discussion of the theory, and for supplying data.

The numerical work, directed by the Co-Investigator, was carried out at the Goddard Space Flight Center with capable assistance from members of the Business and Technological Systems, Inc. staff, especially Webster F. Smith, W. David Wildenhain, and Timothy I. Mann.

Dr. G. David Toot, University of Colorado, contributed numerical skills plus his knowledge of solar physics and data analysis techniques in a variety of useful ways. We also thank Dr. Todd Hoeksema of the Stanford Solar Observatory and Robert Howard, then of Mt. Wilson Observatory, for supplying data on which this study rested. Finally, it is a pleasure to thank Dr. Jeffrey D. Rosendhal, NASA Headquarters, for financial support and encouragement.

I. INTRODUCTION

The line-of-sight component of the solar magnetic field, measured by magnetograph in photospheric lines, has been recorded on an essentially daily basis for more than the past quarter century (e.g. data from Mt. Wilson are available from 9 August 1959 onwards). Those data have been used as one boundary condition for determining potential magnetic field models for the region outside the sun (the second needed boundary condition accounts, crudely, for the effects of the solar wind by assuming that the magnetic field becomes purely radial at a specific spherical surface of radius R_s in the corona, known as the source surface). A comparison of the resulting upward-extrapolated magnetic field models with white light photographs of the corona has led to the realization that the structure of the corona is, to a large extent, controlled by the magnetic field (Newkirk and Altschuler, 1970).

The primary purpose of the work reported here has been to begin the task of determining what the magnetic field patterns are in the region beneath the solar photosphere. Part of our interest in the solar interior has been prompted by the recent concentration of attention on "solar seismology" which uses the global, free oscillations of the sun to probe its interior structure, Deubner and Gough (1984). For example, that technique now suggests that the depth of the solar convection zone is 30% of the solar radius. This is in significant contrast both with the range of values of between 15 and 25% of the solar radius used in most previous models, as well as the 40% figure favored in some calculations by Gilman (1979). An independent method of estimating that depth is clearly of interest, and, at least in the terrestrial setting, a magnetic technique is available (Hide, 1978). It gives a value for the radius of the Earth's core-mantle boundary that is in remarkably good agreement with the value obtained from terrestrial seismology (Voorhies and Benton, 1982). Other topics of interest that can possibly be addressed if reliable models of the interior solar magnetic field can be developed include elucidating the depth of sunspot magnetic fields and the main electric current systems supporting the solar dynamo, plus determining the spin-rate of the radiative core, and the strength of the (possibly primordial) magnetic field present there.

Whereas magnetic probing of the Earth's interior involves the relatively straightforward downward extrapolation of a potential magnetic field, because the Earth's mantle is believed to be only weakly conducting, that physics is totally inappropriate for the solar convection zone. Herein lies final motivation for this project. The problem of downward extrapolation on the sun must rest on a theory of magnetohydrodynamic turbulence, a fascinating subject in its own right, and one in which great theoretical strides have been made beginning with the pioneering "mean-field electrodynamics" approach of Steenbeck, Rädler and Krause (as translated by Roberts and Stix, 1971 and developed further by Moffatt, 1978, Parker, 1979, Krause and Rädler, 1980). Indeed, the following sentence occurs at the end of Steenbeck and Krause (1969), c.f. Roberts and Stix, 1971, p. 245: "We would like to emphasize once more that, in our opinion, the most important application of our theory lies in the possibility of using it as a probe to deduce internal properties of cosmical bodies from the magnetic fields observed on their surfaces."

In Section II of this report we sketch our approach to obtaining a view of the sub-photospheric magnetic field from magnetic measurements taken at the photosphere. The first efforts to implement that theory are then described (Section III) and conclusions are summarized in Section IV.

II. A THEORY FOR THE SUB-PHOTOSPHERIC SOLAR MAGNETIC FIELD

Suppose that at time t the line-of-sight magnetic field has been measured at all points of the solar photosphere, taken to be the sphere $r = R_\odot$ and that our goal is to determine the magnetic field (or at least its vertical component, for a reason to be supplied shortly) throughout the turbulent convection zone. The theory, now developed, is a first step towards this difficult goal.

We first divide the sun into two distinct volumes, the solar interior (subscript i) and the solar exterior (subscript e) which are separated by the photosphere, $r = R_\odot$. It is assumed that electric currents flow in $r < R_\odot$ and $r > R_\odot$ but that no currents flow in or across the photosphere. Then the total magnetic field, $\vec{B}$ (in SI units of tesla, T) at the photosphere is obtainable as the gradient of a magnetic scalar potential which satisfies Laplace's equation. The solution appropriate to spherical coordinates r, θ, ϕ (θ = co-latitude, ϕ = east longitude) is a well known series of spherical harmonic functions. One obtains the three spherical components of $\vec{B}$, say B_r , B_θ , and B_ϕ , by taking the gradient of that scalar function. In this way the measured line-of-sight component is tantamount to knowing the vertical component of the total magnetic field at the photosphere; from here on this last quantity is taken to be the input data.

Next, we decompose the total magnetic field into its parts of internal and external origin:

$$\vec{B} = \vec{B}_i + \vec{B}_e \text{ , where} \qquad (1)$$

$\vec{B}_i$ = that part of $\vec{B}$ produced by currents in $r < R_\odot$

$\vec{B}_e$ = that part of $\vec{B}$ produced by currents in $r > R_\odot$

Under the assumption that classical, low frequency pre-Maxwell electromagnetic theory (in which displacement currents are ignored) is appropriate to the sun, Ampere's law then implies that

$$\nabla \times \vec{B}_i = 0 \quad \text{for} \quad r \geq R_\odot \; ; \; \nabla \times \vec{B}_e = 0 \quad \text{for} \quad r \leq R_\odot \tag{2}$$

Moreover, the absence of monopoles assures us that $\vec{B}$ is solenoidal and we assume that $\vec{B}_i$ and $\vec{B}_e$ separately obey the pre-Maxwell equations and appropriate boundary conditions, so that

$$\nabla \cdot \vec{B}_i = 0 \; , \; \nabla \cdot \vec{B}_e = 0 \quad \text{for all} \quad r \quad . \tag{3}$$

Because $\vec{B}_i$ is both irrotational and solenoidal in the region on and outside the photosphere, its form is the same as that encountered in geomagnetism (Chapman and Bartels, 1940)

$$\vec{B}_i(r,\theta,\phi,t) = -\nabla\{R_\odot \sum_{n=1}^{\infty} \sum_{m=0}^{n} \left(\frac{R_\odot}{r}\right)^{n+1} [g_n^m(t)\cos m\phi + h_n^m(t)\sin m\phi] \, P_n^m(\theta)\} \tag{4}$$

In this expression, which is valid for $r \geq R_\odot$, $g_n^m(t)$, $h_n^m(t)$ are the time-dependent Gauss coefficients, and $P_n^m(\theta)$ is the Schmidt semi-normalized associated Legendre function of order m , degree n . It is next assumed that the solar photosphere is so much closer to strong sub-photospheric electric current sources than it is to weak coronal sources, that the internal magnetic field strongly dominates the external magnetic field right at the photosphere. Then the measured total vertical magnetic field at $r = R_\odot$ is virtually the vertical component of the internal magnetic field which is needed as input to the left hand member of (4). This argument shows that standard spherical harmonic analysis can be applied to determine the magnetic field of internal origin in the region on and outside the solar surface.

Yet, our interest is to extrapolate the internal field into the solar interior where it need no longer be curl-free. This brings up the question of continuity type boundary conditions at the photosphere.

Imagine the photosphere separates a region of internal turbulence from a region of external quiessence. Then, even though temperature and therefore molecular electrical conductivity, σ, remain continuous across $r = R_\odot$, the effective turbulent electrical conductivity changes discontinuously from zero outside the photosphere to some finite, non-zero value just inside the convection zone. Across a finite jump in conductivity, there can be a jump in vertical electric field associated with a surface electric charge, but the tangential components of the electrical field and all components of the magnetic field remain continuous. Therefore, with B_r, B_θ, B_ϕ (actually the components for the internal magnetic field, but with the subscript i usually suppressed from here on) continuous across $r = R_\odot$, the internal magnetic field can be solenoidal only if $\partial B_r/\partial r$ is also continuous across $r = R_\odot$ because in spherical coordinates equation (3) becomes

$$\frac{\partial B_r}{\partial r} + \frac{2}{r} B_r + \frac{1}{r \sin\theta}\left[\frac{\partial}{\partial\theta}(B_\theta \sin\theta) + \frac{\partial B_\phi}{\partial\phi}\right] = 0 \quad . \qquad (5)$$

Therefore, as the photosphere is approached from below, two conditions on the internal magnetic field that follow from equation (4) and these two continuity conditions are

$$B_r(R_\odot, \theta, \phi, t) = \sum_{n=1}^{\infty} \sum_{m=0}^{n} (n+1)\left[g_n^m(t) \cos m\phi + h_n^m(t) \sin m\phi\right] P_n^m(\theta) \qquad (6)$$

$$\partial B_r(R_\odot, \theta, \phi, t)/\partial r =$$

$$- R_\odot^{-1} \sum_{n=1}^{\infty} \sum_{m=0}^{n} (n+1)(n+2)\left[g_n^m(t) \cos m\phi + h_n^m(t) \sin m\phi\right] P_n^m(\theta) \quad . \qquad (7)$$

These expressions connect the internal (vertical) field at the photosphere with the Gauss coefficients determined by fitting the line-of-sight measured field with spherical harmonics. It should be noted at this point that the measurements also determine the tangential components of the internal magnetic field as the photosphere is approached from above, and (by continuity) from below; but the vertical derivative of the tangential components ($\partial B_\theta/\partial r$ and $\partial B_\phi/\partial r$) are not continuous across the surface electric charge, so they cannot generally be determined in the convection zone without considering that distribution itself. Fortunately, all that is required for the magnetic determination of the depth of the convection zone (as well as some aspects of the spin-rate of the radiative core) is the radial component.

It remains to derive differential equations that determine the internal magnetic field in the turbulent solar convection zone. The appropriate fundamental equations, written in SI units, with upper case script quantities $\mathcal{B}(T)$, $\mathcal{E}(Vm^{-1})$, $\mathcal{J}(Am^{-2})$, $\mathcal{Q}(Asm^{-3})$, $\mathcal{V}(ms^{-1})$ denoting, respectively, the (internal) magnetic field, the electric field, electric current density, the electric charge density, and fluid velocity relative to a sun-centered spherical coordinate system that rotates steadily at the Carrington rate, whose period is 27.2753 days, are

$$\nabla \cdot \vec{\mathcal{B}} = 0 \quad , \quad \nabla \cdot \vec{\mathcal{E}} = \varepsilon_0^{-1} \mathcal{Q}$$

$$\nabla \times \vec{\mathcal{B}} = \mu_0 \vec{\mathcal{J}} \quad , \quad \nabla \times \vec{\mathcal{E}} = -\partial \vec{\mathcal{B}}/\partial t \tag{8}$$

$$\vec{\mathcal{J}} = \sigma(\vec{\mathcal{E}} + \vec{\mathcal{V}} \times \vec{\mathcal{B}})$$

Here $\sigma(Sm^{-1})$ is the electrical conductivity, assumed to be a function of radius, at most, and $\varepsilon_0 = 8.854 \times 10^{-12}\ As^2\ m^{-1}\ T^{-1}$, $\mu_0 = 4\pi \cdot 10^{-7}\ T\ m^{-1}\ A^{-1}$ are the dielectric constant and magnetic permeability (taken to be the vacuum values).

Next, the total field values are separated into their large-scale mean-field parts (designated by conventional block capitals) and their small-scale, turbulent or fluctuating parts (denoted by lower case symbols). Thus,

$$\vec{B} = \vec{B} + \vec{b} \ , \ \vec{E} = \vec{E} + \vec{e} \ , \ \vec{J} = \vec{J} + \vec{j} \ , \ Q = Q + q \ , \ \vec{V} = \vec{V} + \vec{v} \ , \qquad (9)$$

where $\vec{B} = \langle \vec{B} \rangle$, $\vec{E} = \langle \vec{E} \rangle$, etc.

and $\langle \ \rangle$ denotes the averaging operation, ideally an "ensemble average", but actually a space-time average because of the way in which solar data are collected. Quantities linear in the lower case variables have zero mean. Introducing this decomposition into the equations in (8) and then averaging, one obtains

$$\nabla \cdot \vec{B} = 0 \qquad \nabla \cdot \vec{E} = \varepsilon_0^{-1} Q$$

$$\nabla \times \vec{B} = \mu_0 \vec{J} \qquad \nabla \times \vec{E} = -\partial \vec{B}/\partial t \qquad (10)$$

$$\vec{J} = \sigma(\vec{E} + \vec{V} \times \vec{B} + \langle \vec{v} \times \vec{b} \rangle)$$

In Ohm's law, σ has been treated as a non-turbulent variable. Subtraction of these equations from (8) gives equations for the fluctuating quantites:

$$\nabla \cdot \vec{b} = 0 \qquad \nabla \cdot \vec{e} = \varepsilon_0^{-1} q$$

$$\nabla \times \vec{b} = \mu_0 \vec{j} \qquad \nabla \times \vec{e} = -\partial \vec{b}/\partial t \qquad (11)$$

$$\vec{j} = \sigma(\vec{e} + \vec{V} \times \vec{b} + \vec{v} \times \vec{B} + \vec{v} \times \vec{b} - \langle \vec{v} \times \vec{b} \rangle)$$

It is the central task of turbulent dynamo theory to achieve closure of these last two sets of equations, for example, by deriving a functional relationship between between $\langle \vec{v} \times \vec{b} \rangle$ and $\vec{B}$. This is the problem solved so persuasively by Steenbeck, Krause and Rädler. We adopt their formalism for isotropic mean-field electromagnetism and write, for the i^{th} component of $\langle \vec{v} \times \vec{b} \rangle$ (not to be confused with the former use of i to designate "internal"):

$$(\langle \vec{v} \times \vec{b} \rangle)_i = \alpha_{ij} B_j + \beta_{ijk} \frac{\partial B_j}{\partial x_k} \tag{12}$$

where $\alpha_{ij} = \alpha \delta_{ij}$, $\beta_{ijk} = \beta e_{ijk}$, and x_k is a Cartesian coordinate. Here, α, β are scalar functions of position, determined by the statistics of the turbulence. In the more familiar vector notation this gives

$$\langle \vec{v} \times b \rangle = \alpha \vec{B} - \beta \nabla \times \vec{B} \quad . \tag{13}$$

Upon substituting (13) into (10) and solving for $\nabla \times \vec{B}$ (proportional to the mean electric current) one obtains

$$\nabla \times \vec{B} = \frac{\mu_0 \sigma}{1 + \mu_0 \sigma \beta} (\vec{E} + \vec{V} \times \vec{B} + \alpha \vec{B}) \quad . \tag{14}$$

This turbulent version of Ampere and Ohm's law, combined, shows the presence of the important α-effect dynamo term, not present in laminar theory and, more importantly for present purposes, that the effective turbulent diffusivity is not $(\mu_0 \sigma)^{-1}$ as in laminar theory, but rather that quantity multiplied by $1 + \mu_0 \sigma \beta$. Because β is the magnetic diffusivity associated with the small scale turbulence, it seems safe to assume that

$$\beta \gg (\mu_0 \sigma)^{-1} \tag{15}$$

throughout the convection zone. Consequently, we ignore 1 compared to $\mu_0 \sigma \beta$ in (14) and have, approximately,

$$\nabla \times \vec{B} \doteq \beta^{-1} (\vec{E} + \vec{V} \times \vec{B} + \alpha \vec{B}) \quad . \tag{16}$$

This suggests that the appropriate conductivity for the large scale magnetic field in the convection zone is the very small value associated with enhanced turbulent magnetic diffusivity. It would seem that, to a leading approximation, large scale electric current does not flow in the convection zone. The solar dynamo currents are therefore buried in the small scales.

This notion can be given mathematical substance by introducing a perturbation expansion for the dependence of the mean-field variables on the small parameter $(1 + \mu_0 \sigma \beta)^{-1}$ that occurs in (14). Let ϵ be a typical value of this parameter (or, for a first theory, assume a constant value). Then the expansions are

$$\vec{B}(\vec{r}, t; \alpha, \epsilon) = \vec{B}_0(\vec{r}, t; \alpha) + \epsilon \vec{B}_1(\vec{r}, t; \alpha) + \epsilon^2 \vec{B}_2(\vec{r}, t; \alpha) + \ldots$$

$$\vec{E}(\vec{r}, t; \alpha, \epsilon) = \vec{E}_0(\vec{r}, t; \alpha) + \epsilon \vec{E}_1(\vec{r}, t; \alpha) + \epsilon^2 \vec{E}_2(\vec{r}, t; \alpha) + \ldots \tag{17}$$

Notice that we have not yet made any assumption about the magnitude of α, only that the dependence of the mean-magnetic and the electric fields on β is analytic so it can be expressed in MacLaurin's series. Upon substitution of these expansions into equation (16) and equating the sum of all terms with like powers of ϵ to zero, a typical hierarchy of problems arises. The first three are

$$\epsilon^0: \quad \nabla \cdot \vec{B}_0 = 0 \quad , \quad \nabla \times \vec{B}_0 = 0 \tag{18}$$

$$\epsilon^1: \quad \nabla \cdot \vec{B}_1 = 0 \quad , \quad \nabla \times \vec{B}_1 = \vec{E}_0 + \vec{V} \times \vec{B}_0 + \alpha \vec{B}_0 \tag{19}$$

$$\epsilon^2: \quad \nabla \cdot \vec{B}_2 = 0 \quad , \quad \nabla \times \vec{B}_2 = \vec{E}_1 + \vec{V} \times \vec{B}_1 + \alpha \vec{B}_1 \tag{20}$$

It is interesting that, in the first approximation (for $\vec{B}_0$) we need only downward continue the vacuum value of the magnetic field, exactly as if the convection zone were an insulator. The two boundary conditions needed for B_0 come immediately from (6) and (7) with B_r replaced by B_{0_r}.

All of the numerical work reported in the next section has been restricted to this zeroth order approximation. However, on the analytic side we have examined the first order correction for finite large-scale current flow in the convection zone. For this purpose, it is convenient to take the radial component of the curl of (19) to eliminate $\vec{E}_0$ in favor of $\vec{B}_0$ so that the first order problem reduces to (for constant β but variable α)

$$\left[\frac{\partial^2}{\partial r^2} + \frac{4}{r}\frac{\partial}{\partial r} + \frac{2}{r^2} + \frac{1}{r^2 \sin\theta}\frac{\partial}{\partial\theta}\left(\sin\theta\frac{\partial}{\partial\theta}\right) + \frac{1}{r^2 \sin^2\theta}\frac{\partial^2}{\partial\phi^2}\right]B_{1_r}$$

$$= \mu_0 \sigma_0 \left\{\frac{\partial B_{0_r}}{\partial t} + \nabla \cdot \left[\hat{r} \times (\vec{V} \times \vec{B}_0)\right] - \frac{1}{r}\frac{\partial\alpha}{\partial\theta} B_{0_\phi}\right\} \qquad (21)$$

subject to B_{1_r} and $\partial B_{1_r}/\partial r$ vanishing at $r = R_\odot$. For a specified mean motion (e.g., large scale differential rotation) and specified latitudinal variation of α effect (e.g., proportional to $\cos\theta$ so it changes sign across the equator, as required by dynamo theory) and with B_0 as determined from the zeroth order problem, equation (21) is a tractable, but complicated problem for determining B_1. In future work it is hoped to work out this correction.

We conclude this section by noting that the magnetic method for determining the depth of the convection zone is a direct extension of the technique introduced by Hide (1978) for the Earth and applied successfully in that context by Voorhies and Benton (1982). One calculates the total absolute magnetic flux (or pole strength) P crossing the sphere of radius r at time t:

$$P(r,t) \equiv \int_0^{2\pi} \int_0^{\pi} |B_r(r, \theta, \phi, t)| r^2 \sin\theta \, d\theta \, d\phi \quad . \qquad (22)$$

Note that calculating this integral only requires knowledge of the vertical component of the magnetic field. This quantity, proportional to the number of field lines crossing the sphere of radius r, has significant variations at the solar surface, but, as argued in the proposal leading to this project, the very high (molecular) electrical conductivity of the radiative core, together with the absence of vertical motion beneath the convection zone, implies that P should be independent of time just beneath the bottom of the convection zone. In the next section values of P were computed from spherical harmonic models of the radial magnetic field (in vacuum approximation) to see if there was any tendency for magnetic flux to be frozen at some depth inside the sun.

III. IMPLEMENTATION OF THE THEORY

To leading order, the theory described in Section II shows that the large scale magnetic field of internal origin remains curl-free within the turbulent convection zone. The appropriate technique for downward extrapolation of the surface observations is then classical spherical harmonic analysis. That technique has been implemented in terms of three data sets made available to us during this project. Details of those sets are as follows:

Code	Name of Data Set	Carrington Rotation Numbers	Time Span of the Data Set
A	Mt. Wilson (I)	1417-1649	Aug. 1959 - Dec. 1976
B	Mt. Wilson (II)	1620-1717	Sept. 1974 - July 1981
C	Stanford	1642-1742	May 1976 - Nov. 1983

Data sets A, B, C were supplied, respectively, by Drs. Gordon A. Newkirk, Robert Howard, and Todd Hoeksema. Sets A and C had already been fit with spherical hamonic expansions truncated at order and degree 9 whereas, set B was raw data.

Initial attention was directed to data set A. The integral in equation (22) above was evaluated numerically on a 2° by 2° latitude-longitude grid covering the full solar disk using the spherical harmonic coefficients of the Mt. Wilson models. The calculations were made for seven different spherical surfaces within the convection zone ($r/R_\odot$ = 1.00, 0.95, 0.90, 0.85, 0.80, 0.75, 0.70), and for a random selection of 84 different times throughout the 17 year span of the data (but some Carrington rotations were selected from each year). The resulting values of P, averaged for all of the selected rotations in a given year were then plotted as a function of radius ratio, $r/R_\odot$. Smooth curves passed through the discrete points of such plots would then ideally, cross each other at a distinct radius, thereby determining the depth at which absolute magnetic flux becomes invariant with time. We would interpret that depth as being close to the bottom of the convection zone.

These first computations produced very few indications that such a depth exists. Instead of two of the curves converging towards each other, as depth increases, they mostly diverged, indicating that when the solar flux was, say, relatively small at the surface, it remained small at all depths sampled. Actually some of the curves did cross each other, but at angles two small to be considered significant.

In attempting to assess this failure, we came to the belief that perhaps the high harmonics in the series were not well determined by the data and yet they were dominating the flux integral. Studies of the energy spectra for those models, as well as the examination of contour plots of the radial magnetic field at several different depths confirmed this suspicion. The spectra revealed dominance by the eighth or ninth degree terms, much small scale structure in the contour maps, and a lot of temporal variability in both quantities. In addition, the spurious monopole terms were found to be surprisingly large (refer to Figure 1).

It was, therefore, decided to work with the lower-resolution but less noisy data available from the Stanford Solar Observatory, to see whether it suffered from the same problems. First, though, the entire span of those data (in the form spherical harmonic model coefficients) were passed through a low-pass filter (with a cut-off near 2.3 years) designed to remove high-frequency noise while retaining the low-frequency solar cycle variations. Next, five nearly uniformly spaced Carrington rotations were selected (numbers 1648, 1672, 1696, 1716, 1736) and flux computations made, as on the Mt. Wilson data. It was again found that there is no depth at which absolute magnetic flux appears to be conserved. We believe that the main source of difficulty is that noise in the high harmonics is being selectively amplified during the downward extrapolation more than that in the low harmonics, so that eventually the signal to noise ratio degenerates too much. The data should therefore be smoothed in the spatial domain before downward extrapolation. There are sophisticated modern techniques for doing this (known as "harmonic splines" and "stochastic inversion" in the geophysical literature) but here, we tried only the straightforward technique of truncating the spherical harmonic expansions back to lower degress than that to which the data were fitted.

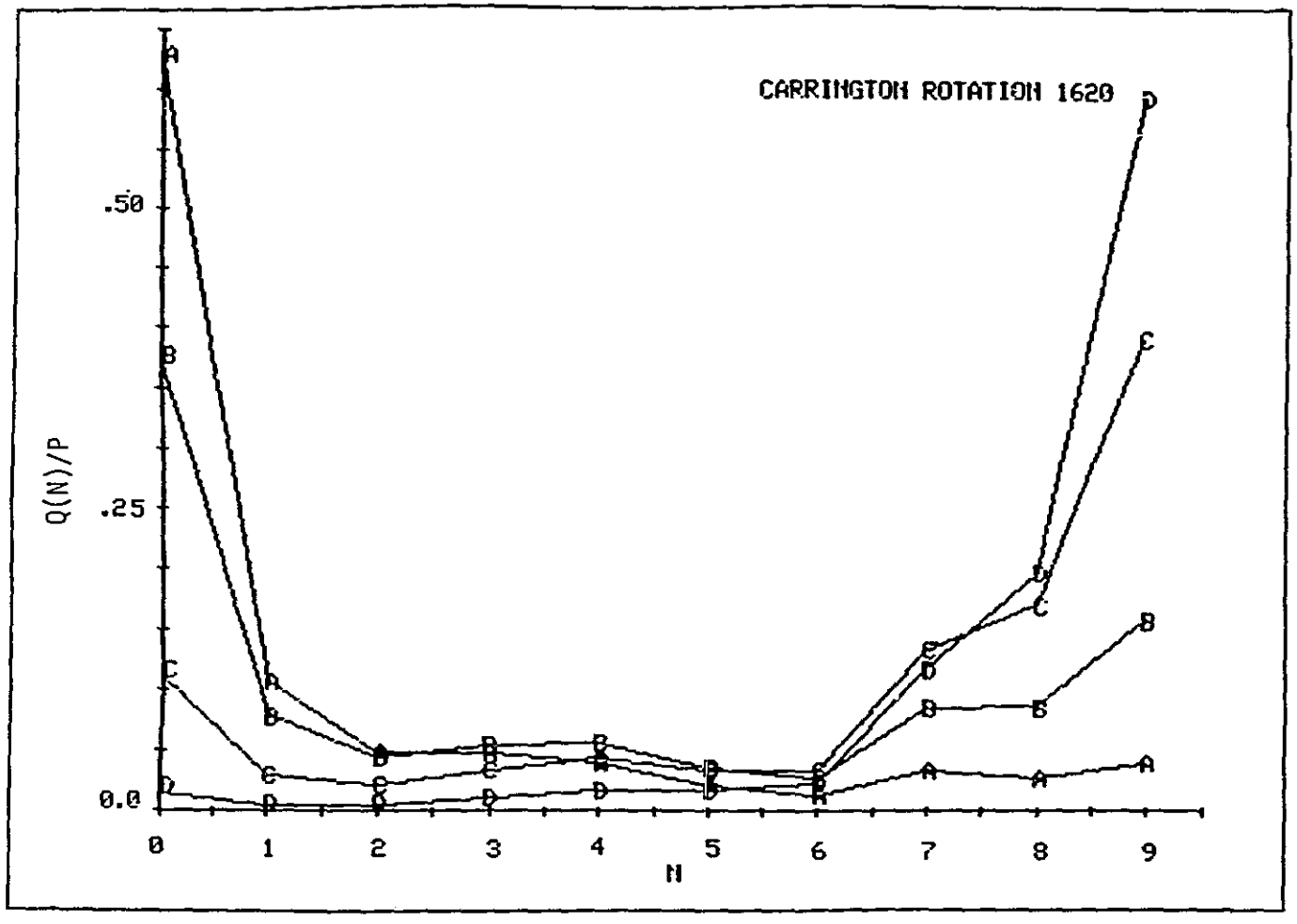

Figure 1. Normalized energy spectra for Carrington rotation 1620. The four different traces A, B, C and D refer to different depths; 1.0, 0.9, 0.8 and 0.7, of a solar radius, respectively.

The results of this exercise are encouraging but not definitive. A great number of the flux curves now do indeed cross each other, but the range of depths at which this occurs is substantial. This shows a strong model-dependence of the flux conservation depth that will have to be removed before we can get results that are really believable. The large amount of numerical work on which this rests is summarized in the three large fold-out matrices, Tables III-1, III-2, and III-3. The degree of truncation is $N = 5, 7$ or 9. Each entry box of each matrix is at the intersection of the two Carrington rotations being compared (so, close to the main diagonal we are comparing two epochs closely separated, while time separation increases as one moves toward the upper right corner). The key on each matrix shows the meaning of some of the symbols. The numbers entered into the boxes show between what radius ratios flux was invariant at the two epochs in question. Clearly, as the truncation level is lowered from 9 to 7 to 5, there is a substantial growth in the number of "successful" events. The region close to the main diagonal should be discounted because the pairs of rotations in question are not sufficiently distinct. At $N = 9$, what crossings there are occur at unrealistically large depth, but shallower depths, typically down to a few tenths of a solar radius, are indicated frequently at $N = 7$ and $N = 5$. These results are regarded as encouraging but it would certainly be inappropriate to regard them as definitive. There is too much sensitivity to the pair of rotations being compared, and probably an overabundance of depths too shallow to be believed.

Our final effort to work with data consisted of a careful fitting of spherical harmonics to the second Mt. Wilson data set (Code B). The details of this work are included in the Appendix, briefly summarized here. Spherical harmonic coefficients, to order and degree 9 (99 internal coefficients excluding the monopole) were determined by two different solution techniques (Type I and Type II). In solution Type I, all available observations for each Carrington rotation were used, with equal weighting, and a single iteration of the least squares algorithm was performed. For solution Type II, five iterations were performed with equal weighting within each iteration, but with each data point rejected whose residual of fit at that location was 2.5 times (or more) the rms of fit for all data used in the previous iteration. This

Carrington Rotation Flux Crossing Table
Filtered Stanford Data

N = 5

	1643	1644	1645	1646	1648*	1660	1670	1671	1672*	1673	1674	1684	1686	1688	1690	1692
1643		0	0	0	0	0	0	0	0	0	0	0	0	0	0	0
1644			0	0	0	0	0	0	0	0	0	0	0	0	0	0
1645				0	0	0	0	0	0	0	0	0	0	0	0	0
1646					0	0	0	0	0	0	0	0	0	0	0	0
1648						0	0	0	0	0	0	0	0	0	0	0
1660							0	0	0	0	0	0	0	0	0	0
1670								0	0	0	0	=.15	.55-.6	.7-.75	.8-.85	.85-.9
1671									0	0	0	<	.65-.7	.8-.85	.85-.9	.9-.95
1672										0	0	.6-.65	.75-.8	.85-.9	.9-.95	.9-.95
1673											0	.7-.75	.8-.85	.95-1.0	.95-1.0	.95-1.0
1674												.8-.85	.9-.95	.95-1.0	.95-1.0	.95-1.0
1684													0	0	0	0
1686														0	0	0
1688															0	0
1690																=1.0
1692																
1694																
1695																
1696																
1697																
1698																
1699																
1700																
1702																
1704																
1706																
1708																
1710																
1716																
1726																
1736																

TABLE III-

0 Flux lines did not cross
2 Flux lines crossed twice
3 Flux lines crossed three times
· Flux not calculated for given carrington rotation
< Flux lines crossed at less than .5 of a solar radii
* Flux not calculated for less than .5 of a solar radii

1690	1692	1694	1695	1696*	1697	1698	1699	1700	1702	1704	1706	1708	1710	1716*	1726	1736*
0	0	0	0	0	0	0	0	0	0	0	0	0	0	0	<	.8-.85
0	0	0	0	0	0	0	0	0	0	0	0	0	0	0	<	.8-.85
0	0	0	0	0	0	0	0	0	0	0	0	0	0	0	<	.85-.9
0	0	0	0	0	0	0	0	0	0	0	0	0	0	0	<	.85-.9
0	0	0	0	0	0	0	0	0	0	0	0	0	0	0	0	.9-.95
0	0	0	<	<	<	<	.5-.55	.55-.6	.6-.65	.6-.65	.6-.65	.6-.65	.6-.65	.65-.7	.75-.8	0
-.85	.85-.9	.85-.9	.85-.9	.85-.9	.85-.9	.85-.9	.85-.9	.85-.9	.85-.9	.85-.9	.85-.9	.85-.9	.85-.9	.85-.9	.9-.95	0
5-.9	.9-.95	.9-.95	.9-.95	.9-.95	.9-.95	.9-.95	.85-.9	.85-.9	.85-.9	.85-.9	.85-.9	.85-.9	.85-.9	.85-.9	.9-.95	0
-.95	.9-.95	.9-.95	.9-.95	.9-.95	.9-.95	.9-.95	.9-.95	.9-.95	.85-.9	.85-.9	.85-.9	.85-.9	.85-.9	.85-.9	.95-1.0	0
5-1.0	.95-1.0	.95-1.0	.95-1.0	.9-.95	.9-.95	.9-.95	.9-.95	.9-.95	.9-.95	=.9	.85-.9	.85-.9	.85-.9	.85-.9	.95-1.0	0
5-1.0	.95-1.0	.95-1.0	.95-1.0	.95-1.0	.9-.95	.9-.95	.9-.95	.9-.95	.9-.95	.9-.95	.9-.95	.85-.9	.85-.9	.9-.95	.95-1.0	0
0	0	0	.95-1.0	.95-1.0	.95-1.0	.95-1.0	.9-.95	.9-.95	.9-.95	.9-.95	.9-.95	.9-.95	.85-.9	.9-.95	.95-1.0	0
0	0	0	.95-1.0	.95-1.0	.95-1.0	.9-.95	.9-.95	.9-.95	.9-.95	.9-.95	=.9	.85-.9	.8-.85	.9-.95	.95-1.0	0
0	0	.95-1.0	.95-1.0	.95-1.0	.9-.95	.9-.95	.9-.95	.85-.9	.9-.95	.85-.9	.85-.9	.85-.9	.8-.85	.85-.9	.95-1.0	0
	=1.0	.95-1.0	.95-1.0	.9-.95	.9-.95	.9-.95	.9-.95	.85-.9	.85-.9	.85-.9	.85-.9	.85-.9	.8-.85	.85-.9	.95-1.0	0
		=.95	.9-.95	.9-.95	.9-.95	.85-.9	.85-.9	.85-.9	.85-.9	.85-.9	.8-.85	.8-.85	.8-.85	.85-.9	.95-1.0	0
			.9-.95	.85-.9	.85-.9	.85-.9	.85-.9	.85-.9	.8-.85	.8-.85	.8-.85	.8-.85	.8-.85	.85-.9	.95-1.0	0
				.85-.9	.85-.9	.85-.9	=.85	.8-.85	.8-.85	.8-.85	.8-.85	.8-.85	.8-.85	.8-.85	.95-1.0	0
					.85-.9	.85-.9	.8-.85	.8-.85	.8-.85	.8-.85	.8-.85	.8-.85	.8-.85	.8-.85	.95-1.0	0
						.8-.85	.8-.85	.8-.85	.8-.85	.8-.85	.75-.8	.75-.8	.75-.8	.8-.85	.95-1.0	0
							.8-.85	.8-.85	.75-.8	.75-.8	.75-.8	.75-.8	.75-.8	.8-.85	0	0
								.75-.8	.75-.8	.75-.8	.75-.8	.75-.8	.75-.8	.8-.85	0	0
									.75-.8	.75-.8	.75-.8	.7-.75	.75-.8	.85-.9	0	0
										.7-.75	.7-.75	.7-.75	.75-.8	.85-.9	0	0
											.65-.7	.7-.75	.75-.8	.85-.9	0	0
												.7-.75	.75-.8	.9-.95	0	0
													3	.9-.95	0	0
														.95-1.0	0	0
															0	0
																0

TABLE III-1

2 FOLDOUT FRAME

Carrington Rotation Flux Crossing Table
Filtered Stanford Data

N = 7

	1643	1644	1645	1646	1648	1660	1670	1671	1672	1673	1674	1684	1686	1688	1690	1692	1694	1695
1643		0	0	0	0	0	<	<	<	<	=.15	0	0	0	0	0	0	0
1644			0	0	0	<	<	<	<	<	<	0	0	0	0	0	0	0
1645				0	0	<	<	<	<	<	<	0	0	0	0	0	0	0
1646					0	<	<	<	<	<	<	0	0	0	0	0	0	0
1648						<	<	<	<	<	<	0	0	0	0	0	0	0
1660							<	<	<	<	<	0	0	0	0	0	0	0
1670								.0	0	0	0	0	0	0	0	0	0	0
1671									0	0	0	0	0	0	0	0	0	0
1672										0	0	0	0	0	0	0	0	0
1673											0	0	0	0	0	0	0	2
1674												0	0	0	0	2	2	2
1684													=.65	=.65	.6-.65	.6-.65	.6-.65	=.
1686														.6-.65	.6-.65	.6-.65	.55-.6	2
1688															=.6	.55-.6	2	2
1690																2	2	2
1692																	2	.9-
1694																		.9-
1695																		
1696																		
1697																		
1698																		
1699																		
1700																		
1702																		
1704																		
1706																		
1708																		
1710																		
1716																		
1726																		
1736																		

FOLDOUT FRAME

TABLE III-2

0 Flux lines did not cross
2 Flux lines crossed twice
3 Flux lines crossed three times
• Flux not calculated for given carrington rotation
< Flux lines crossed at less than .5 of a solar radii
* Flux not calculated for less than .5 of a solar radii

692	1694	1695	1696	1697	1698	1699	1700	1702	1704	1706	1708	1710	1716	1726	1736
0	0	0	0	0	0	0	0	0	0	0	0	0	0	0	0
0	0	0	0	0	0	0	0	0	0	0	0	0	0	0	0
0	0	0	0	0	0	0	0	0	0	0	0	0	0	0	0
[illegible]	0	0	0	0	0	0	0	0	0	0	0	0	0	0	0
[illegible]	0	0	0	0	0	0	0	0	0	0	0	0	0	0	0
0	0	0	0	0	0	0	0	0	0	0	0	0	0	0	0
0	0	0	0	0	0	0	0	0	0	0	0	0	0	0	.6-.65
0	0	0	0	0	0	0	0	0	0	0	0	0	0	0	.6-.65
0	0	0	0	0	0	0	0	0	0	0	0	0	0	0	.55-.6
0	0	2	2	2	2	2	2	2	0	0	0	0	0	0	.55-.6
2	2	2	2	2	2	2	2	2	2	2	0	0	0	0	.5-.55
6-.65	.6-.65	*.6	2	2	2	2	2	2	2	2	2"	2	0	2	<
6-.65	.55-.6	2	2	2	2	2	2	2	2	.9-.95	2	2	0	2	0
55-.6	2	2	2	2	2	2	2	2	2	.85-.9	2	2	0	0	0
2	2	2	2	2	.9-.95	.9-.95	.9-.95	.85-.9	.85-.9	.85-.9	.8-.85	<	0	0	0
	2	.9-.95	.9-.95	.9-.95	.9-.95	.85-.9	.85-.9	.85-.9	.85-.9	.8-.85	.75-.8	.5-.55	0	0	0
		.9-.95	.85-.9	.85-.9	.85-.9	.85-.9	.85-.9	.85-.9	.8-.85	.8-.85	.7-.75	.5-.55	0	0	0
			.85-.9	.85-.9	.85-.9	.85-.9	.85-.9	.85-.9	.8-.85	.75-.8	*.65	<	0	0	0
				.85-.9	.85-.9	.85-.9	.85-.9	.8-.85	.8-.85	*.75	.6-.65	<	0	0	0
					.85-.9	.85-.9	.85-.9	.8-.85	.75-.8	.7-.75	.55-.6	<	0	0	0
						.85-.9	*.85	.8-.85	.75-.8	.65-.7	*.55	<	0	0	0
							.8-.85	.75-.8	.7-.75	*.65	*.5	<	0	0	0
								.75-.8	.7-.75	*.65	<	<	0	0	0
									.65-.7	*.5	<	0	0	0	0
										<	0	0	0	0	0
											0	0	0	0	0
												0	0	.9-.95	0
													0	.8-.85	0
														0	0
															0

LE III-2

2 FOLDOUT FRAME

Carrington Rotation Flux Crossing Table
Filtered Stanford Data

N = 9

	1643	1644	1645*	1646	1648*	1660	1670	1671	1672	1673	1674	1684	1686	1688	1690	1692	1694
1643		0	0	0	0	•	•	•	0	•	•	•	0	0	0	0	0
1644			0	0	0	•	•	•	0	•	•	•	0	0	0	0	0
1645				0	0	•	•	•	0	•	•	•	0	0	0	0	0
1646					0	•	•	•	0	•	•	•	0	0	0	0	0
1648						•	•	•	0	•	•	•	0	0	0	0	0
1660							•	•	•	•	•	•	•	•	•	•	•
1670								•	•	•	•	•	•	•	•	•	•
1671									•	•	•	•	•	•	•	•	•
1672										•	•	•	0	0	0	0	0
1673											•	•	•	•	•	•	•
1674												•	•	•	•	•	•
1684													•	•	•	•	•
1686														.65-.7	.6-.65	.55-.6	.55-.6
1688															.55-.6	.55-.6	.5-.55
1690																.5-.55	.5-.55
1692																	2
1694																	
1695																	
1696																	
1697																	
1698																	
1699																	
1700																	
1702																	
1704																	
1706																	
1708																	
1710																	
1716																	
1726																	
1736																	

FOLDOUT FRAME

TABLE III-3

0 Flux lines did not cross
2 Flux lines crossed twice
3 Flux lines crossed three times
• Flux not calculated for given carrington rotation
< Flux lines crossed at less than .5 of a solar radii
* Flux not calculated for less than .5 of a solar radii

1690	1692	1694	1695	1696	1697	1698	1699	1700	1702	1704	1706	1708	1710	1716	1726	1736
0	0	0	0	0	0	0	0	0	0	0	•	0	0	0	•	0
0	0	0	0	0	0	0	0	0	0	0	•	0	0	0	•	0
0	0	0	0	0	0	0	0	0	0	0	•	0	0	0	•	0
0	0	0	0	0	0	0	0	0	0	0	•	0	0	0	•	0
0	0	0	0	0	0	0	0	0	0	0	•	0	0	0	•	0
•	•	•	•	•	•	•	•	•	•	•	•	•	•	•	•	•
•	•	•	•	•	•	•	•	•	•	•	•	•	•	•	•	•
•	•	•	•	•	•	•	•	•	•	•	•	•	•	•	•	•
0	0	0	0	0	0	0	0	0	0	0	•	0	0	0	•	0
•	•	•	•	•	•	•	•	•	•	•	•	•	•	•	•	•
•	•	•	•	•	•	•	•	•	•	•	•	•	•	•	•	•
•	•	•	•	•	•	•	•	•	•	•	•	•	•	•	•	•
-.65	.55-.6	.55-.6	.55-.6	.55-.6	.55-.6	2	2	2	2	2	•	2	0	0	•	0
5-.6	.55-.6	.5-.55	.5-.55	.5-.55	2	2	2	2	2	2	•	2	0	0	•	0
	.5-.55	.5-.55	.5-.55	2	2	2	2	2	2	2	•	0	0	<	•	0
		2	2	2	2	2	2	2	2	2	•	0	0	<	•	0
			2	2	2	2	2	2	2	2	•	0	0	<	•	0
				2	2	2	2	2	2	0	•	0	0	<	•	0
					2	2	2	2	2	0	•	0	0	<	•	0
						2	2	2	0	0	•	0	0	<	•	0
							2	2	0	0	•	0	0	<	•	0
								0	0	0	•	0	0	<	•	0
									0	0	•	<	<	.55	•	0
										0	•	<	<	.55	•	0
											•	<	<	.55	•	0
												•	•	•	•	•
													.55	.6	•	0
														.65	•	0
															•	0
																•

TABLE III-3

2 FOLDOUT FRAME

procedure has produced two different models (with N = 9) for every rotation from #1620 to #1717. These models are included in the microfiche packet attached to this report.

To illustrate the type of behaviour encountered in these data, three typical Carrington rotations were selected for detailed study. Rotation #1620 contains no substantial data gaps, but there are large spatial gradients present so the data are noisy (refer to Tables A1-A5 which pertain to solution Type I and Tables A16-A20 for solution Type II). Rotation #1625 (see Tables A6-A10 for solution Type I and Tables A21-A25 for solution Type II) contained data neither excessively noisy nor plagued with data gaps. Rotation #1663 (Tables A11-A15 for solution Type I and Tables A26-A30 for solution Type II) illustrates a poor distribution of relatively good quality data. The five members of these sets of tables reveal, respectively, the distribution of (i) the residuals, (ii) their root mean square, (iii) the number of observations, (iv) the line-of-sight magnetic field calculated from the model, and (v) the line-of-sight magnetic field as observed.

These calculations will permit culling of the data so as to work with a reduced set of the more reliably determined models. We believe that such "cleaning procedures" are a necessary step before proceeding further with this line of work. The models for the selected Carrington rotations 1620, 1625 and 1663 appear in Tables A-31, A-32, and A-33, respectively, for solution Type I and in Tables A-34 through A-36 for solution Type II.

One of the conclusions reached in this study is that, when compared with geomagnetic data collected at ground observatories and occasionally by satellite, the solar data are far less easy to analyze. A discouragingly long list of potential problems exists and it exacerbates the question of testing our theoretical ideas. We do not readily see how to isolate whether the theory needs major revision (or refinement) or whether the data are inadequate for the task at hand (or, as is quite possible, both areas require further attention). The sources of error which are of concern include these:

1) Instrument error - magnetographs do not provide a perfect measure of the line-of-sight field even within the saturation limits.

2) Instrument saturation - fields in excess of about 200 Gauss fail to be delineated.

3) Absence of strong sunspot field measurements - insufficient light emerges from sunspots to enable spectroscopic determination of their strong fields to be recorded.

4) Absence of limb measurements - line-of-sight fields can weaken progressively towards the limb (especially the poles) and fade below the limit for detectability.

5) Data gaps are produced by instrument failure and poor or no seeing.

6) Asynoptic data are gathered but synoptic data are required - because reliable data can only be gathered in the region close to central meridian, it takes about 27 days to acquire enough data for a global model. Time and space aliasing are produced by the time evolution during that period.

7) The tilt of the solar rotation axis by 7° to the ecliptic leaves polar caps without data coverage during much of the year.

8) Differential rotation of the photosphere is not accounted for in assigning the location to a given measurement - some locations are oversampled while others are not sampled at all.

9) The source surface, where $\vec{B}$ is assumed to become radial, is probably a crude model of solar wind effects because it is taken as a sphere of fixed radius.

10) Data are, typically, selected off of a grid on which the spherical harmonics are not orthogonal, so there is model dependence on truncation level.

11) There are not trustworthy estimates of modeling and other errors available.

IV. CONCLUSIONS

A concise description of our accomplishments and conclusions are as follows:

A. An approximate method for downward extrapolation of line-of-sight magnetic field measurements taken at the solar photosphere has been developed. It utilizes the mean-field theory of electromagnetism in a form thought to be appropriate for the solar convection zone.

B. A way to test that theory has been proposed. It is based on calculating the depth at which the vertical absolute magnetic flux remains constant in time and then comparing that value with the depth of the solar convection zone as determined by helioseismology. Accordingly, existing spherical harmonic models of photospheric magnetograph data from Mt. Wilson Observatory were used to calculate flux as a function of depth for many different solar rotations.

C. The straightforward application of the lowest-order-theory with the complete model fit to these data does not indicate the existence of any reasonable depth at which flux conservation is achieved.

D. Spherical harmonic models, fit to data from Stanford Solar Observatory at degree N = 9, were first low-pass filtered to remove high-frequency noise ($\omega > 1/2.3$ years). Downward extrapolation was undertaken on the full models (with N = 9) and also on models spatially smoothed by truncating back to N = 7 or N = 5. A host of depths at which absolute magnetic flux appears to be possibly conserved is then found. However, the range of depths is substantial, so there is significant model dependence in these results. A definitive frozen-flux depth may well be contained in the data, but extracting it in unambiguous fashion

will require a considerable amount of improvement in data quality, and perhaps duration of the data span.

E. Spherical harmonic models, truncated at degree N = 9, have been constructed for a span of Mt. Wilson data from Sept. 1974 to July 1981 to complement the models previously fit to the Mt. Wilson data for the interval Aug. 1959 to Dec. 1976. This gives a 22 year continuous record from the same observatory for subsequent use.

F. We speculate that the methods developed and given initial testing in this project, may ultimately provide a satisfactory magnetic estimate for the depth of the solar convection zone. Alternatively, if the value from helioseismology is adopted, then the present theory presumably places constraints on the α and β turbulence parameters.

V. REFERENCES

Chapman, S. and J. Bartels, Geomagnetism (2 volumes), Oxford University Press, 1940.

Deubner, F.-L. and D. Gough, "Helioseismology: Oscillations as a Diagnostic of the Solar Interior", Ann. Rev. Astron. Astrophys. 22, 593-619, 1984.

Gilman, P.A., "Model calculations concerning rotation at high solar latitudes and the depth of the solar convection zone", Ap. J. 231, 284, 1979.

Hide, R., "How to locate the electrically-conducting core of a planet from external magnetic observations," Nature 271, 640, 1978.

Hoeksema, J. Todd, Structure and Evolution of the Large Scale Solar and Heliospheric Magnetic Fields, Ph.D. Thesis, Stanford University, 222 pages, 1984.

Krause, F. and K.-H. Rädler, Mean-Field Magnetohydrodynamics and Dynamo Theory, Pergamon Press, 1980.

Moffatt, H.K., Magnetic Field Generation in Electrically Conducting Fluids, Cambridge University Press, 1978.

Newkirk, G.A., Jr. and M.D. Altschuler, "Magnetic Fields and the Solar Corona. III. The Observed Connection Between Magnetic Fields and the Density Structure of the Corona", Solar Physics 13, 131, 1970.

Parker, E.N., Cosmical Magnetic Fields - Their Origin and Their Activity, Oxford University Press, 1979.

Roberts, P.H. and M. Stix, "The Turbulent Dynamo - A Translation of a Series of Papers by F. Krause, K.-H. Rädler, and M. Steenbeck", NCAR-TN/IA-60, Boulder, Colorado, 318 pages, 1971.

Steenbeck, M. and F. Krause, "On the Dynamo Theory of Stellar and Planetary Magnetic Fields, II. D.C. Dynamos of Planetary Type", Astron. Nachr. 291, 271-286, 1969.

Voorhies, C.V. and E.R. Benton, "Pole-Strength of the Earth from MAGSAT and Magnetic Determination of the Core Radius", Geophys. Res. Lett. 9, 258-261, 1982.

APPENDIX: SOLAR MAGNETIC FIELD MODELS FROM PHOTOSPHERIC MEASUREMENTS

The source-free coronal magnetic field may be represented by a scalar potential expanded in spherical harmonics

$$\overline{B} = -\nabla V$$

where (see Chapman and Bartels)

$$V = a \sum_{n=0}^{\infty} \sum_{m=0}^{n} P_n^m(\theta) \{[c_n^m (\tfrac{r}{a})^n + (1 - c_n^m)(\tfrac{a}{r})^{n+1}] A_n^m \cos m\phi + [s_n^m (\tfrac{r}{a})^n + (1 - s_n^m)(\tfrac{a}{r})^{n+1}] B_n^m \sin m\phi\} \quad . \qquad \text{A.1}$$

The expansion may be alternatively written in the form

$$V = a \sum_{n=0}^{\infty} \sum_{m=0}^{n} (\tfrac{a}{r})^{n+1} [g_{nm} \cos m\phi + h_{nm} \sin m\phi] P_n^m(\theta) + a \sum_{n=1}^{\infty} \sum_{m=0}^{\infty} (\tfrac{r}{a})^n [q_{nm} \cos m\phi + t_{nm} \sin m\phi] P_n^m(\theta) \qquad \text{A.2}$$

where the coefficients g_{nm} , h_{nm} represent sources internal to the radius a and s_{nm} , t_{nm} represent sources external to a . Then clearly

$$A_n^m = g_{nm} + q_{nm}$$

$$B_n^m = h_{nm} + t_{nm} \qquad \text{A.3}$$

$$c_n^m = \frac{q_{nm}}{g_{nm} + q_{nm}}$$

$$s_n^m = \frac{t_{nm}}{h_{nm} + t_{nm}} \quad .$$

Both Altschuler and Newkirk (1969) and Hoeksema (1984) have utilized scalar potential expansions to determine coronal fields from line-of-sight magnetic measurements at the photosphere. Because their notations are slightly different from each other, we briefly review the mathematical procedure.

Denote by $R_\odot$ the radius of the photosphere and R_s the radius of the source surface in the corona. Then applying the boundary condition that the field be radial at R_s ($V(R_s) = 0$) we have from Eq. A.1 with $a = R_\odot$

$$c_n^m \left(\frac{R_s}{R_\odot}\right)^n + (1 - c_n^m) \left(\frac{R_\odot}{R_s}\right)^{n+1} = 0$$

$$s_n^m \left(\frac{R_s}{R_\odot}\right)^n + (1 - s_n^m) \left(\frac{R_\odot}{R_s}\right)^{n+1} = 0$$

for arbitrary n and m, so that

$$c_n^m = s_n^m = \frac{1}{1 - \left(\frac{R_s}{R_\odot}\right)^{2n+1}} \quad .$$

The scalar potential which describes the coronal field is then

$$V = R_\odot \sum \sum \frac{1}{1 - \lambda_n} \left[\left(\frac{R_\odot}{r}\right)^{n+1} - \lambda_n \left(\frac{r}{R_\odot}\right)^n\right] \left[A_n^m \cos m\phi + B_n^m \sin m\phi\right] P_n^m(\theta) \qquad \text{A.4}$$

where

$$\lambda_n = \left(\frac{R_\odot}{R_s}\right)^{2n+1} \quad . \qquad \text{A.5}$$

Note that

$$g_{nm} = \left(\frac{1}{1-\lambda_n}\right) A_n^m$$

$$\text{A.6}$$

$$h_{nm} = \left(\frac{1}{1-\lambda_n}\right) B_n^m \quad .$$

In the limit as n gets large, λ_n approaches zero so that A_n^m and B_n^m approach the internal field coefficients g_{nm} and h_{nm}. The mathematical procedure used by Altschuler and Newkirk (1969) and by Newkirk, et al. (1973) assumes their limit to be zero. Hoeksema (1984) describes his potential in the form

$$V = R_\odot \sum \sum \left[\left(\frac{R_\odot}{r}\right)^{n+1} - \frac{R_s}{R_\odot}\left(\frac{R_\odot}{R_s}\right)^{n+2}\left(\frac{r}{R_s}\right)^n\right]\left[a_{nm}\cos m\phi + b_{nm}\sin m\phi\right] P_n^m(\theta) \qquad \text{A.7}$$

so that

$$a_{nm} = g_{nm} = \left(\frac{1}{1-\lambda_n}\right) A_{nm}$$

$$\text{A.8}$$

$$b_{nm} = h_{nm} = \left(\frac{1}{1-\lambda_n}\right) B_{nm} \quad .$$

Hoeksema uses Schmit normalization for his Legendre polynomials and coefficients, while Newkirk et al use fully normalized polynomials and coefficients. Note that Hoeksema's coefficients are the internal field coefficients, while those of Newkirk et al are equal to the internal coefficients in the limit as λ_n approaches zero.

In this appendix we present least squares solar corona field models computed using Equation A.4 and additional photspheric line-of-sight magnetic measurements available from the Mt. Wilson magnetograph for Carrington rotations 1620 through 1717. These models complement those computed by Altschuler, et al (1969) for rotations 1417 through 1649 and by Hoeksema using Stanford magnetograph data for rotations 1642 through 1742. The line-of-sight measurement at the photosphere is given by

$$B_L = \vec{B} \cdot \hat{L} = \alpha_1 B_r + \alpha_2 B_\theta + \alpha_3 B_\phi$$

where

$$\alpha_1 = \delta \sin^2 \theta \cos \varepsilon - \sin \theta + \delta \cos^2 \theta$$

$$\alpha_2 = \delta \sin \theta \cos \theta (\cos \varepsilon - 1) - \cos \theta$$

$$\alpha_3 = \delta \sin \theta \sin \varepsilon$$

and $\hat{L}$ is the unit line-of-sight vector, ε is the angular Carrington longitude increment from the central meridian (CM) to the observation point and

$$\delta = \frac{R_\odot}{a_E}$$

with a_E the earth-sun distance. Altschuler et al (1969) assume δ and ε to be zero. While the measurements are linear functions of the potential coefficients, we use an iterative least squares algorithm so that a data editing criterion may be applied on sequential iterations. The least squares matrix equations

$$\delta \hat{p}_{n+1} = (A^T W A)^{-1} A^T W \delta y_n$$

where

A is the partial derivative matrix of the measurements with respect to the parameters

$\hat{p}$ is the vector of adjusted spherical harmonic potential coefficients

δy is the vector of residuals, i.e. measured data minus predicted value from previous iteration

w is the weight matrix for the measurements

and the estimate at the (n+1)st iteration is

$$\hat{p}_{n+1} = \hat{p}_n + \delta\hat{p}_{n+1} \quad .$$

The weight matrix W is the inverse of the noise covariance matrix. We assume W to be a diagonal matrix. The matrix $(A^T W A)^{-1}$ is the covariance matrix of the estimated coefficients.

The observation technique for the Mt. Wilson magnetograph and some of the limitations of the data are discussed by Altschuler et al (1974). Using this data we have computed two different solutions for each Carrington rotation from 1620 to 1717; 1) a solution with W set to the unit matrix using all data available for that rotation (1080 observations maximum) in a single iteration of the least squares equations and 2) a solution computed thorugh five iterations with W set to the unit matrix and with data rejected in each iteration step whose residual exceeds 2.5 times the rms sigma of fit for the previous iteration (or a minimum of 5 Gauss).

The solutions for some Carrington rotations suffer from very noisy data, while others suffer from poor data distribution. Three representative Carrington rotations were chosen; 1620, characterized by noisy data, 1625,

characterized by good quality data and 1663, characterized by poor data distribution, due to gaps in the data. The sigma value and number of data points for the three Carrington rotations for solution type I and the fifth iteration of solution type II are given below.

CARRINGTON ROTATION	I		II	
	SIGMA (GAUSS)	NUMBER OF DATA POINTS	SIGMA (GAUSS)	NUMBER OF DATA POINTS
1620	3.34	1056	0.963	1026
1625	0.817	1053	0.799	1052
1663	2.22	745	1.192	722

For these Carrington rotations spatial distributions averaged on a global 10° x 10° equiangular grid for the solution residual means, RMS, observed values, and computed solution values for the two solution types, together with the number of observations within each bin, are presented in Tables A-1 through A-30. The type II (iterated) solutions clearly remove local regions of high intensity as seen by comparing the rms values in Tables A-2 and A-17.

The solutions obtained using the first method (which corresponds to the procedure used by Altschuler et al (1969)) are presented in Tables A-31 through A-33. All units are in Gauss. The rms of fit and the number of observations are given for each rotation together with the A_{nm}, B_{nm} coefficients and their unit weight standard deviations (from the solution covariance matrix) in both Schmidt and fully normalized form. The formal errors for the coefficients should be scaled from their unit weight values by the factor

$$\sqrt{\frac{M}{M-N}} \times \text{rms}$$

where M is the number of observations and N is the number of solution coefficients. The solutions obtained using the second method which edits data so as to exclude anomalous regions of high field strength are presented in Tables A-34 through A-36. Solutions (I & II) for all the Carrington rotations have been copied onto microfiche and have been included.

Mean Deviation for solution Type I for Carrington Rotation 1620. Units are Gauss with values meaned within a 10° x 10° equiangular grid.
σ = 3.34

	-80	-70	-60	-50	-40	-30	-20	-10	0	10	20	30	40	50	60	70	80	90
1	0	31	9	-1	-5	-3	4	14	-9	1	6	-1	1	-4	-1	3	-3	0
2	0	-3	-2	7	-10	-2	-7	1	3	-10	-28	-7	3	-5	-2	-4	7	0
3	0	3	4	0	-14	-4	0	-23	4	14	2	0	-4	-4	0	-6	-4	0
4	0	-13	-4	-3	0	0	12	10	-1	10	14	7	1	5	6	0	0	0
5	0	-18	4	0	14	9	0	15	-10	-12	-1	-2	5	6	6	4	0	0
6	0	-20	-9	0	7	-1	-21	1	-6	-15	-16	-6	-3	0	4	-1	-2	0
7	0	-17	-6	0	-1	-6	-8	1	23	19	9	-5	-12	-7	-5	-5	0	0
8	0	1	-6	-2	-14	-3	12	-3	22	21	27	10	-1	-7	-1	3	-13	0
9	0	-28	4	-10	-5	-11	27	-66	-53	-166	38	23	3	-3	0	0	-13	0
10	0	-30	-3	6	-7	-8	11	72	-21	329	-180	12	3	0	0	-14	-14	0
11	0	-32	5	3	2	0	-10	-54	-78	-120	45	18	-1	-1	0	-2	-1	0
12	0	-1	1	-7	0	-3	1	54	-4	62	-20	10	-5	-12	2	2	-3	0
13	0	24	19	4	2	3	4	14	21	-64	39	17	-3	-1	14	5	-5	0
14	0	17	11	2	0	12	-36	-6	3	13	4	-10	-10	-1	3	2	3	0
15	0	-17	6	2	-7	8	2	43	-4	1	2	-11	-2	6	2	0	2	0
16	0	19	1	-9	-1	3	-28	5	-5	6	-5	-3	7	9	-2	-1	9	0
17	0	0	3	-5	-9	3	25	-10	-11	-12	-1	8	8	-1	0	8	15	0
18	0	0	14	4	-8	2	1	-20	55	4	7	0	0	0	0	0	0	0
19	0	5	-7	0	-7	-7	-4	-17	15	-41	2	-4	-6	-12	-5	-11	4	0
20	0	21	2	1	7	-3	13	-7	-41	10	11	-1	-4	-2	0	-9	5	0
21	0	5	4	7	11	-2	0	17	39	4	13	3	1	6	3	9	-1	0
22	0	1	0	3	6	6	-6	-4	-3	-21	-6	-7	1	10	2	1	-22	0
23	0	-22	0	-6	-4	0	-3	3	1	-7	6	2	0	4	3	-7	2	0
24	0	0	0	-3	-8	-2	4	-24	-6	6	9	2	-1	-3	1	3	-3	0
25	0	0	0	0	-12	0	8	26	6	7	2	-8	-5	-3	0	-10	1	0
26	0	0	0	1	0	-2	0	-7	-10	-5	-6	-1	3	-8	-1	6	0	0
27	0	0	0	-9	1	0	-1	-1	0	-2	-10	6	7	-3	-5	1	-4	0
28	0	0	0	3	12	1	-3	-1	5	6	0	6	4	7	-8	12	5	0
29	0	0	0	5	7	7	-5	11	7	4	-6	-1	2	5	-2	10	6	0
30	0	-7	-8	-5	-6	2	-1	-6	-11	-5	-12	-9	-8	0	0	0	0	0
31	0	8	6	-4	-10	2	7	-1	-2	0	8	9	-1	11	0	-4	-2	0
32	0	3	3	0	-7	-4	1	13	0	2	10	5	-1	0	6	17	10	0
33	0	-5	0	0	-2	2	-8	5	-1	1	0	-7	4	-2	2	0	1	0
34	0	2	13	4	1	14	-11	2	3	-10	-7	-10	0	-3	-3	-13	-4	0
35	0	6	6	6	-2	4	5	-5	5	-1	-4	6	4	-1	0	5	-1	0
36	0	10	3	0	1	-3	12	-24	8	5	8	8	1	0	-2	3	6	0

TABLE A-1

RMS Deviation for solution Type I for Carrington Rotation 1620.
Units are Gauss with values meaned within a 10° x 10° equiangular grid.

1	0	31	9	5	5	5	9	19	10	2	7	5	4	4	5	3	3	0
2	0	3	2	7	10	6	10	3	5	19	30	7	4	5	4	4	7	0
3	0	3	4	0	14	9	6	24	5	14	4	0	4	4	4	6	4	0
4	0	13	4	4	0	2	14	11	3	10	14	11	1	5	9	0	0	0
5	0	18	4	3	14	9	10	27	11	17	1	5	6	6	9	4	0	0
6	0	20	9	10	7	5	21	5	6	16	17	8	4	0	5	1	2	0
7	0	17	6	0	1	6	10	2	23	20	10	6	12	7	5	5	0	0
8	0	1	6	5	14	7	15	3	24	21	27	12	1	7	4	3	13	0
9	0	28	4	11	5	14	36	127	57	178	46	23	5	3	4	0	13	0
10	0	30	3	10	7	8	23	73	52	394	198	14	9	0	4	14	14	0
11	0	32	5	3	2	2	10	70	81	238	53	18	7	1	6	2	1	0
12	0	1	1	9	0	5	7	60	20	72	48	11	12	12	5	2	3	0
13	0	24	19	5	2	5	4	14	21	109	39	17	6	1	15	5	5	0
14	0	17	11	2	0	14	62	15	4	13	9	11	12	1	4	2	3	0
15	0	17	6	2	7	10	6	53	8	8	14	11	5	6	5	0	2	0
16	0	19	1	10	1	4	55	9	9	10	6	12	7	9	6	1	9	0
17	0	0	3	5	9	12	26	16	17	12	2	9	8	1	3	8	15	0
18	0	0	14	6	8	5	4	20	57	5	7	0	0	0	0	0	0	0
19	0	5	7	1	7	7	5	17	17	77	2	4	6	12	5	11	4	0
20	0	21	2	7	7	6	17	17	51	11	12	7	4	2	1	9	5	0
21	0	5	4	8	11	6	6	24	65	5	13	10	3	6	3	9	1	0
22	0	1	0	8	6	6	7	5	12	21	9	9	5	10	3	1	22	0
23	0	22	0	7	4	1	7	17	6	11	9	3	4	4	4	7	2	0
24	0	0	0	3	8	3	4	24	17	11	10	7	2	3	5	3	3	0
25	0	0	0	0	12	5	8	32	8	9	3	10	5	3	2	10	1	0
26	0	0	0	1	0	2	6	8	12	6	8	1	6	8	4	6	0	0
27	0	0	0	9	1	2	5	3	5	4	11	6	7	3	5	1	4	0
28	0	0	0	3	12	5	6	3	11	9	3	6	4	7	8	12	5	0
29	0	0	0	5	7	7	9	12	9	4	6	2	3	5	3	10	6	0
30	0	7	8	5	6	2	4	7	11	7	12	9	10	0	6	0	0	0
31	0	8	6	7	10	4	10	1	4	4	9	13	3	11	3	4	2	0
32	0	3	3	2	7	4	8	13	4	8	10	6	5	0	6	17	10	0
33	0	5	0	0	2	3	11	15	10	6	6	9	6	2	2	0	1	0
34	0	2	13	4	1	15	17	18	4	11	7	10	2	3	6	13	4	0
35	0	6	6	10	2	5	13	6	7	6	4	8	4	1	0	5	1	0
36	0	10	3	2	1	7	16	24	9	5	9	9	5	0	3	3	6	0

TABLE A-2

Distribution of observations (multiplied by ten) for Carrington Rotation 1620 used in solution Type I meaned within a 10° x 10° equiangular grid.

1	0	10	10	20	10	20	30	20	30	30	20	20	30	10	20	10	10	0
2	0	10	10	20	10	20	30	20	30	30	20	20	30	10	20	10	10	0
3	0	10	10	20	10	20	30	20	30	30	20	20	30	10	20	10	10	0
4	0	10	10	20	10	20	30	20	30	30	20	20	30	10	20	10	10	0
5	0	10	10	20	10	20	30	20	30	30	20	20	30	10	20	10	10	0
6	0	10	10	20	10	20	30	20	30	30	20	20	30	0	20	10	10	0
7	0	10	10	20	10	20	30	20	30	30	20	20	30	10	20	10	10	0
8	0	10	10	20	10	20	30	20	30	30	20	20	30	10	20	10	10	0
9	0	10	10	20	10	20	30	20	30	30	20	20	30	10	20	10	10	0
10	0	10	10	20	10	20	30	20	30	30	20	20	30	10	20	10	10	0
11	0	10	10	20	10	20	30	20	30	30	20	20	30	10	20	10	10	0
12	0	10	10	20	10	20	30	20	30	30	20	20	30	10	20	10	10	0
13	0	10	10	20	10	20	30	20	30	30	20	20	30	10	20	10	10	0
14	0	10	10	20	10	20	30	20	30	30	20	20	30	10	20	10	10	0
15	0	10	10	20	10	20	30	20	30	30	20	20	30	10	20	10	10	0
16	0	10	10	20	10	20	30	20	30	30	20	20	30	10	20	10	10	0
17	0	0	10	20	10	20	30	20	30	30	20	20	30	10	20	10	10	0
18	0	0	10	20	10	20	30	20	30	30	20	0	0	0	0	0	0	0
19	0	10	10	20	10	20	30	20	30	30	20	20	30	10	20	10	10	0
20	0	10	10	20	10	20	30	20	30	30	20	20	30	10	20	10	10	0
21	0	10	10	20	10	20	30	20	30	30	20	20	30	10	20	10	10	0
22	0	10	10	20	10	20	30	20	30	30	20	20	30	10	20	10	10	0
23	0	10	10	20	10	20	30	20	30	30	20	20	30	10	20	10	10	0
24	0	0	0	10	10	20	30	20	30	30	20	20	30	10	20	10	10	0
25	0	0	0	10	10	20	30	20	30	30	20	20	30	10	20	10	10	0
26	0	0	0	10	10	20	30	20	30	30	20	20	30	10	20	10	10	0
27	0	0	0	10	10	20	30	20	30	30	20	20	30	10	20	10	10	0
28	0	0	0	10	10	20	30	20	30	30	20	20	30	10	20	10	10	0
29	0	0	0	10	10	20	30	20	30	30	20	20	30	10	20	10	10	0
30	0	10	10	20	10	20	30	20	30	30	10	20	30	10	20	10	10	0
31	0	10	10	20	10	20	30	20	30	30	20	20	30	10	20	10	10	0
32	0	10	10	20	10	20	30	20	30	30	20	20	30	10	20	10	10	0
33	0	10	10	20	10	20	30	20	30	30	20	20	30	10	20	10	10	0
34	0	10	10	20	10	20	30	20	30	20	20	20	30	10	20	10	10	0
35	0	10	10	20	10	20	30	20	30	30	20	20	30	10	20	10	10	0
36	0	10	10	20	10	20	30	20	30	20	20	20	30	10	20	10	10	0

TABLE A-3

Computed Line-of-Sight Magnetic field measurements from solution Type I for Carrington Rotation 1620. Units are Gauss with values meaned within a 10° x 10° grid.

1	0	-5	-14	-3	15	23	17	8	10	11	7	5	9	12	15	19	17	0
2	0	-6	-12	-1	15	23	23	19	20	18	15	15	15	13	15	19	17	0
3	0	-7	-9	0	11	17	18	13	5	-1	3	11	14	11	13	19	17	0
4	0	-8	-7	0	5	10	19	20	7	-6	-2	7	10	6	10	20	18	0
5	0	-8	-5	-1	0	7	29	46	41	22	15	15	10	3	7	19	19	0
6	0	-7	-4	-3	0	8	32	51	52	38	28	23	13	0	7	19	20	0
7	0	-5	-5	-5	1	11	19	18	14	11	11	13	13	8	8	18	20	0
8	0	-3	-6	-6	3	12	4	-10	-10	-6	-7	-3	8	11	9	17	21	0
9	0	-2	-7	-8	2	10	5	7	27	28	0	-11	2	12	10	16	22	0
10	0	0	-7	-10	0	6	12	41	80	69	14	-12	-1	11	9	16	22	0
11	0	0	-7	-10	-4	0	11	43	74	50	0	-17	0	10	8	15	23	0
12	0	0	-6	-8	-4	-1	5	22	27	-3	-26	-16	9	11	6	17	23	0
13	0	-1	-6	-4	0	0	4	13	6	-20	-21	1	20	11	5	17	22	0
14	0	-2	-5	1	7	2	0	13	17	6	7	20	23	10	6	19	21	0
15	0	-3	-5	7	12	2	-13	-2	18	23	19	19	15	8	10	21	19	0
16	0	-4	-5	10	16	2	-25	-22	1	13	8	4	4	8	14	22	18	0
17	0	0	-5	8	16	6	-16	-19	-5	4	0	-1	2	10	18	23	17	0
18	0	0	-4	4	11	10	4	2	2	2	4	0	0	0	0	0	0	0
19	0	-3	-2	0	3	8	17	16	3	-2	6	14	14	11	16	22	17	0
20	0	-2	-1	-2	-3	0	15	19	4	-5	3	12	9	5	12	21	18	0
21	0	-3	0	-1	-6	-4	11	25	19	7	6	8	2	0	7	20	19	0
22	0	-4	1	2	-2	-3	9	27	29	17	9	6	0	-2	5	18	20	0
23	0	-5	2	7	4	0	5	14	14	6	3	4	3	1	6	17	20	0
24	0	0	0	12	8	3	0	1	-3	-6	-1	4	7	6	9	15	19	0
25	0	0	0	12	7	1	2	6	4	2	5	6	6	9	12	15	18	0
26	0	0	0	8	0	-4	6	20	19	14	11	4	0	7	14	15	17	0
27	0	0	0	5	-5	-11	3	16	10	5	5	0	-4	5	15	16	16	0
28	0	0	0	4	-6	-15	-4	3	-7	-9	-1	-1	-3	6	16	16	16	0
29	0	0	0	6	-3	-14	-10	-1	-5	-4	3	5	2	8	15	15	16	0
30	0	-4	-1	8	4	-8	-13	0	9	10	9	8	7	11	15	15	16	0
31	0	-4	-6	9	12	-1	-15	-3	13	12	4	2	7	11	13	14	17	0
32	0	-3	-10	7	17	5	-17	-12	7	10	1	0	6	10	12	15	17	0
33	0	-2	-13	3	18	11	-14	-14	2	13	9	5	6	8	11	15	18	0
34	0	-2	-15	-1	16	14	-10	-21	-7	11	10	7	5	7	11	17	18	0
35	0	-2	-16	-4	14	16	-6	-25	-20	-7	-2	0	2	7	12	18	17	0
36	0	-3	-16	-5	14	19	3	-14	-15	-9	-7	-4	2	9	14	18	17	0

TABLE A-4

Mt. Wilson Line-of-Sight Magnetic field measurements for Carrington Rotation 1620 used in solution Type I. Units are Gauss with values meaned within a 10° x 10° equiangular grid.

1	0	26	-5	-5	9	20	21	23	0	12	13	4	10	8	13	22	13	0
2	0	-10	-14	6	4	21	15	21	23	7	-13	7	18	8	12	15	25	0
3	0	-4	-5	1	-2	13	19	-9	9	12	6	12	10	6	12	13	12	0
4	0	-22	-12	-3	5	10	31	31	6	4	11	14	11	12	16	20	19	0
5	0	-26	-1	-2	15	16	28	61	30	9	13	13	16	10	14	24	18	0
6	0	-27	-13	-2	6	7	11	53	45	23	11	17	10	0	11	17	17	0
7	0	-22	-11	-4	0	5	10	19	38	31	20	8	1	1	2	12	20	0
8	0	-1	-13	-9	-11	8	17	-13	12	15	19	6	6	4	7	20	7	0
9	0	-30	-2	-19	-2	0	32	-59	-25	-138	39	11	5	8	9	17	8	0
10	0	-31	-11	-4	-7	-1	23	113	59	398	-165	0	2	11	8	2	8	0
11	0	-32	-1	-7	-2	0	0	-10	-3	-70	44	0	0	9	8	14	21	0
12	0	-1	-5	-15	-3	-5	6	76	22	58	-47	-5	3	-1	8	19	20	0
13	0	23	13	0	2	3	8	27	27	-84	17	18	17	10	19	23	17	0
14	0	15	5	3	6	15	-35	6	20	19	11	10	13	8	10	22	25	0
15	0	-21	0	9	5	10	-10	41	13	25	21	8	12	14	12	21	22	0
16	0	15	-3	0	14	5	-53	-16	-4	19	2	0	11	17	12	21	27	0
17	0	0	-1	3	7	9	8	-30	-16	-8	0	7	11	9	18	32	32	0
18	0	0	10	8	3	13	6	-17	57	6	12	0	0	0	0	0	0	0
19	0	2	-10	0	-3	1	12	-1	19	-44	8	10	7	3	10	11	21	0
20	0	18	1	0	3	-2	28	11	-37	4	14	10	5	3	12	12	23	0
21	0	2	4	5	5	-7	12	42	59	11	19	11	4	5	10	30	18	0
22	0	-3	1	5	3	2	2	23	26	-3	3	0	1	7	8	20	-1	0
23	0	-28	2	1	0	0	1	18	16	-1	10	7	2	6	9	9	22	0
24	0	0	0	8	0	0	5	-23	-9	0	8	6	5	3	11	18	16	0
25	0	0	0	11	-5	0	11	33	11	9	7	-2	0	5	12	5	20	0
26	0	0	0	9	1	-6	6	12	8	9	4	3	4	0	13	22	17	0
27	0	0	0	-3	-3	-12	1	14	10	3	-5	6	2	2	10	17	12	0
28	0	0	0	7	5	-14	-8	1	-1	-3	0	5	0	13	7	28	21	0
29	0	0	0	11	4	-6	-16	9	2	0	-2	3	5	13	13	26	23	0
30	0	-12	-9	3	-2	-5	-14	-6	-1	4	-3	-1	-1	10	15	15	15	0
31	0	4	0	4	1	1	-8	-5	10	12	12	11	6	22	13	10	14	0
32	0	0	-6	7	9	1	-15	1	6	12	12	5	4	10	18	32	28	0
33	0	-7	-13	3	16	13	-23	-11	0	15	8	-1	10	6	13	16	19	0
34	0	0	-2	3	17	28	-21	-19	-3	0	3	-3	5	3	8	3	13	0
35	0	3	-10	2	11	21	0	-31	-15	-8	-6	5	6	6	13	23	16	0
36	0	6	-12	-4	15	16	16	-38	-6	-3	1	3	4	9	12	22	23	0

TABLE A-5

Mean Deviation for solution Type I for Carrington Rotation 1625. Units are Gauss with values meaned within a 10° x 10° equiangular grid.
σ = .817

1	0	1	8	5	-10	4	3	-2	2	6	0	-13	-2	-7	5	-4	0	0
2	0	-5	0	-8	-2	2	-5	0	4	1	-4	0	-1	2	1	-5	-4	0
3	0	11	-4	-3	-3	2	3	0	0	-6	-3	10	6	-3	4	5	0	0
4	0	9	4	5	-6	-1	0	-5	0	8	-4	5	-1	0	-5	1	9	0
5	0	-4	0	7	9	1	3	-4	-1	0	-5	-3	-3	3	2	4	11	0
6	0	6	0	-5	2	-5	2	8	2	4	-1	0	-1	8	0	-3	5	0
7	0	-9	1	7	-1	-1	0	-10	-3	3	2	2	6	-4	0	0	9	0
8	0	-4	3	-4	-4	0	-2	0	-5	-2	-2	-6	2	-10	2	-3	0	0
9	0	-19	0	-1	0	-2	5	10	5	3	-5	-2	2	5	5	2	0	0
10	0	-12	-11	-4	9	-3	0	-6	-2	2	0	4	-6	-15	3	-1	0	0
11	0	-1	2	-5	1	-3	0	-5	-1	-1	-4	7	1	0	3	0	-14	0
12	0	1	-8	-1	3	2	-4	4	3	-8	-1	3	-3	-2	0	-9	0	0
13	0	-10	-1	2	3	6	1	2	0	10	0	-5	-2	10	0	-2	0	0
14	0	-21	0	-4	-7	-7	2	-11	-6	1	0	0	2	0	-2	-2	0	0
15	0	-1	4	2	-11	4	0	8	-1	2	0	1	4	-6	0	-9	0	0
16	0	0	-2	-5	-10	3	-9	1	-3	1	-8	-1	-10	-7	-3	-4	0	0
17	0	12	9	10	3	9	4	3	2	8	3	0	5	2	4	3	3	0
18	0	3	12	1	5	-1	1	-4	0	-3	-6	3	1	1	9	7	9	0
19	0	14	8	-5	-14	-6	-3	-3	-1	0	-5	4	-4	7	0	11	0	0
20	0	3	10	3	6	8	1	2	5	7	3	3	0	-5	-4	6	0	0
21	0	-2	3	0	3	-1	0	-2	2	-2	-9	0	2	-4	0	-1	0	0
22	0	8	-4	-3	-3	0	0	2	-4	5	-2	0	0	3	-3	-5	0	0
23	0	-25	-6	-3	5	2	0	-20	-6	0	7	-3	1	-8	-6	-1	0	0
24	0	0	8	-4	0	-1	2	26	4	3	-3	-2	2	-2	6	3	0	0
25	0	6	-2	0	-6	0	-3	-7	-4	11	-4	-2	6	1	5	-4	0	0
26	0	1	-12	5	-3	-5	3	-10	-8	-14	-12	-3	-1	-8	5	-2	0	0
27	0	-10	7	8	1	-1	1	14	3	22	5	8	-1	5	-6	-3	0	0
28	0	-8	-2	-3	1	3	-1	8	1	-16	11	-1	-3	-1	4	-2	0	0
29	0	-3	-5	-1	-1	-1	-1	-19	-3	10	-26	-13	5	-2	2	2	7	0
30	0	0	-9	-1	0	-3	0	11	0	-1	5	8	5	-6	-2	-2	-20	0
31	0	-7	8	-6	-10	0	2	2	-13	30	-5	-2	0	3	-2	3	29	0
32	0	16	0	5	1	5	7	3	8	-29	0	-6	0	-3	-3	-10	-24	0
33	0	-1	5	-5	10	0	-2	-32	4	5	6	-3	1	-4	6	12	9	0
34	0	12	0	4	10	1	-6	31	3	1	8	2	1	-6	-8	-1	-34	0
35	0	6	8	0	1	2	-7	2	-4	-8	0	-1	-3	2	0	3	0	0
36	0	9	5	-3	4	11	-3	-1	-1	-3	12	1	4	1	-2	-4	0	0

TABLE A-6

RMS Deviation for solution Type I for Carrington Rotation 1625.
Units are Gauss with values meaned within a 10° x 10° equiangular grid.

1	0	1	8	5	10	4	5	3	4	8	2	13	7	7	5	4	0	0
2	0	5	0	8	2	3	6	0	7	4	5	1	4	2	4	5	4	0
3	0	11	4	3	3	2	4	2	2	10	8	10	8	3	9	5	0	0
4	0	9	4	6	6	1	2	5	5	8	5	6	4	0	6	1	9	0
5	0	4	0	10	9	6	5	7	5	1	5	4	3	3	5	4	11	0
6	0	6	0	5	2	5	6	9	3	4	5	5	7	8	2	3	5	0
7	0	9	1	8	1	2	3	14	3	5	4	3	7	4	0	0	9	0
8	0	4	3	4	4	7	3	0	5	3	2	6	5	10	5	3	0	0
9	0	19	0	1	0	2	6	10	6	4	7	5	3	5	6	2	0	0
10	0	12	11	5	9	5	0	6	6	7	1	4	7	15	3	1	0	0
11	0	1	2	6	1	3	5	5	8	6	7	8	4	0	5	0	14	0
12	0	1	8	2	3	5	7	6	5	8	1	3	4	2	3	9	0	0
13	0	10	1	3	3	8	2	3	2	14	0	6	3	10	1	2	0	0
14	0	21	0	7	7	7	6	12	7	3	0	0	5	0	4	2	0	0
15	0	1	4	5	11	4	4	8	2	4	2	8	6	6	0	9	0	0
16	0	0	2	6	10	4	9	6	4	5	9	2	11	7	3	4	0	0
17	0	12	9	10	3	10	4	4	2	8	3	0	5	2	4	3	3	0
18	0	3	12	3	5	2	3	6	4	3	6	5	2	1	9	7	9	0
19	0	14	8	5	14	6	5	4	3	1	5	5	4	7	2	11	0	0
20	0	3	10	4	6	8	6	3	6	7	4	3	3	5	6	6	0	0
21	0	2	3	2	3	1	1	2	3	4	9	0	5	4	4	1	0	0
22	0	8	4	3	3	2	7	2	4	6	3	3	4	3	3	5	0	0
23	0	25	6	3	5	2	4	25	8	4	7	6	2	8	6	1	0	0
24	0	0	8	7	0	3	3	33	5	7	6	9	3	2	9	3	0	0
25	0	6	2	6	6	1	4	7	5	14	4	2	7	1	6	4	0	0
26	0	1	12	5	3	5	4	12	9	14	12	5	5	8	10	2	0	0
27	0	10	7	8	1	5	7	14	6	23	6	8	8	5	6	3	0	0
28	0	8	2	3	1	3	1	9	8	25	11	4	3	1	4	2	0	0
29	0	3	5	1	1	2	8	19	7	11	27	16	11	2	4	2	7	0
30	0	0	9	2	0	3	2	28	20	11	5	8	5	6	2	2	20	0
31	0	7	8	6	10	0	3	2	20	35	8	3	7	3	2	3	29	0
32	0	16	0	6	1	5	8	7	8	31	2	6	2	3	4	10	24	0
33	0	1	5	5	10	2	4	32	6	6	6	3	1	4	6	12	9	0
34	0	12	0	4	10	2	9	32	5	1	8	5	3	6	8	1	34	0
35	0	6	8	2	1	5	8	3	8	12	0	3	7	2	3	3	0	0
36	0	9	5	3	4	12	6	6	6	6	12	5	6	1	2	4	0	0

TABLE A-7

Distribution of observations (multiplied by ten) for Carrington Rotation 1625 used in solution Type I meaned within a 10° x 10° equiangular grid.

1	0	10	10	20	10	20	30	20	30	30	20	20	30	10	20	10	0	0
2	0	10	10	20	10	20	30	20	30	30	20	20	30	10	20	10	10	0
3	0	10	10	20	10	20	30	20	30	30	20	20	30	10	20	10	0	0
4	0	10	10	20	10	20	30	20	30	30	20	20	30	10	20	10	10	0
5	0	10	10	20	10	20	30	20	30	30	20	20	30	10	20	10	10	0
6	0	10	10	20	10	20	30	20	30	30	20	20	30	10	20	10	10	0
7	0	10	10	20	10	20	30	20	30	30	20	20	30	10	20	10	10	0
8	0	10	10	20	10	20	30	20	30	30	20	20	30	10	20	10	0	0
9	0	10	10	20	10	20	30	20	30	30	20	20	30	10	20	10	0	0
10	0	10	10	20	10	20	30	20	30	30	20	20	30	10	20	10	0	0
11	0	10	10	20	10	20	30	20	30	30	20	20	30	10	20	10	10	0
12	0	10	10	20	10	20	30	20	30	30	20	20	30	10	20	10	0	0
13	0	10	10	20	10	20	30	20	30	30	20	20	30	10	20	10	0	0
14	0	10	10	20	10	20	30	20	30	30	20	20	30	10	20	10	0	0
15	0	10	10	20	10	20	30	20	30	30	20	20	30	10	20	10	0	0
16	0	10	10	20	10	20	30	20	30	30	20	20	30	10	20	10	0	0
17	0	10	10	20	10	20	30	20	30	30	20	20	30	10	20	10	10	0
18	0	10	10	20	10	20	30	20	30	30	20	20	30	10	20	10	10	0
19	0	10	10	20	10	20	30	20	30	30	20	20	30	10	20	10	0	0
20	0	10	10	20	10	20	30	20	30	20	20	20	30	10	20	10	0	0
21	0	10	10	20	10	20	30	10	30	30	20	20	30	10	20	10	0	0
22	0	10	10	20	10	20	30	20	30	30	20	20	30	10	20	10	0	0
23	0	10	10	20	10	20	30	20	30	30	20	20	30	10	20	10	0	0
24	0	10	10	20	10	20	30	20	30	30	20	20	30	10	20	10	0	0
25	0	10	10	20	10	20	30	20	30	30	20	20	30	10	20	10	0	0
26	0	10	10	20	10	20	30	20	30	30	20	20	30	10	20	10	0	0
27	0	10	10	20	10	20	30	20	20	30	20	20	30	10	20	10	0	0
28	0	10	10	20	10	20	30	20	30	30	20	20	30	10	20	10	0	0
29	0	10	10	20	10	20	30	20	30	30	20	20	30	10	20	10	10	0
30	0	10	10	20	10	20	30	20	30	30	20	20	30	10	20	10	10	0
31	0	10	10	20	10	20	30	20	30	30	20	20	30	10	20	10	10	0
32	0	10	10	20	10	20	20	20	30	30	20	20	30	10	20	10	10	0
33	0	10	10	20	10	20	30	20	30	30	20	20	30	10	20	10	10	0
34	0	10	10	10	10	20	30	20	30	30	20	20	30	10	20	10	10	0
35	0	10	10	20	10	20	30	20	30	30	20	20	30	10	20	10	0	0
36	0	10	10	20	10	20	30	20	30	30	20	20	30	10	20	10	0	0

TABLE A-8

Computed Line-of-Sight Magnetic field measurements from solution Type I for Carrington Rotation 1625. Units are Gauss with values meaned within a 10° x 10° grid.

1	0	-22	-13	-4	1	5	3	-3	-6	-4	-4	-3	1	3	3	7	0	0
2	0	-22	-14	-5	1	7	8	0	-9	-15	-16	-11	0	4	3	6	12	0
3	0	-21	-14	-7	0	6	10	4	-3	-11	-14	-10	0	4	2	6	0	0
4	0	-21	-14	-8	-2	4	10	6	3	3	1	0	2	3	2	6	12	0
5	0	-20	-13	-9	-4	3	9	6	5	11	13	8	4	2	2	6	12	0
6	0	-20	-13	-9	-5	2	11	7	3	8	11	7	2	1	2	6	12	0
7	0	-20	-13	-9	-7	0	11	12	5	3	3	1	0	0	2	7	12	0
8	0	-19	-13	-9	-8	-4	9	15	11	4	1	0	-1	0	3	8	0	0
9	0	-19	-13	-9	-10	-8	3	13	12	5	1	0	0	0	2	8	0	0
10	0	-18	-13	-9	-10	-9	0	8	6	0	-1	0	0	-1	1	8	0	0
11	0	-18	-13	-9	-9	-8	0	5	2	-4	-4	-2	-3	-5	0	9	14	0
12	0	-18	-13	-9	-9	-7	0	6	6	0	-1	-3	-7	-8	-2	9	0	0
13	0	-18	-13	-8	-9	-9	-3	6	12	10	3	-2	-8	-10	-3	9	0	0
14	0	-19	-13	-8	-9	-12	-8	2	11	9	0	-4	-8	-8	-2	9	0	0
15	0	-19	-13	-6	-7	-11	-9	-1	3	0	-6	-6	-4	-3	0	9	0	0
16	0	-20	-13	-4	-3	-5	-4	0	0	-3	-5	-2	1	1	2	9	0	0
17	0	-21	-13	-3	0	1	3	4	3	3	4	5	5	4	4	9	12	0
18	0	-22	-14	-2	2	5	9	7	4	8	12	10	5	4	6	9	11	0
19	0	-22	-13	-2	0	4	9	4	-1	3	8	6	1	2	7	10	0	0
20	0	-21	-13	-4	-3	0	5	0	-8	-3	1	0	-3	1	7	11	0	0
21	0	-20	-12	-6	-8	-7	0	-2	-7	-6	-2	-5	-7	0	8	12	0	0
22	0	-19	-12	-8	-12	-12	-4	0	0	-1	-4	-10	-10	0	7	12	0	0
23	0	-18	-12	-9	-13	-13	-4	4	8	2	-8	-16	-12	-1	6	11	0	0
24	0	-17	-13	-10	-11	-11	-3	7	12	4	-10	-17	-10	0	4	10	0	0
25	0	-16	-14	-10	-9	-9	-5	3	9	4	-5	-8	-2	1	2	8	0	0
26	0	-16	-15	-9	-8	-9	-10	-4	2	2	0	2	5	3	1	7	0	0
27	0	-16	-15	-8	-7	-11	-13	-8	-2	-2	-3	1	6	3	0	7	0	0
28	0	-16	-15	-8	-8	-12	-13	-3	1	-7	-15	-11	-1	1	1	8	0	0
29	0	-17	-14	-7	-7	-12	-12	0	6	-7	-22	-21	-8	0	3	9	15	0
30	0	-17	-14	-5	-5	-11	-13	-3	3	-4	-17	-18	-8	0	5	10	14	0
31	0	-18	-14	-4	-3	-8	-15	-14	-8	-5	-6	-6	-2	3	6	10	13	0
32	0	-19	-14	-2	0	-4	-11	-17	-16	-8	-2	0	2	5	7	10	12	0
33	0	-20	-13	-2	1	0	-3	-9	-12	-8	-2	0	1	4	7	10	11	0
34	0	-21	-13	-4	1	2	2	1	0	0	0	-1	0	2	6	10	11	0
35	0	-21	-13	-2	1	2	3	3	6	10	7	1	0	1	5	9	0	0
36	0	-22	-13	-3	1	3	1	-1	2	8	7	3	1	2	3	8	0	0

TABLE A-9

Mt. Wilson Line-of-Sight Magnetic field measurements for Carrington Rotation 1625 used in solution Type I. Units are Gauss with values meaned within a 10° x 10° equiangular grid.

1	0	-20	-5	0	-8	9	6	-5	-3	2	-4	-16	-1	-3	8	3	0	0
2	0	-27	-14	-14	-1	9	2	0	-4	-14	-21	-11	-1	7	4	0	7	0
3	0	-9	-18	-10	-3	9	14	5	-4	-17	-17	0	7	1	7	11	0	0
4	0	-11	-9	-2	-9	2	9	0	2	11	-3	5	1	4	-3	7	21	0
5	0	-25	-13	-1	5	5	13	1	3	10	8	5	0	5	4	10	23	0
6	0	-14	-14	-14	-2	-2	13	16	5	12	9	6	0	9	2	3	17	0
7	0	-29	-11	-1	-8	-1	11	1	2	7	6	4	5	-3	3	6	21	0
8	0	-23	-9	-14	-13	-4	6	15	5	2	0	-6	1	-9	5	4	0	0
9	0	-39	-12	-10	-10	-10	8	23	17	9	-3	-1	2	6	8	10	0	0
10	0	-31	-24	-14	0	-12	0	2	3	2	-1	4	-6	-17	4	7	0	0
11	0	-19	-11	-15	-7	-11	0	0	0	-6	-8	4	-2	-5	2	9	0	0
12	0	-16	-22	-10	-5	-5	-4	10	10	-7	-2	0	-10	-10	-2	0	0	0
13	0	-29	-15	-5	-5	-3	-1	9	12	20	2	-8	-11	0	-3	7	0	0
14	0	-40	-13	-12	-17	-19	-5	-9	4	10	0	-4	-5	-8	-4	7	0	0
15	0	-21	-9	-4	-19	-6	-8	6	1	1	-5	-5	0	-9	0	0	0	0
16	0	-21	-15	-10	-14	-2	-14	0	-2	-2	-14	-4	-9	-5	-1	4	0	0
17	0	-9	-4	7	3	10	7	8	6	11	8	6	10	6	9	12	15	0
18	0	-18	-1	0	7	4	10	2	4	4	5	13	7	6	15	16	21	0
19	0	-7	-4	-7	-13	-1	5	0	-3	2	3	11	-3	10	8	22	0	0
20	0	-17	-2	0	3	8	7	3	-2	4	4	2	-3	-4	3	18	0	0
21	0	-23	-8	-7	-4	-8	0	-5	-5	-8	-12	-6	-4	-4	7	10	0	0
22	0	-10	-16	-12	-15	-13	-5	3	-4	4	-7	-10	-10	2	4	6	0	0
23	0	-44	-19	-13	-7	-10	-3	-15	2	2	-1	-19	-10	-9	0	9	0	0
24	0	-17	-5	-14	-11	-12	0	34	16	7	-13	-19	-8	-3	11	13	0	0
25	0	-10	-17	-10	-15	-9	-9	-3	5	16	-9	-10	3	2	8	4	0	0
26	0	-15	-27	-4	-11	-14	-6	-14	-5	-11	-11	-1	3	-5	6	5	0	0
27	0	-26	-8	0	-6	-12	-11	6	1	19	1	9	4	8	-5	4	0	0
28	0	-25	-17	-11	-6	-9	-14	4	2	-24	-3	-12	-4	0	5	5	0	0
29	0	-20	-20	-8	-8	-14	-14	-18	2	2	-48	-35	-3	-2	5	12	22	0
30	0	-17	-24	-7	-4	-14	-13	8	3	-6	-11	-9	-3	-5	2	7	-6	0
31	0	-26	-5	-10	-13	-9	-13	-12	-21	25	-11	-9	-1	6	4	14	42	0
32	0	-3	-13	2	1	1	-3	-13	-8	-38	-1	-5	1	1	3	0	-12	0
33	0	-22	-8	-7	11	1	-6	-41	-7	-2	1	-4	2	0	14	23	21	0
34	0	-8	-14	0	12	3	-4	32	3	1	8	1	0	-3	-1	8	-22	0
35	0	-15	-4	-3	3	5	-4	6	2	1	7	0	-4	4	5	12	0	0
36	0	-12	-8	-6	5	14	-2	-2	0	5	20	5	5	3	1	4	0	0

TABLE A-10

Mean Deviation for solution Type I for Carrington Rotation 1663. Units are Gauss with values meaned within a 10° x 10° equiangular grid.
σ = 2.22

1	0	-2	-21	7	11	5	23	-45	9	-3	22	-1	8	13	0	-9	80	0
2	0	18	-5	3	1	8	-19	28	-5	-2	1	-6	1	4	-13	4	19	0
3	0	10	5	8	-7	-12	-1	16	-10	3	5	-2	0	1	-10	-11	-37	0
4	0	-26	-11	1	9	-6	8	-16	1	1	0	3	-5	15	4	0	0	0
5	0	0	0	0	0	0	0	0	0	0	0	0	0	0	0	0	0	0
6	0	0	0	0	0	0	0	0	0	0	0	0	0	0	0	0	0	0
7	0	0	0	0	0	0	0	0	0	0	0	0	0	0	0	0	0	0
8	0	0	0	0	0	0	0	0	0	0	0	0	0	0	0	0	0	0
9	0	0	0	0	0	0	0	0	0	0	0	0	0	0	0	0	0	0
10	0	0	0	0	0	0	0	0	0	0	0	0	0	0	0	0	0	0
11	0	0	0	0	0	0	0	0	0	0	0	0	0	0	0	0	0	0
12	0	0	0	0	0	0	0	0	0	0	0	0	0	0	0	0	0	0
13	0	0	0	0	0	0	0	0	0	0	0	0	0	0	0	0	0	0
14	0	0	0	0	0	0	0	0	0	0	0	0	0	0	0	0	0	0
15	0	0	0	0	0	0	0	0	0	0	0	0	0	0	0	0	0	0
16	0	135	-41	38	12	-2	2	16	-10	-4	8	-6	0	24	-33	-26	37	0
17	0	-27	-11	-3	-21	-30	-4	-5	-5	2	6	2	-5	13	9	17	-7	0
18	0	-164	-4	-17	-10	10	35	7	-6	-6	6	0	-8	-3	12	0	-2	0
19	0	-31	15	-9	5	28	-69	18	5	-8	9	2	4	10	7	-14	-10	0
20	0	23	-1	-3	1	16	12	9	2	-8	-1	3	-1	-12	-2	-15	32	0
21	0	21	-1	-5	-5	-3	0	-4	0	4	7	-3	2	-14	-7	1	7	0
22	0	-16	1	2	-2	-6	-1	-7	-2	4	0	-39	7	-1	4	-10	-4	0
23	0	50	-11	4	-7	2	12	-1	1	-5	10	14	-1	10	8	1	-15	0
24	0	55	5	0	3	-4	0	2	9	-16	28	0	-1	0	0	1	-14	0
25	0	9	10	7	4	5	-11	-1	4	-6	-8	-4	-14	-16	0	-11	-19	0
26	0	-15	-8	8	0	6	-4	0	-2	7	13	-11	4	3	9	2	-3	0
27	0	-15	10	0	4	16	7	9	-5	-6	3	3	10	5	0	3	-7	0
28	0	2	-4	-5	-9	0	-4	2	-1	1	0	5	-1	-6	-7	-6	-9	0
29	0	-3	-9	0	-20	-15	-18	-9	11	0	-11	-1	-20	0	-7	-10	-10	0
30	0	12	-5	5	-18	6	33	-9	4	1	-20	7	-3	5	-2	-4	11	0
31	0	8	0	8	-2	-16	17	-3	-4	0	39	17	17	14	1	-6	20	0
32	0	8	-9	3	14	11	-83	16	-6	-3	-20	-71	12	0	3	1	1	0
33	0	2	-6	0	13	25	16	18	9	-1	11	53	-25	-4	5	3	-4	0
34	0	-6	-3	0	-4	8	-18	-11	-1	-1	-43	11	6	3	13	2	28	0
35	0	3	-2	-3	-12	-14	3	18	-6	-5	51	-13	-2	7	12	-12	-15	0
36	0	16	-6	1	-6	-14	-7	20	2	-4	-12	-12	-6	-2	3	5	-5	0

TABLE A-11

RMS Deviation for solution Type I for Carrington Rotation 1663.
Units are Gauss with values meaned within a 10° x 10° equiangular grid.

1	0	2	21	7	11	6	35	105	9	4	23	2	8	13	2	9	80	0
2	0	18	5	10	1	8	29	31	9	3	3	6	3	4	14	4	19	0
3	0	10	5	8	7	12	45	44	12	5	10	8	3	1	21	11	37	0
4	0	26	11	2	9	6	19	55	9	9	18	5	11	15	5	0	0	0
5	0	0	0	0	0	0	0	0	0	0	0	0	0	0	0	0	0	0
6	0	0	0	0	0	0	0	0	0	0	0	0	0	0	0	0	0	0
7	0	0	0	0	0	0	0	0	0	0	0	0	0	0	0	0	0	0
8	0	0	0	0	0	0	0	0	0	0	0	0	0	0	0	0	0	0
9	0	0	0	0	0	0	0	0	0	0	0	0	0	0	0	0	0	0
10	0	0	0	0	0	0	0	0	0	0	0	0	0	0	0	0	0	0
11	0	0	0	0	0	0	0	0	0	0	0	0	0	0	0	0	0	0
12	0	0	0	0	0	0	0	0	0	0	0	0	0	0	0	0	0	0
13	0	0	0	0	0	0	0	0	0	0	0	0	0	0	0	0	0	0
14	0	0	0	0	0	0	0	0	0	0	0	0	0	0	0	0	0	0
15	0	0	0	0	0	0	0	0	0	0	0	0	0	0	0	0	0	0
16	0	135	41	39	12	4	7	16	18	13	18	16	3	24	33	26	37	0
17	0	27	11	5	21	31	6	8	7	5	14	7	6	13	17	17	7	0
18	0	164	4	18	10	11	36	7	7	6	6	12	8	3	12	0	2	0
19	0	31	15	9	5	29	114	19	5	8	16	4	10	10	8	14	10	0
20	0	23	1	3	1	17	12	9	5	8	2	4	17	12	7	15	32	0
21	0	21	1	8	5	5	4	8	2	4	10	3	16	14	7	1	7	0
22	0	16	1	4	2	8	5	8	4	5	5	43	9	1	4	10	4	0
23	0	50	11	4	7	4	21	8	1	5	20	14	1	10	15	1	15	0
24	0	55	5	3	3	5	8	3	10	17	34	9	1	0	0	1	14	0
25	0	9	10	7	4	8	12	5	5	8	8	4	15	16	5	11	19	0
26	0	15	8	8	0	6	7	5	2	7	13	12	12	3	10	2	3	0
27	0	15	10	5	4	16	8	9	7	7	3	11	12	5	1	3	7	0
28	0	2	4	5	9	0	4	4	1	4	1	6	4	6	8	6	9	0
29	0	3	9	4	20	17	19	15	11	6	11	5	21	0	11	10	10	0
30	0	12	5	5	18	32	61	11	6	5	38	8	13	5	6	4	11	0
31	0	8	0	8	2	19	26	4	5	5	39	18	18	14	6	6	20	0
32	0	8	9	11	14	14	101	16	10	6	28	73	15	0	3	1	1	0
33	0	2	6	1	13	25	16	19	9	3	20	122	32	4	6	3	4	0
34	0	6	3	1	4	9	26	12	5	6	43	23	51	3	15	2	28	0
35	0	3	2	4	12	19	23	30	7	7	62	13	25	7	12	12	15	0
36	0	16	6	6	6	14	23	60	7	4	14	13	7	2	3	5	5	0

TABLE A-12

Distribution of observations (multiplied by ten) for Carrington Rotation 1663 used in solution Type I meaned within a 10° x 10° equiangular grid.

1	0	10	10	20	10	20	30	20	30	30	20	20	20	10	20	10	10	0
2	0	10	10	20	10	20	30	20	30	30	20	20	30	10	20	10	10	0
3	0	10	10	20	10	20	30	20	30	30	20	20	30	10	20	10	10	0
4	0	10	10	20	10	20	30	20	30	30	20	20	30	10	20	0	0	0
5	0	0	0	0	0	0	0	0	0	0	0	0	0	0	0	0	0	0
6	0	0	0	0	0	0	0	0	0	0	0	0	0	0	0	0	0	0
7	0	0	0	0	0	0	0	0	0	0	0	0	0	0	0	0	0	0
8	0	0	0	0	0	0	0	0	0	0	0	0	0	0	0	0	0	0
9	0	0	0	0	0	0	0	0	0	0	0	0	0	0	0	0	0	0
10	0	0	0	0	0	0	0	0	0	0	0	0	0	0	0	0	0	0
11	0	0	0	0	0	0	0	0	0	0	0	0	0	0	0	0	0	0
12	0	0	0	0	0	0	0	0	0	0	0	0	0	0	0	0	0	0
13	0	0	0	0	0	0	0	0	0	0	0	0	0	0	0	0	0	0
14	0	0	0	0	0	0	0	0	0	0	0	0	0	0	0	0	0	0
15	0	0	0	0	0	0	0	0	0	0	0	0	0	0	0	0	0	0
16	0	10	10	20	10	20	30	20	30	30	20	20	30	10	10	10	10	0
17	0	10	10	20	10	20	30	20	30	30	20	20	30	10	20	10	10	0
18	0	10	10	20	10	20	30	20	30	30	20	20	30	10	20	10	10	0
19	0	10	10	20	10	20	30	20	30	30	20	20	30	10	20	10	10	0
20	0	10	10	20	10	20	30	20	30	30	20	20	30	10	20	10	10	0
21	0	10	10	20	10	20	30	20	30	30	20	20	30	10	20	10	10	0
22	0	10	10	20	10	20	30	20	30	30	20	20	30	10	20	10	10	0
23	0	10	10	20	10	20	30	20	30	30	20	20	30	10	20	10	10	0
24	0	10	10	20	10	20	30	20	30	30	20	20	30	10	20	10	10	0
25	0	10	10	20	10	20	30	20	30	30	20	20	30	10	20	10	10	0
26	0	10	10	20	10	20	30	20	30	30	20	20	30	10	20	10	10	0
27	0	10	10	20	10	20	30	20	30	30	20	20	30	10	20	10	10	0
28	0	10	10	20	10	20	30	20	30	30	20	20	30	10	20	10	10	0
29	0	10	10	20	10	20	30	20	30	30	20	20	30	10	20	10	10	0
30	0	10	10	20	10	20	30	20	30	30	20	20	30	10	20	10	10	0
31	0	10	10	20	10	20	30	20	30	30	20	20	30	10	20	10	10	0
32	0	10	10	20	10	20	20	20	30	30	20	20	30	10	20	10	10	0
33	0	10	10	20	10	20	30	20	30	30	20	20	30	10	20	10	10	0
34	0	10	10	20	10	20	30	20	30	30	20	20	30	10	20	10	10	0
35	0	10	10	20	10	20	30	20	30	30	20	20	30	10	20	10	10	0
36	0	10	10	20	10	20	30	20	30	30	20	20	30	10	20	10	10	0

TABLE A-13

Computed Line-of-Sight Magnetic field measurements from solution Type I for Carrington Rotation 1663. Units are Gauss with values meaned within a 10° x 10° grid.

1	0	-12	4	-1	-2	-1	-6	-9	0	12	11	4	-3	0	13	19	-4	0
2	0	-10	4	2	-2	-2	0	5	13	17	9	-1	-4	5	16	15	-2	0
3	0	0	5	8	14	21	26	20	15	16	12	5	4	13	17	10	5	0
4	0	28	13	0	-1	3	2	0	6	11	0	-8	6	26	22	0	0	0
5	0	0	0	0	0	0	0	0	0	0	0	0	0	0	0	0	0	0
6	0	0	0	0	0	0	0	0	0	0	0	0	0	0	0	0	0	0
7	0	0	0	0	0	0	0	0	0	0	0	0	0	0	0	0	0	0
8	0	0	0	0	0	0	0	0	0	0	0	0	0	0	0	0	0	0
9	0	0	0	0	0	0	0	0	0	0	0	0	0	0	0	0	0	0
10	0	0	0	0	0	0	0	0	0	0	0	0	0	0	0	0	0	0
11	0	0	0	0	0	0	0	0	0	0	0	0	0	0	0	0	0	0
12	0	0	0	0	0	0	0	0	0	0	0	0	0	0	0	0	0	0
13	0	0	0	0	0	0	0	0	0	0	0	0	0	0	0	0	0	0
14	0	0	0	0	0	0	0	0	0	0	0	0	0	0	0	0	0	0
15	0	0	0	0	0	0	0	0	0	0	0	0	0	0	0	0	0	0
16	0	108	23	-27	-20	-3	3	0	9	19	14	5	-2	-6	-3	17	70	0
17	0	53	1	9	28	25	11	9	8	-2	-2	8	11	1	-5	6	44	0
18	0	19	-2	16	15	-10	-28	-6	12	7	3	5	3	0	0	6	25	0
19	0	2	-2	14	4	-21	-37	-18	3	15	17	10	-3	-4	5	11	12	0
20	0	-4	-2	10	8	-2	-9	-3	6	15	13	1	-12	-6	10	16	5	0
21	0	-6	-4	7	16	17	13	12	13	7	-7	-20	-19	-3	13	19	2	0
22	0	-6	-6	4	16	21	14	6	7	1	-13	-21	-13	2	13	19	2	0
23	0	-5	-6	0	12	16	7	-5	-3	8	10	6	4	7	11	17	3	0
24	0	-3	-5	-1	7	11	7	-4	-5	17	35	33	18	8	8	15	6	0
25	0	-2	-3	-1	2	4	6	3	0	12	27	27	13	4	5	14	8	0
26	0	-2	-3	1	0	-5	-5	4	7	3	3	2	0	1	5	14	10	0
27	0	-2	-3	4	5	-4	-13	-1	8	3	-4	-6	-3	3	7	13	11	0
28	0	-2	-4	6	16	15	3	-2	0	4	5	2	2	9	10	13	11	0
29	0	-2	-4	5	25	39	35	9	-6	1	9	3	3	12	13	14	11	0
30	0	-2	-2	3	22	42	46	19	0	3	0	-12	-7	10	13	14	11	0
31	0	-2	0	1	7	15	17	10	12	12	-7	-25	-14	7	10	15	10	0
32	0	-2	2	1	-3	-14	-24	-13	9	13	-5	-13	0	8	5	15	8	0
33	0	-3	3	3	0	-13	-29	-18	0	4	5	19	27	11	1	16	6	0
34	0	-5	1	5	16	17	10	9	6	1	21	48	46	12	0	17	2	0
35	0	-7	0	4	24	40	42	30	16	10	30	51	40	7	2	19	0	0
36	0	-10	2	1	14	27	25	12	9	14	24	29	17	1	7	20	-4	0

TABLE A-14

Mt. Wilson Line-of-Sight Magnetic field measurements for Carrington Rotation 1663 used in solution Type I. Units are Gauss with values meaned within a 10° x 10° equiangular grid.

1	0	-15	-17	5	8	3	16	-55	9	9	34	2	4	14	12	10	75	0
2	0	7	0	5	-1	6	-16	34	7	14	10	-8	-3	9	3	20	17	0
3	0	10	11	16	7	9	24	36	5	19	18	3	3	15	6	-1	-31	0
4	0	1	1	0	8	-2	10	-17	8	12	0	-5	1	42	26	0	0	0
5	0	0	0	0	0	0	0	0	0	0	0	0	0	0	0	0	0	0
6	0	0	0	0	0	0	0	0	0	0	0	0	0	0	0	0	0	0
7	0	0	0	0	0	0	0	0	0	0	0	0	0	0	0	0	0	0
8	0	0	0	0	0	0	0	0	0	0	0	0	0	0	0	0	0	0
9	0	0	0	0	0	0	0	0	0	0	0	0	0	0	0	0	0	0
10	0	0	0	0	0	0	0	0	0	0	0	0	0	0	0	0	0	0
11	0	0	0	0	0	0	0	0	0	0	0	0	0	0	0	0	0	0
12	0	0	0	0	0	0	0	0	0	0	0	0	0	0	0	0	0	0
13	0	0	0	0	0	0	0	0	0	0	0	0	0	0	0	0	0	0
14	0	0	0	0	0	0	0	0	0	0	0	0	0	0	0	0	0	0
15	0	0	0	0	0	0	0	0	0	0	0	0	0	0	0	0	0	0
16	0	243	-18	11	-8	-5	5	16	0	15	23	0	-1	17	-36	-9	107	0
17	0	25	-9	5	6	-5	6	4	3	0	4	11	6	15	3	23	36	0
18	0	-144	-7	-1	4	0	6	1	6	0	9	6	-4	-4	12	6	22	0
19	0	-28	13	5	10	6	-106	0	9	6	27	13	1	5	12	-3	1	0
20	0	18	-4	7	10	13	2	5	8	7	11	4	-14	-18	8	0	38	0
21	0	15	-5	1	10	13	14	8	12	11	0	-23	-16	-18	5	20	9	0
22	0	-22	-5	6	13	14	12	-1	5	6	-13	-60	-6	0	18	8	-2	0
23	0	45	-17	5	5	19	19	-6	-1	3	21	20	3	17	20	19	-11	0
24	0	52	0	0	10	6	6	-1	4	0	63	34	16	8	7	17	-8	0
25	0	6	6	6	6	10	-5	1	5	6	19	22	-1	-12	4	3	-10	0
26	0	-17	-11	9	1	1	-10	5	5	11	16	-9	4	4	14	16	6	0
27	0	-18	7	5	10	11	-5	7	2	-3	0	-3	6	9	8	17	4	0
28	0	0	-8	0	7	15	-1	0	0	6	6	8	1	3	3	6	2	0
29	0	-6	-14	6	4	24	16	0	4	2	-2	2	-17	12	5	3	1	0
30	0	10	-8	8	4	48	79	10	4	4	-20	-4	-11	15	10	10	22	0
31	0	6	0	10	5	-1	35	6	7	11	31	-8	3	21	11	8	31	0
32	0	5	-6	4	10	-2	-108	3	3	10	-25	-84	12	7	9	17	10	0
33	0	-1	-3	4	14	11	-12	0	9	2	17	73	2	7	7	20	1	0
34	0	-12	-1	5	11	26	-7	-2	4	0	-21	60	53	15	13	19	30	0
35	0	-4	-1	1	12	26	45	49	10	5	82	38	38	15	14	7	-16	0
36	0	5	-4	2	7	12	17	33	11	10	12	16	10	0	11	26	-9	0

TABLE A-15

Mean Deviation for the fifth iteration of solution Type II for Carrington Rotation 1620. Units are Gauss with values meaned within a 10° x 10° equiangular grid.
σ = .963

	-80	-70	-60	-50	-40	-30	-20	-10	0	10	20	30	40	50	60	70	80	90
1	0	32	10	0	-3	-2	4	16	-7	2	6	0	3	-1	1	4	-5	0
2	0	-3	0	11	-6	2	-3	6	8	-5	-24	-2	7	-1	1	-2	6	0
3	0	3	7	4	-10	-1	0	-26	0	11	1	0	-4	-3	2	-3	-5	0
4	0	-12	-1	-1	-1	-3	7	5	-7	4	8	1	-3	2	6	2	1	0
5	0	-16	8	-1	9	3	-1	20	-4	-7	2	0	2	1	3	6	1	0
6	0	-17	-6	-2	2	-2	-14	11	2	-7	-9	1	0	0	1	-1	0	0
7	0	-13	-5	-3	-1	0	-5	-5	10	6	1	-4	-4	-4	-8	-6	3	0
8	0	6	-8	-6	-9	5	5	-28	0	1	6	-3	2	0	-3	2	-9	0
9	0	-23	2	-13	2	-3	11	19	-23	0	25	1	1	4	-1	-2	-8	0
10	0	-25	-7	4	0	-3	-3	0	2	0	0	-9	0	8	-1	-17	-9	0
11	0	-27	1	0	8	2	-21	-12	-14	5	17	-3	-3	7	0	-5	3	0
12	0	2	-1	-9	4	0	-4	20	-1	24	-5	-8	-1	-5	0	0	2	0
13	0	27	18	2	4	6	4	8	4	-33	12	10	6	1	9	5	0	0
14	0	20	11	1	-1	11	-2	-6	-2	0	-2	-4	-2	-3	-1	5	7	0
15	0	-16	6	3	-8	1	-6	12	1	6	6	-5	-1	0	-1	4	5	0
16	0	19	2	-5	0	-3	-8	0	0	11	-5	-5	3	4	-3	3	11	0
17	0	0	4	-1	-5	1	18	-11	-8	-13	-6	5	7	-1	3	14	15	0
18	0	0	13	7	-3	6	4	-15	44	-1	3	9	0	0	0	0	6	0
19	0	4	-9	0	-4	-4	-2	-16	9	-6	-3	0	1	-6	-1	-7	3	0
20	0	21	0	0	6	-5	9	-13	-16	-3	3	-2	-2	-1	1	-6	5	0
21	0	6	1	4	8	-6	-3	15	2	2	11	0	-1	2	1	10	0	0
22	0	1	-3	0	4	5	-5	1	6	-11	-1	-6	-1	5	0	0	-21	0
23	0	-23	-4	-8	-2	2	-1	7	7	-4	8	4	0	3	0	-10	2	0
24	0	0	0	-1	-5	0	3	-28	-11	0	5	1	1	0	0	0	-3	0
25	0	0	0	2	-10	0	4	23	4	4	0	-10	-3	0	0	-14	0	0
26	0	0	0	3	1	-4	-1	-3	-5	0	-3	-1	1	-6	0	2	-2	0
27	0	0	0	-6	0	-3	0	2	0	0	-6	6	2	-3	-3	-2	-6	0
28	0	0	0	5	12	-1	-1	-1	-2	0	2	7	0	6	-5	8	2	0
29	0	0	0	7	7	4	-4	13	3	1	-2	0	0	5	0	7	3	0
30	0	-10	-12	-3	-5	0	-2	-2	-5	0	-8	-7	-9	1	2	-2	-3	0
31	0	7	2	-3	-7	2	3	0	0	0	6	6	-1	13	0	-8	-4	0
32	0	3	-1	0	-3	-2	-1	9	-4	-2	6	3	0	1	5	13	9	0
33	0	-4	-4	-1	0	5	-7	5	-2	0	0	-4	5	-3	0	-2	0	0
34	0	3	9	1	0	15	-8	6	8	-5	-2	-6	-1	-7	-5	-14	-4	0
35	0	7	4	3	-6	2	3	-6	5	-2	-5	5	1	-4	0	4	-2	0
36	0	11	2	0	-1	-6	8	-28	4	0	3	5	0	0	-1	4	5	0

TABLE A-16

RMS Deviation for the fifth iteration of solution Type II for Carrington Rotation 1620. Units are Gauss with values meaned within a 10° x 10° equiangular grid.

	-80	-70	-60	-50	-40	-30	-20	-10	0	10	20	30	40	50	60	70	80	90
1	8	32	10	4	3	4	9	20	8	3	7	5	6	1	5	4	5	0
2	0	3	0	11	6	6	7	6	9	17	25	2	8	1	4	2	6	0
3	0	3	7	4	10	7	7	26	3	11	3	0	4	3	5	3	5	0
4	0	12	1	3	1	5	10	7	7	4	10	8	3	2	8	2	1	0
5	0	16	8	2	9	4	12	29	5	13	3	4	5	1	6	6	1	0
6	0	17	6	9	2	4	14	12	2	9	9	6	4	0	2	1	0	0
7	0	13	5	3	1	1	6	5	10	7	6	6	4	4	8	6	3	0
8	0	6	8	9	9	7	5	28	10	4	6	10	4	0	4	0	9	0
9	0	23	2	13	2	7	21	19	23	0	32	4	3	4	1	2	8	0
10	0	25	7	12	0	5	19	0	30	0	0	11	1	8	1	17	9	0
11	0	27	1	4	8	5	21	12	16	5	17	5	3	7	3	5	3	0
12	0	2	1	10	4	2	8	20	19	24	5	8	5	5	2	0	2	0
13	0	27	18	2	4	7	4	8	6	36	12	10	7	1	11	5	0	0
14	0	20	11	1	1	13	4	15	5	2	6	5	7	3	3	5	7	0
15	0	16	6	3	8	4	10	12	6	10	15	5	2	0	3	4	5	0
16	0	19	2	7	0	5	9	9	6	13	6	12	4	4	4	3	11	0
17	0	0	4	2	5	10	19	16	15	13	6	6	8	1	5	14	15	0
18	0	0	13	8	3	7	5	15	44	4	3	0	0	0	0	0	0	0
19	0	4	9	2	4	5	3	17	10	6	4	0	2	6	1	7	3	0
20	0	21	0	7	6	7	14	21	16	5	7	6	2	1	2	6	5	0
21	0	6	1	6	8	8	7	22	13	3	12	9	3	2	1	10	0	0
22	0	1	3	8	4	5	6	5	12	12	5	8	5	5	0	0	21	0
23	0	23	4	10	2	2	6	18	9	9	11	4	3	3	4	10	2	0
24	0	0	0	1	5	0	3	28	19	10	7	6	1	0	6	0	3	0
25	0	0	0	2	10	7	5	30	6	7	1	12	4	0	1	14	0	0
26	0	0	0	3	1	4	5	4	7	3	6	2	4	6	3	2	2	0
27	0	0	0	6	0	4	4	3	5	3	7	6	4	3	3	2	6	0
28	0	0	0	5	12	5	5	4	3	3	3	7	1	6	5	8	2	0
29	0	0	0	7	7	4	10	14	5	3	2	0	1	5	2	7	3	0
30	0	10	12	3	5	1	4	3	5	5	8	7	11	1	8	2	3	0
31	0	7	2	5	7	5	7	2	3	3	8	11	3	13	4	8	4	0
32	0	3	1	0	3	4	8	9	6	8	6	5	4	1	6	13	9	0
33	0	4	4	2	0	5	10	15	11	6	6	7	6	3	1	2	0	0
34	0	3	9	1	0	16	15	20	8	7	2	6	1	7	7	14	4	0
35	0	7	4	9	6	2	11	6	6	6	5	7	1	4	1	4	2	0
36	0	11	2	2	1	9	13	28	5	0	4	6	5	0	3	4	5	0

TABLE A-17

Distribution of observations (multiplied by ten) for Carrington Rotation 1620 used in the fifth iteration of solution Type II meaned within a 10° x 10° equiangular grid.

1	0	10	10	20	10	20	30	20	30	30	20	20	30	10	20	10	10	0
2	0	10	10	20	10	20	30	20	30	30	20	20	30	10	20	10	10	0
3	0	10	10	20	10	20	30	20	30	30	20	20	30	10	20	10	10	0
4	0	10	10	20	10	20	30	20	30	30	20	20	30	10	20	10	10	0
5	0	10	10	20	10	20	30	20	30	30	20	20	30	10	20	10	10	0
6	0	10	10	20	10	20	30	20	30	30	20	20	30	0	20	10	10	0
7	0	10	10	20	10	20	30	20	30	30	20	20	30	10	20	10	10	0
8	0	10	10	20	10	20	30	20	30	30	20	20	30	10	20	10	10	0
9	0	10	10	20	10	20	30	10	20	0	20	20	30	10	20	10	10	0
10	0	10	10	20	10	20	30	0	20	0	0	20	30	10	20	10	10	0
11	0	10	10	20	10	20	30	10	20	10	10	20	30	10	20	10	10	0
12	0	10	10	20	10	20	30	10	30	20	10	20	30	10	20	10	10	0
13	0	10	10	20	10	20	30	20	30	20	20	20	30	10	20	10	10	0
14	0	10	10	20	10	20	20	20	30	30	20	20	30	10	20	10	10	0
15	0	10	10	20	10	20	30	10	30	30	20	20	30	10	20	10	10	0
16	0	10	10	20	10	20	20	20	30	30	20	20	30	10	20	10	10	0
17	0	0	10	20	10	20	30	20	30	30	20	20	30	10	20	10	10	0
18	0	0	10	20	10	20	30	20	20	30	20	0	0	0	0	0	0	0
19	0	10	10	20	10	20	30	20	30	20	20	20	30	10	20	10	10	0
20	0	10	10	20	10	20	30	20	10	30	20	20	30	10	20	10	10	0
21	0	10	10	20	10	20	30	20	20	30	20	20	30	10	20	10	10	0
22	0	10	10	20	10	20	30	20	30	30	20	20	30	10	20	10	10	0
23	0	10	10	20	10	20	30	20	30	30	20	20	30	10	20	10	10	0
24	0	0	0	10	10	20	30	20	30	30	20	20	30	10	20	10	10	0
25	0	0	0	10	10	20	30	20	30	30	20	20	30	10	20	10	10	0
26	0	0	0	10	10	20	30	20	30	30	20	20	30	10	20	10	10	0
27	0	0	0	10	10	20	30	20	30	30	20	20	30	10	20	10	10	0
28	0	0	0	10	10	20	30	20	30	30	20	20	30	10	20	10	10	0
29	0	0	0	10	10	20	30	20	30	30	20	20	30	10	20	10	10	0
30	0	10	10	20	10	20	30	20	30	30	10	20	30	10	20	10	10	0
31	0	10	10	20	10	20	30	20	30	30	20	20	30	10	20	10	10	0
32	0	10	10	20	10	20	30	20	30	30	20	20	30	10	20	10	10	0
33	0	10	10	20	10	20	30	20	30	30	20	20	30	10	20	10	10	0
34	0	10	10	20	10	20	30	20	30	20	20	20	30	10	20	10	10	0
35	0	10	10	20	10	20	30	20	30	30	20	20	30	10	20	10	10	0
36	0	10	10	20	10	20	30	20	30	20	20	20	30	10	20	10	10	0

TABLE A-18

Computed Line-of-Sight Magnetic field measurements from the fifth iteration of solution Type II for Carrington Rotation 1620. Units are Gauss with values meaned within a 10° x 10° grid.

	-80	-70	-60	-50	-40	-30	-20	-10	0	10	20	30	40	50	60	70	80	90
1	0	-5	-15	-5	13	22	16	7	8	10	6	4	6	9	12	17	18	0
2	0	-6	-14	-4	10	18	18	15	14	13	10	10	11	10	11	17	18	0
3	0	-8	-13	-3	7	15	19	16	8	1	5	12	15	10	10	17	17	0
4	0	-9	-11	-2	6	13	23	26	14	0	2	12	15	10	10	17	17	0
5	0	-10	-9	0	5	12	29	41	34	16	11	14	13	8	10	18	17	0
6	0	-10	-7	0	3	9	26	42	43	30	20	15	9	0	10	18	17	0
7	0	-9	-5	-1	1	5	15	25	27	24	19	12	6	5	11	19	16	0
8	0	-8	-4	-3	-1	3	12	14	12	13	13	9	4	4	11	20	17	0
9	0	-6	-4	-6	-5	3	20	25	18	0	13	10	3	3	11	20	17	0
10	0	-5	-3	-8	-8	2	27	0	32	0	0	9	3	2	10	20	17	0
11	0	-4	-3	-8	-10	-2	21	37	31	22	8	4	2	2	9	19	18	0
12	0	-4	-4	-5	-8	-5	10	24	24	8	1	3	4	4	9	18	17	0
13	0	-4	-4	-1	-1	-3	4	18	22	11	5	8	10	8	10	17	17	0
14	0	-4	-5	2	7	3	0	13	23	20	14	15	15	12	12	17	17	0
15	0	-4	-6	6	13	8	-4	1	12	18	14	13	14	14	14	17	16	0
16	0	-4	-6	6	15	9	-8	-17	-3	8	7	5	8	13	15	17	16	0
17	0	0	-5	4	12	8	-9	-18	-8	5	5	1	3	10	15	18	16	0
18	0	0	-3	1	6	7	1	-2	0	8	9	0	0	0	0	0	0	0
19	0	-2	-1	-1	0	6	14	15	9	9	11	10	5	6	12	18	17	0
20	0	-2	0	-1	-2	2	19	25	11	7	11	12	7	4	10	19	18	0
21	0	-3	3	1	-3	0	15	27	20	9	8	10	6	3	9	19	19	0
22	0	-4	5	5	0	-2	8	21	19	8	5	5	3	2	9	19	19	0
23	0	-5	6	9	3	-1	2	10	9	2	1	3	2	3	9	19	19	0
24	0	0	0	10	5	0	2	4	2	0	3	5	4	4	10	19	19	0
25	0	0	0	9	4	1	6	9	6	5	7	8	4	5	11	20	19	0
26	0	0	0	5	0	-2	7	16	13	9	7	5	2	5	12	20	19	0
27	0	0	0	2	-4	-8	2	12	10	4	0	0	0	5	13	20	19	0
28	0	0	0	1	-6	-12	-6	2	1	-2	-3	-2	1	6	13	19	19	0
29	0	0	0	3	-3	-11	-11	-4	-1	-1	0	2	5	8	13	19	19	0
30	0	-2	2	6	2	-6	-12	-4	4	5	5	6	8	9	12	18	19	0
31	0	-2	-1	7	8	0	-12	-4	10	11	5	4	7	9	12	18	19	0
32	0	-3	-5	7	13	3	-13	-8	10	15	6	2	5	9	12	18	19	0
33	0	-3	-9	5	16	8	-15	-16	3	14	7	2	5	10	13	18	19	0
34	0	-3	-12	2	17	13	-13	-25	-11	6	5	3	6	10	13	18	18	0
35	0	-3	-14	0	17	19	-4	-25	-20	-5	-1	0	5	10	13	18	18	0
36	0	-4	-15	-3	16	23	7	-10	-10	-3	-1	-1	4	10	13	18	18	0

TABLE A-19

Mt. Wilson Line-of-Sight Magnetic field measurements for Carrington Rotation 1620 used in the fifth iteration of solution Type II. Units are Gauss with values meaned within a 10° x 10° equiangular grid.

1	0	26	-5	-5	9	20	21	23	0	12	13	4	10	8	13	22	13	0
2	0	-10	-14	6	4	21	15	21	23	7	-13	7	18	8	12	15	25	0
3	0	-4	-5	1	-2	13	19	-9	9	12	6	12	10	6	12	13	12	0
4	0	-22	-12	-3	5	10	31	31	6	4	11	14	11	12	16	20	19	0
5	0	-26	-1	-2	15	16	28	61	30	9	13	13	16	10	14	24	18	0
6	0	-27	-13	-2	6	7	11	53	45	23	11	17	10	0	11	17	17	0
7	0	-22	-11	-4	0	5	10	19	38	31	20	8	1	1	2	12	20	0
8	0	-1	-13	-9	-11	8	17	-13	12	15	19	6	6	4	7	20	7	0
9	0	-30	-2	-19	-2	0	32	45	-5	0	39	11	5	8	9	17	8	0
10	0	-31	-11	-4	-7	-1	23	0	34	0	0	0	2	11	8	2	8	0
11	0	-32	-1	-7	-2	0	0	25	16	27	25	0	0	9	8	14	21	0
12	0	-1	-5	-15	-3	-5	6	45	22	32	-4	-5	3	-1	8	19	20	0
13	0	23	13	0	2	3	8	27	27	-21	17	18	17	10	19	23	17	0
14	0	15	5	3	6	15	-1	6	20	19	11	10	13	8	10	22	25	0
15	0	-21	0	9	5	10	-10	13	13	25	21	8	12	14	12	21	22	0
16	0	15	-3	0	14	5	-16	-16	-4	19	2	0	11	17	12	21	27	0
17	0	0	-1	3	7	9	8	-30	-16	-8	0	7	11	9	18	32	32	0
18	0	0	10	8	3	13	6	-17	45	6	12	0	0	0	0	0	0	0
19	0	2	-10	0	-3	1	12	-1	19	2	8	10	7	0	10	11	21	0
20	0	18	1	0	3	-2	28	11	-4	4	14	10	5	3	12	12	23	0
21	0	2	4	5	5	-7	12	42	22	11	19	11	4	5	10	30	18	0
22	0	-3	1	5	3	2	2	23	26	-3	3	0	1	7	8	20	-1	0
23	0	-28	2	1	0	0	1	18	16	-1	10	7	2	6	9	9	22	0
24	0	0	0	8	0	0	5	-23	-9	0	8	6	5	3	11	18	16	0
25	0	0	0	11	-5	0	11	33	11	9	7	-2	0	5	12	5	20	0
26	0	0	0	9	1	-6	6	12	8	9	4	3	4	0	13	22	17	0
27	0	0	0	-3	-3	-12	1	14	10	3	-5	6	2	2	10	17	12	0
28	0	0	0	7	5	-14	-8	1	-1	-3	0	5	0	13	7	28	21	0
29	0	0	0	11	4	-6	-16	9	2	0	-2	3	5	13	13	26	23	0
30	0	-12	-9	3	-2	-5	-14	-6	-1	4	-3	-1	-1	10	15	15	15	0
31	0	4	0	4	1	1	-8	-5	10	12	12	11	6	22	13	10	14	0
32	0	0	-6	7	9	1	-15	1	6	12	12	5	4	10	18	32	28	0
33	0	-7	-13	3	16	13	-23	-11	0	15	8	-1	10	6	13	16	19	0
34	0	0	-2	3	17	28	-21	-19	-3	0	3	-3	5	3	8	3	13	0
35	0	3	-10	2	11	21	0	-31	-15	-8	-6	5	6	6	13	23	16	0
36	0	6	-12	-4	15	16	16	-38	-6	-3	1	3	4	9	12	22	23	0

TABLE A-20

Mean Deviation for the fifth iteration of solution Type II for Carrington Rotation 1625. Units are Gauss with values meaned within a 10° x 10° equiangular grid.
σ = .799

	-80	-70	-60	-50	-40	-30	-20	-10	0	10	20	30	40	50	60	70	80	90
1	0	1	8	5	-10	4	3	-2	2	6	0	-13	-2	-7	5	-4	0	0
2	0	-5	0	-8	-2	2	-5	0	3	0	-5	0	-1	2	1	-5	-4	0
3	0	11	-4	-3	-3	3	3	0	0	-6	-3	10	7	-3	4	5	0	0
4	0	9	4	5	-6	-1	0	-5	0	8	-4	5	-1	0	-5	1	9	0
5	0	-4	0	7	9	1	3	-5	-1	0	-5	-3	-3	3	2	4	11	0
6	0	6	0	-5	2	-5	2	8	2	4	-1	-1	-1	8	0	-3	5	0
7	0	-9	1	7	-1	-1	0	-10	-2	4	2	2	6	-4	0	0	9	0
8	0	-4	3	-4	-4	0	-2	0	-5	-2	-2	-6	2	-10	2	-3	0	0
9	0	-20	0	-1	0	-2	5	10	5	3	-5	-1	2	5	5	2	0	0
10	0	-12	-11	-4	9	-3	0	-6	-2	2	0	4	-6	-15	3	-1	0	0
11	0	-1	2	-5	1	-3	0	-5	-1	-1	-4	7	1	0	3	0	-13	0
12	0	1	-8	-1	3	2	-4	4	3	-8	0	3	-3	-2	0	-9	0	0
13	0	-10	-1	3	3	6	1	2	0	10	0	-5	-2	10	0	-2	0	0
14	0	-21	0	-4	-7	-7	3	-11	-7	1	0	0	2	0	-2	-2	0	0
15	0	-1	4	2	-11	4	0	8	-1	2	0	1	4	-5	0	-9	0	0
16	0	0	-2	-5	-10	2	-9	1	-3	1	-8	-1	-10	-7	-3	-4	0	0
17	0	12	9	11	3	9	3	3	2	8	3	0	5	2	4	3	3	0
18	0	3	12	1	5	0	1	-4	0	-3	-6	3	1	1	9	7	9	0
19	0	14	8	-5	-14	-5	-3	-3	-1	0	-5	4	-4	7	0	11	0	0
20	0	3	10	3	6	8	1	2	5	7	2	2	0	-5	-4	6	0	0
21	0	-2	3	-1	3	-1	0	-2	2	-2	-9	0	2	-4	0	-1	0	0
22	0	8	-4	-3	-3	0	0	2	-4	6	-2	0	0	3	-3	-5	0	0
23	0	-25	-6	-3	5	3	0	-20	-5	0	7	-3	1	-8	-5	-1	0	0
24	0	0	8	-4	0	0	2	26	4	2	-3	-2	1	-2	6	3	0	0
25	0	6	-2	0	-6	0	-4	-7	-4	11	-4	-2	6	1	5	-4	0	0
26	0	1	-11	5	-3	-5	3	-10	-7	-14	-11	-3	-1	-8	5	-2	0	0
27	0	-10	7	8	0	-1	2	14	3	22	5	9	-1	5	-6	-3	0	0
28	0	-8	-1	-3	1	3	0	8	0	-17	10	-1	-2	-1	4	-3	0	0
29	0	-2	-5	-1	-1	-1	-1	-19	-4	11	-26	-14	4	-2	3	2	7	0
30	0	0	-9	-1	1	-3	0	11	1	2	7	8	4	-5	-2	-3	-20	0
31	0	-7	8	-6	-10	0	1	1	-10	26	-1	-1	0	4	-1	3	29	0
32	0	16	1	5	1	5	7	3	10	-25	2	-6	-1	-3	-3	-10	-24	0
33	0	-1	5	-5	10	1	-2	-32	4	6	4	-4	0	-4	6	12	9	0
34	0	12	0	4	10	1	-6	31	3	0	7	2	2	-6	-8	-1	-34	0
35	0	6	9	0	1	2	-7	3	-4	-8	0	-1	-3	2	0	2	0	0
36	0	9	5	-3	4	11	-3	0	0	-3	12	2	4	1	-2	-4	0	0

TABLE A-21

RMS Deviation for the fifth iteration of solution Type II for Carrington Rotation 1625. Units are Gauss with values meaned within a 10° x 10° equiangular grid.

	-80	-70	-60	-50	-40	-30	-20	-10	0	10	20	30	40	50	60	70	80	90
1	0	1	8	5	10	4	4	3	4	8	2	13	7	7	5	4	0	0
2	0	5	0	8	2	3	6	0	7	4	5	1	4	2	4	5	4	0
3	0	11	4	3	3	3	4	2	2	10	8	10	8	3	9	5	0	0
4	0	9	4	6	6	1	2	5	5	9	5	6	4	0	5	1	9	0
5	0	4	0	10	9	6	4	7	5	1	5	4	3	3	5	4	11	0
6	0	6	0	5	2	5	6	9	3	4	5	5	7	8	2	3	5	0
7	0	9	1	8	1	2	3	14	3	5	4	3	7	4	0	0	9	0
8	0	4	3	4	4	7	3	0	5	3	2	6	5	10	5	3	0	0
9	0	20	0	1	0	2	6	10	6	4	7	5	3	5	6	2	0	0
10	0	12	11	5	9	5	0	6	6	7	1	4	7	15	3	1	0	0
11	0	1	2	6	1	3	5	5	8	6	7	7	4	0	5	0	13	0
12	0	1	8	2	3	4	7	6	5	8	1	3	4	2	3	9	0	0
13	0	10	1	3	3	7	2	3	2	14	0	6	3	10	1	2	0	0
14	0	21	0	7	7	8	6	12	8	3	0	0	5	0	4	2	0	0
15	0	1	4	5	11	4	4	9	2	5	1	8	6	5	1	9	0	0
16	0	0	2	6	10	4	9	6	4	5	10	2	11	7	3	4	0	0
17	0	12	9	11	3	10	4	4	2	8	3	0	5	2	4	3	3	0
18	0	3	12	3	5	2	3	5	4	3	6	5	2	1	9	7	9	0
19	0	14	8	5	14	5	5	3	2	1	5	5	4	7	2	11	0	0
20	0	3	10	3	6	8	6	3	6	7	4	2	3	5	6	6	0	0
21	0	2	3	2	3	1	1	2	3	4	9	0	5	4	4	1	0	0
22	0	8	4	3	3	2	7	2	4	6	3	3	4	3	3	5	0	0
23	0	25	6	3	5	3	4	24	7	4	7	6	2	8	6	1	0	0
24	0	0	8	6	0	3	3	33	5	6	6	9	3	2	9	3	0	0
25	0	6	2	6	6	1	4	8	5	14	4	2	7	1	6	4	0	0
26	0	1	11	5	3	5	4	12	8	14	12	5	5	8	10	2	0	0
27	0	10	7	8	0	5	7	14	6	23	6	9	8	5	6	3	0	0
28	0	8	1	3	1	4	0	8	8	25	10	4	3	1	4	3	0	0
29	0	2	5	1	1	2	8	20	7	11	27	17	11	2	4	2	7	0
30	0	0	9	2	1	3	2	28	19	11	7	8	5	5	2	3	20	0
31	0	7	8	6	10	0	3	1	18	29	6	4	7	4	2	3	29	0
32	0	16	1	5	1	5	7	7	10	28	3	7	3	3	4	10	24	0
33	0	1	5	5	10	2	4	33	6	6	6	4	1	4	6	12	9	0
34	0	12	0	4	10	2	9	32	5	1	7	4	3	6	8	1	34	0
35	0	6	9	3	1	5	8	3	8	12	0	3	7	2	3	2	0	0
36	0	9	5	3	4	12	6	6	5	6	13	5	6	1	3	4	0	0

TABLE A-22

Distribution of observations (multiplied by ten) for Carrington Rotation 1625 used in the fifth iteration of solution Type II meaned within a 10° x 10° equiangular grid.

1	0	10	10	20	10	20	30	20	30	30	20	20	30	10	20	10	0	0
2	0	10	10	20	10	20	30	20	30	30	20	20	30	10	20	10	10	0
3	0	10	10	20	10	20	30	20	30	30	20	20	30	10	20	10	0	0
4	0	10	10	20	10	20	30	20	30	30	20	20	30	10	20	10	10	0
5	0	10	10	20	10	20	30	20	30	30	20	20	30	10	20	10	10	0
6	0	10	10	20	10	20	30	20	30	30	20	20	30	10	20	10	10	0
7	0	10	10	20	10	20	30	20	30	30	20	20	30	10	20	10	10	0
8	0	10	10	20	10	20	30	20	30	30	20	20	30	10	20	10	0	0
9	0	10	10	20	10	20	30	20	30	30	20	20	30	10	20	10	0	0
10	0	10	10	20	10	20	30	20	30	30	20	20	30	10	20	10	0	0
11	0	10	10	20	10	20	30	20	30	30	20	20	30	10	20	10	10	0
12	0	10	10	20	10	20	30	20	30	30	20	20	30	10	20	10	0	0
13	0	10	10	20	10	20	30	20	30	30	20	20	30	10	20	10	0	0
14	0	10	10	20	10	20	30	20	30	30	20	20	30	10	20	10	0	0
15	0	10	10	20	10	20	30	20	30	30	20	20	30	10	20	10	0	0
16	0	10	10	20	10	20	30	20	30	30	20	20	30	10	20	10	0	0
17	0	10	10	20	10	20	30	20	30	30	20	20	30	10	20	10	10	0
18	0	10	10	20	10	20	30	20	30	30	20	20	30	10	20	10	10	0
19	0	10	10	20	10	20	30	20	30	30	20	20	30	10	20	10	0	0
20	0	10	10	20	10	20	30	20	30	20	20	20	30	10	20	10	0	0
21	0	10	10	20	10	20	30	10	30	30	20	20	30	10	20	10	0	0
22	0	10	10	20	10	20	30	20	30	30	20	20	30	10	20	10	0	0
23	0	10	10	20	10	20	30	20	30	30	20	20	30	10	20	10	0	0
24	0	10	10	20	10	20	30	20	30	30	20	20	30	10	20	10	0	0
25	0	10	10	20	10	20	30	20	30	30	20	20	30	10	20	10	0	0
26	0	10	10	20	10	20	30	20	30	30	20	20	30	10	20	10	0	0
27	0	10	10	20	10	20	30	20	20	30	20	20	30	10	20	10	0	0
28	0	10	10	20	10	20	30	20	30	30	20	20	30	10	20	10	0	0
29	0	10	10	20	10	20	30	20	30	30	20	20	30	10	20	10	10	0
30	0	10	10	20	10	20	30	20	30	30	20	20	30	10	20	10	10	0
31	0	10	10	20	10	20	30	20	30	20	20	20	30	10	20	10	10	0
32	0	10	10	20	10	20	20	20	30	30	20	20	30	10	20	10	10	0
33	0	10	10	20	10	20	30	20	30	30	20	20	30	10	20	10	10	0
34	0	10	10	10	10	20	30	20	30	30	20	20	30	10	20	10	10	0
35	0	10	10	20	10	20	30	20	30	30	20	20	30	10	20	10	0	0
36	0	10	10	20	10	20	30	20	30	30	20	20	30	10	20	10	0	0

TABLE A-23

Computed Line-of-Sight Magnetic field measurements from the fifth iteration of solution Type II for Carrington Rotation 1625. Units are Gauss with values meaned within a 10° x 10° grid.

	-80	-70	-60	-50	-40	-30	-20	-10	0	10	20	30	40	50	60	70	80	90
1	0	-22	-14	-4	1	5	3	-3	-6	-4	-4	-3	1	3	3	7	0	0
2	0	-21	-14	-5	1	7	8	0	-8	-15	-16	-11	0	4	3	6	12	0
3	0	-21	-14	-7	0	6	10	4	-3	-11	-14	-10	0	4	2	6	0	0
4	0	-21	-14	-8	-2	4	10	6	3	3	1	0	2	3	2	5	12	0
5	0	-20	-13	-9	-4	3	9	6	5	11	13	8	4	2	2	6	12	0
6	0	-20	-13	-9	-5	2	11	7	3	8	11	7	2	1	2	6	11	0
7	0	-20	-13	-9	-7	0	11	12	5	3	3	1	0	0	3	7	11	0
8	0	-19	-13	-9	-9	-4	8	15	11	4	1	0	-1	0	3	8	0	0
9	0	-19	-13	-9	-10	-8	3	13	12	5	2	0	0	0	2	8	0	0
10	0	-18	-13	-9	-10	-9	0	8	6	0	-1	0	0	-1	1	9	0	0
11	0	-18	-13	-9	-9	-8	0	5	1	-5	-4	-2	-3	-5	0	9	14	0
12	0	-18	-13	-9	-8	-7	0	6	6	0	-1	-3	-6	-8	-2	10	0	0
13	0	-18	-13	-8	-9	-9	-3	6	13	10	2	-2	-8	-10	-3	10	0	0
14	0	-18	-13	-8	-9	-12	-8	2	11	9	0	-4	-8	-8	-2	9	0	0
15	0	-19	-13	-6	-7	-10	-9	-2	3	0	-6	-6	-4	-3	0	9	0	0
16	0	-20	-13	-4	-4	-5	-4	0	0	-3	-5	-2	1	1	2	9	0	0
17	0	-21	-13	-3	0	1	3	4	3	3	5	5	5	4	4	9	12	0
18	0	-22	-13	-2	2	5	8	7	4	8	12	10	5	4	6	9	11	0
19	0	-22	-13	-2	0	4	9	4	-1	3	8	6	1	2	7	10	0	0
20	0	-21	-12	-4	-2	0	5	0	-8	-3	1	0	-3	1	7	11	0	0
21	0	-20	-12	-6	-8	-6	0	-2	-7	-5	-2	-5	-7	0	7	12	0	0
22	0	-19	-12	-8	-12	-12	-4	0	0	-1	-5	-11	-10	-1	7	11	0	0
23	0	-18	-12	-9	-13	-13	-4	4	8	2	-8	-16	-12	-1	6	11	0	0
24	0	-17	-13	-10	-12	-11	-3	7	12	4	-9	-16	-10	0	4	10	0	0
25	0	-16	-14	-10	-9	-9	-4	3	9	4	-5	-8	-2	1	2	8	0	0
26	0	-16	-15	-9	-7	-9	-9	-4	2	2	0	1	5	3	1	7	0	0
27	0	-16	-15	-8	-7	-11	-14	-8	-2	-2	-3	0	5	3	0	8	0	0
28	0	-16	-15	-8	-7	-12	-13	-3	2	-6	-14	-11	-1	1	1	8	0	0
29	0	-17	-14	-6	-7	-13	-12	1	7	-8	-22	-21	-8	0	2	10	15	0
30	0	-17	-14	-5	-5	-11	-13	-3	1	-8	-19	-18	-7	0	4	10	14	0
31	0	-18	-14	-3	-3	-9	-15	-13	-11	-10	-10	-7	-1	2	6	11	13	0
32	0	-19	-14	-2	0	-4	-10	-17	-18	-12	-4	0	2	4	7	11	12	0
33	0	-20	-14	-2	1	0	-3	-8	-11	-8	-2	0	1	4	7	11	11	0
34	0	-21	-14	-4	1	2	2	1	0	1	0	0	-1	2	6	10	11	0
35	0	-22	-13	-2	1	3	2	2	6	10	7	1	-1	1	5	9	0	0
36	0	-22	-14	-3	1	3	1	-1	1	8	7	3	0	2	4	8	0	0

TABLE A-24

Mt. Wilson Line-of-Sight Magnetic field measurements for Carrington Rotation 1625 used in the fifth iteration of solution Type II. Units are Gauss with values meaned within a 10° x 10° equiangular grid.

1	0	-20	-5	0	-8	9	6	-5	-3	2	-4	-16	-1	-3	8	3	0	0
2	0	-27	-14	-14	-1	9	2	0	-4	-14	-21	-11	-1	7	4	0	7	0
3	0	-9	-18	-10	-3	9	14	5	-4	-17	-17	0	7	1	7	11	0	0
4	0	-11	-9	-2	-9	2	9	0	2	11	-3	5	1	4	-3	7	21	0
5	0	-25	-13	-1	5	5	13	1	3	10	8	5	0	5	4	10	23	0
6	0	-14	-14	-14	-2	-2	13	16	5	12	9	6	0	9	2	3	17	0
7	0	-29	-11	-1	-8	-1	11	1	2	7	6	4	5	-3	3	6	21	0
8	0	-23	-9	-14	-13	-4	6	15	5	2	0	-6	1	-9	5	4	0	0
9	0	-39	-12	-10	-10	-10	8	23	17	9	-3	-1	2	6	8	10	0	0
10	0	-31	-24	-14	0	-12	0	2	3	2	-1	4	-6	-17	4	7	0	0
11	0	-19	-11	-15	-7	-11	0	0	0	-6	-8	4	-2	-5	2	9	0	0
12	0	-16	-22	-10	-5	-5	-4	10	10	-7	-2	0	-10	-10	-2	0	0	0
13	0	-29	-15	-5	-5	-3	-1	9	12	20	2	-8	-11	0	-3	7	0	0
14	0	-40	-13	-12	-17	-19	-5	-9	4	10	0	-4	-5	-8	-4	7	0	0
15	0	-21	-9	-4	-19	-6	-8	6	1	1	-5	-5	0	-9	0	0	0	0
16	0	-21	-15	-10	-14	-2	-14	0	-2	-2	-14	-4	-9	-5	-1	4	0	0
17	0	-9.	-4	.7	3	10	7	8	6	11	8	6	10	8	9	12	15	0
18	0	-18	-1	0	7	4	10	2	4	4	5	13	7	6	15	16	21	0
19	0	-7	-4	-7	-13	-1	5	0	-3	2	3	11	-3	10	8	22	0	0
20	0	-17	-2	0	3	8	7	3	-2	4	4	2	-3	-4	3	18	0	0
21	0	-23	-8	-7	-4	-8	0	-5	-5	-8	-12	-6	-4	-4	7	10	0	0
22	0	-10	-16	-12	-15	-13	-5	3	-4	4	-7	-10	-10	2	4	6	0	0
23	0	-44	-19	-13	-7	-10	-3	-15	2	2	-1	-19	-10	-9	0	9	0	0
24	0	-17	-5	-14	-11	-12	0	34	16	7	-13	-19	-8	-3	11	13	0	0
25	0	-10	-17	-10	-15	-9	-9	-3	5	16	-9	-10	3	2	8	4	0	0
26	0	-15	-27	-4	-11	-14	-6	-14	-5	-11	-11	-1	3	-5	6	5	0	0
27	0	-26	-8	0	-6	-12	-11	6	1	19	1	9	4	8	-5	4	0	0
28	0	-25	-17	-11	-6	-9	-14	4	2	-24	-3	-12	-4	0	5	5	0	0
29	0	-20	-20	-8	-8	-14	-14	-18	2	2	-48	-35	-3	-2	5	12	22	0
30	0	-17	-24	-7	-4	-14	-13	8	3	-6	-11	-9	-3	-5	2	7	-6	0
31	0	-26	-5	-10	-13	-9	-13	-12	-21	15	-11	-9	-1	6	4	14	42	0
32	0	-3	-13	2	1	1	-3	-13	-8	-38	-1	-5	1	1	3	0	-12	0
33	0	-22	-8	-7	11	1	-6	-41	-7	-2	1	-4	2	0	14	23	21	0
34	0	-8	-14	0	12	3	-4	32	3	1	8	1	0	-3	-1	8	-22	0
35	0	-15	-4	-3	3	5	-4	6	2	1	7	0	-4	4	5	12	0	0
36	0	-12	-8	-6	5	14	-2	-2	0	5	20	5	5	3	1	4	0	0

TABLE A-25

Mean Deviation for the fifth iteration of solution Type II for Carrington Rotation 1663. Units are Gauss with values meaned within a 10° x 10° equiangular grid.
σ = 1.192

	-80	-70	-60	-50	-40	-30	-20	-10	0	10	20	30	40	50	60	70	80	90
1	0	-11	-17	5	6	-2	7	29	-2	-1	24	-4	4	13	0	-8	0	0
2	0	12	-4	1	-4	5	-18	28	-8	-3	0	-7	2	4	-15	4	30	0
3	0	14	5	7	-5	0	-6	1	2	0	2	0	1	0	-13	-7	-21	0
4	0	-3	-10	0	10	-4	1	22	-10	0	3	4	-8	14	9	0	0	0
5	0	0	0	0	0	0	0	0	0	0	0	0	0	0	0	0	0	0
6	0	0	0	0	0	0	0	0	0	0	0	0	0	0	0	0	0	0
7	0	0	0	0	0	0	0	0	0	0	0	0	0	0	0	0	0	0
8	0	0	0	0	0	0	0	0	0	0	0	0	0	0	0	0	0	0
9	0	0	0	0	0	0	0	0	0	0	0	0	0	0	0	0	0	0
10	0	0	0	0	0	0	0	0	0	0	0	0	0	0	0	0	0	0
11	0	0	0	0	0	0	0	0	0	0	0	0	0	0	0	0	0	0
12	0	0	0	0	0	0	0	0	0	0	0	0	0	0	0	0	0	0
13	0	0	0	0	0	0	0	0	0	0	0	0	0	0	0	0	0	0
14	0	0	0	0	0	0	0	0	0	0	0	0	0	0	0	0	0	0
15	0	0	0	0	0	0	0	0	0	0	0	0	0	0	0	0	0	0
16	0	0	-20	18	-3	-6	1	14	-9	-3	9	-5	-1	21	-24	-16	29	0
17	0	22	-12	-1	1	-6	3	-1	-1	-3	0	6	0	9	5	19	-14	0
18	0	0	-9	-9	0	2	6	-4	2	-2	3	0	-6	-8	7	0	-7	0
19	0	-30	13	-1	5	8	-33	5	6	-8	7	2	4	7	5	-14	-14	0
20	0	16	0	2	0	8	4	5	0	-9	0	5	-1	-11	0	-14	30	0
21	0	11	1	-2	-4	-1	3	-3	0	6	7	-6	0	-12	-4	3	6	0
22	0	-25	4	2	-2	-4	-2	-9	0	5	-8	-31	3	1	6	-9	-3	0
23	0	42	-8	2	-9	2	10	-3	3	-6	2	4	-1	13	9	1	-12	0
24	0	0	7	-3	0	-3	0	1	9	-15	28	2	2	3	-2	0	-10	0
25	0	6	12	2	1	7	-9	-2	2	-4	-3	0	-12	-17	-4	-12	-14	0
26	0	-17	-7	3	-2	4	-6	0	-2	7	12	-14	1	0	5	1	1	0
27	0	-16	10	-2	3	13	3	9	-3	-6	0	-1	6	5	0	2	-2	0
28	0	1	-5	-7	-6	2	-4	3	-1	1	3	9	1	-1	-5	-7	-5	0
29	0	-3	-10	0	-13	-5	-11	-7	8	-2	-8	3	-15	7	-2	-9	-7	0
30	0	12	-4	4	-11	15	8	-5	3	-4	3	0	-6	9	2	-1	13	0
31	0	7	3	8	-2	-18	13	-1	0	-4	25	0	7	12	3	-2	23	0
32	0	6	-4	2	7	-3	-45	9	-3	-2	-23	0	8	-7	0	6	3	0
33	0	-1	0	0	6	10	0	10	5	0	28	-30	-15	-13	0	9	-2	0
34	0	-12	2	0	-6	6	-14	-5	-1	-1	-21	26	40	-5	6	6	30	0
35	0	-4	3	-2	-9	-6	5	10	1	-3	27	6	3	0	7	-8	-13	0
36	0	7	-1	1	-6	-11	-6	-37	2	0	-7	-10	-9	-7	2	8	-1	0

TABLE A-26

RMS Deviation for the fifth iteration of solution Type II for Carrington Rotation 1663. Units are Gauss with values meaned within a 10° x 10° equiangular grid.

	-80	-70	-60	-50	-40	-30	-20	-10	0	10	20	30	40	50	60	70	80	90
1	9	11	17	5	6	4	29	29	6	2	25	5	4	13	2	8	0	0
2	0	12	4	7	4	5	28	31	11	4	3	7	3	4	16	4	30	0
3	0	14	5	7	5	4	8	1	2	6	8	8	3	0	22	7	21	0
4	0	3	10	0	10	5	14	22	15	9	18	5	13	14	11	0	0	0
5	0	0	0	0	0	0	0	0	0	0	0	0	0	0	0	0	0	0
6	0	0	0	0	0	0	0	0	0	0	0	0	0	0	0	0	0	0
7	0	0	0	0	0	0	0	0	0	0	0	0	0	0	0	0	0	0
8	0	0	0	0	0	0	0	0	0	0	0	0	0	0	0	0	0	0
9	0	0	0	0	0	0	0	0	0	0	0	0	0	0	0	0	0	0
10	0	0	0	0	0	0	0	0	0	0	0	0	0	0	0	0	0	0
11	0	0	0	0	0	0	0	0	0	0	0	0	0	0	0	0	0	0
12	0	0	0	0	0	0	0	0	0	0	0	0	0	0	0	0	0	0
13	0	0	0	0	0	0	0	0	0	0	0	0	0	0	0	0	0	0
14	0	0	0	0	0	0	0	0	0	0	0	0	0	0	0	0	0	0
15	0	0	0	0	0	0	0	0	0	0	0	0	0	0	0	0	0	0
16	0	0	20	21	3	6	5	14	18	13	18	15	2	21	24	16	29	0
17	0	22	12	3	1	7	3	8	3	8	10	7	3	9	17	19	14	0
18	0	0	9	12	0	4	8	5	4	2	3	10	6	8	8	0	7	0
19	0	30	13	1	5	8	34	6	7	9	14	4	10	7	7	14	14	0
20	0	16	0	2	0	11	5	7	5	9	2	6	17	11	6	14	30	0
21	0	11	1	6	4	4	5	7	2	6	10	6	14	12	4	3	6	0
22	0	25	4	4	2	7	5	10	3	6	10	31	5	1	6	9	3	0
23	0	42	8	2	9	4	20	9	3	7	16	5	4	13	14	1	12	0
24	0	0	7	5	0	3	7	2	10	17	34	10	2	3	3	0	10	0
25	0	6	12	3	1	8	9	5	4	7	4	1	12	17	6	12	14	0
26	0	17	7	3	2	4	8	5	3	7	12	15	11	0	7	1	1	0
27	0	16	10	6	3	13	6	10	6	8	0	10	8	5	2	2	2	0
28	0	1	5	7	6	2	4	5	2	3	3	9	4	1	7	7	5	0
29	0	3	10	2	13	9	14	13	8	5	8	6	16	7	10	9	7	0
30	0	12	4	5	11	35	33	7	5	7	3	3	15	9	7	1	13	0
31	0	7	3	8	2	22	23	4	2	4	25	7	8	12	6	2	23	0
32	0	6	4	9	7	12	45	9	7	4	29	0	13	7	2	6	3	0
33	0	1	0	0	6	10	2	11	6	5	34	30	19	13	0	9	2	0
34	0	12	2	0	6	8	23	6	3	1	21	26	40	5	7	6	30	0
35	0	4	3	2	9	16	13	10	3	8	27	7	21	0	7	8	13	0
36	0	7	1	5	6	12	22	37	7	0	11	11	10	7	3	8	1	0

TABLE A-27

Distribution of observations (multiplied by ten) for Carrington Rotation 1663 used in the fifth iteration of solution Type II meaned within a 10° x 10° equiangular grid.

1	0	10	10	20	10	20	30	10	30	30	20	20	20	10	20	10	0	0
2	0	10	10	20	10	20	30	20	30	30	20	20	30	10	20	10	10	0
3	0	10	10	20	10	20	20	10	30	30	20	20	30	10	20	10	10	0
4	0	10	10	20	10	20	30	10	30	30	20	20	30	10	20	0	0	0
5	0	0	0	0	0	0	0	0	0	0	0	0	0	0	0	0	0	0
6	0	0	0	0	0	0	0	0	0	0	0	0	0	0	0	0	0	0
7	0	0	0	0	0	0	0	0	0	0	0	0	0	0	0	0	0	0
8	0	0	0	0	0	0	0	0	0	0	0	0	0	0	0	0	0	0
9	0	0	0	0	0	0	0	0	0	0	0	0	0	0	0	0	0	0
10	0	0	0	0	0	0	0	0	0	0	0	0	0	0	0	0	0	0
11	0	0	0	0	0	0	0	0	0	0	0	0	0	0	0	0	0	0
12	0	0	0	0	0	0	0	0	0	0	0	0	0	0	0	0	0	0
13	0	0	0	0	0	0	0	0	0	0	0	0	0	0	0	0	0	0
14	0	0	0	0	0	0	0	0	0	0	0	0	0	0	0	0	0	0
15	0	0	0	0	0	0	0	0	0	0	0	0	0	0	0	0	0	0
16	0	0	10	20	10	20	30	20	30	30	20	20	30	10	10	10	10	0
17	0	10	10	20	10	20	30	20	30	30	20	20	30	10	20	10	10	0
18	0	0	10	20	10	20	30	20	30	30	20	20	30	10	20	10	10	0
19	0	10	10	20	10	20	20	20	30	30	20	20	30	10	20	10	10	0
20	0	10	10	20	10	20	30	20	30	30	20	20	30	10	20	10	10	0
21	0	10	10	20	10	20	30	20	30	30	20	20	30	10	20	10	10	0
22	0	10	10	20	10	20	30	20	30	30	20	10	30	10	20	10	10	0
23	0	10	10	20	10	20	30	20	30	30	20	20	30	10	20	10	10	0
24	0	0	10	20	10	20	30	20	30	30	20	20	30	10	20	10	10	0
25	0	10	10	20	10	20	30	20	30	30	20	20	30	10	20	10	10	0
26	0	10	10	20	10	20	30	20	30	30	20	20	30	10	20	10	10	0
27	0	10	10	20	10	20	30	20	30	30	20	20	30	10	20	10	10	0
28	0	10	10	20	10	20	30	20	30	30	20	20	30	10	20	10	10	0
29	0	10	10	20	10	20	30	20	30	30	20	20	30	10	20	10	10	0
30	0	10	10	20	10	20	20	20	30	30	10	20	30	10	20	10	10	0
31	0	10	10	20	10	20	30	20	30	30	20	20	30	10	20	10	10	0
32	0	10	10	20	10	20	10	20	30	30	20	0	30	10	20	10	10	0
33	0	10	10	20	10	20	30	20	30	30	20	10	30	10	20	10	10	0
34	0	10	10	20	10	20	30	20	30	30	20	10	10	10	20	10	10	0
35	0	10	10	20	10	20	20	10	30	30	10	20	30	10	20	10	10	0
36	0	10	10	20	10	20	30	10	30	30	20	20	30	10	20	10	10	0

TABLE A-28

Computed Line-of-Sight Magnetic field measurements from the fifth iteration of solution Type II for Carrington Rotation 1663. Units are Gauss with values meaned within a 10° x 10° grid.

	-80	-70	-60	-50	-40	-30	-20	-10	0	10	20	30	40	50	60	70	80	90
1	0	-3	0	0	2	6	9	11	12	10	9	7	0	1	13	18	0	0
2	0	-5	3	4	3	0	0	6	16	18	9	-1	-5	5	18	15	-13	0
3	0	-3	5	9	12	10	0	-8	2	18	15	3	2	15	20	6	-10	0
4	0	5	12	0	-2	2	8	12	19	13	-4	-10	9	27	17	0	0	0
5	0	0	0	0	0	0	0	0	0	0	0	0	0	0	0	0	0	0
6	0	0	0	0	0	0	0	0	0	0	0	0	0	0	0	0	0	0
7	0	0	0	0	0	0	0	0	0	0	0	0	0	0	0	0	0	0
8	0	0	0	0	0	0	0	0	0	0	0	0	0	0	0	0	0	0
9	0	0	0	0	0	0	0	0	0	0	0	0	0	0	0	0	0	0
10	0	0	0	0	0	0	0	0	0	0	0	0	0	0	0	0	0	0
11	0	0	0	0	0	0	0	0	0	0	0	0	0	0	0	0	0	0
12	0	0	0	0	0	0	0	0	0	0	0	0	0	0	0	0	0	0
13	0	0	0	0	0	0	0	0	0	0	0	0	0	0	0	0	0	0
14	0	0	0	0	0	0	0	0	0	0	0	0	0	0	0	0	0	0
15	0	0	0	0	0	0	0	0	0	0	0	0	0	0	0	0	0	0
16	0	0	2	-6	-5	0	4	2	8	18	14	4	0	-3	-12	7	77	0
17	0	3	3	6	4	1	3	6	4	2	4	5	7	5	-1	3	50	0
18	0	0	2	8	3	-1	0	5	3	3	6	5	2	4	4	5	30	0
19	0	1	0	6	4	-2	-7	-5	2	15	20	10	-3	-2	7	10	16	0
20	0	2	-3	4	9	5	-2	0	8	16	12	0	-12	-6	9	14	7	0
21	0	3	-7	4	14	15	11	11	13	5	-7	-16	-17	-5	10	17	3	0
22	0	2	-9	3	16	19	14	8	5	0	-5	-11	-9	0	11	18	1	0
23	0	2	-9	3	14	16	9	-2	-4	9	19	16	5	4	11	17	1	0
24	0	0	-7	3	9	10	6	-3	-4	16	34	32	14	5	10	16	1	0
25	0	0	-5	4	5	3	3	4	2	11	23	22	10	4	9	16	3	0
26	0	0	-3	5	4	-3	-3	5	8	6	4	5	3	3	8	15	5	0
27	0	-1	-3	7	7	-1	-9	-2	6	3	-1	-2	0	4	8	14	6	0
28	0	-2	-3	8	13	12	3	-3	0	4	2	0	0	4	8	13	8	0
29	0	-2	-3	6	18	29	27	6	-3	4	5	-1	-2	5	8	13	8	0
30	0	-1	-3	3	15	33	36	15	0	9	5	-4	-4	5	8	12	8	0
31	0	-1	-2	2	7	17	21	8	6	16	6	-8	-3	9	8	11	8	0
32	0	0	-2	2	2	0	-6	-6	6	13	-2	0	3	15	8	10	6	0
33	0	0	-2	4	7	1	-12	-10	4	2	-10	-1	17	20	7	11	3	0
34	0	0	-4	5	18	19	6	1	6	1	0	8	34	21	6	12	0	0
35	0	0	-4	3	22	32	28	11	9	9	14	31	34	15	6	15	-3	0
36	0	-1	-2	0	13	24	23	11	8	11	19	26	20	6	8	18	-8	0

TABLE A-29

Mt. Wilson Line-of-Sight Magnetic field measurements for Carrington Rotation 1663 used in the fifth iteration of solution Type II. Units are Gauss with values meaned within a 10° x 10° equiangular grid.

1	0	-15	-17	5	8	3	16	40	9	9	34	2	4	14	12	10	0	0
2	0	7	0	5	-1	6	-18	34	7	14	10	-8	-3	8	3	20	17	0
3	0	10	11	16	7	9	-6	-6	5	19	18	3	3	15	6	-1	-31	0
4	0	1	1	0	8	-2	10	35	8	12	0	-5	1	42	26	0	0	0
5	0	0	0	0	0	0	0	0	0	0	0	0	0	0	0	0	0	0
6	0	0	0	0	0	0	0	0	0	0	0	0	0	0	0	0	0	0
7	0	0	0	0	0	0	0	0	0	0	0	0	0	0	0	0	0	0
8	0	0	0	0	0	0	0	0	0	0	0	0	0	0	0	0	0	0
9	0	0	0	0	0	0	0	0	0	0	0	0	0	0	0	0	0	0
10	0	0	0	0	0	0	0	0	0	0	0	0	0	0	0	0	0	0
11	0	0	0	0	0	0	0	0	0	0	0	0	0	0	0	0	0	0
12	0	0	0	0	0	0	0	0	0	0	0	0	0	0	0	0	0	0
13	0	0	0	0	0	0	0	0	0	0	0	0	0	0	0	0	0	0
14	0	0	0	0	0	0	0	0	0	0	0	0	0	0	0	0	0	0
15	0	0	0	0	0	0	0	0	0	0	0	0	0	0	0	0	0	0
16	0	0	-18	11	-8	-5	5	16	0	15	23	0	-1	17	-36	-9	107	0
17	0	-25	-9	5	6	-5	6	4	3	0	4	11	6	15	3	23	36	0
18	0	0	-7	-1	4	0	6	1	6	0	9	6	-4	-4	12	6	22	0
19	0	-28	13	5	10	6	-40	0	9	6	27	13	1	5	12	-3	1	0
20	0	18	-4	7	10	13	2	5	8	7	11	4	-14	-18	8	0	38	0
21	0	15	-5	1	10	13	14	8	12	11	0	-23	-16	-18	5	20	9	0
22	0	-22	-5	6	13	14	12	-1	5	6	-13	-42	-6	0	18	8	-2	0
23	0	45	-17	5	5	19	19	-6	-1	3	21	20	3	17	20	19	-11	0
24	0	0	0	0	10	6	6	-1	4	0	63	34	16	8	7	17	-8	0
25	0	6	6	6	6	10	-5	1	5	6	19	22	-1	-12	4	3	-10	0
26	0	-17	-11	9	1	1	-10	5	5	11	16	-9	4	4	14	16	6	0
27	0	-18	7	5	10	11	-5	7	2	-3	0	-3	6	9	8	17	4	0
28	0	0	-8	0	7	15	-1	0	0	6	6	8	1	3	3	6	2	0
29	0	-6	-14	6	4	24	16	0	4	2	-2	2	-17	12	5	3	1	0
30	0	10	-8	8	4	48	45	10	4	4	8	-4	-11	15	10	10	22	0
31	0	6	0	10	5	-1	35	6	7	11	31	-8	3	21	11	8	31	0
32	0	5	-6	4	10	-2	-51	3	3	10	-25	0	12	7	9	17	10	0
33	0	-1	-3	4	14	11	-12	0	9	2	17	-32	2	7	7	20	1	0
34	0	-12	-1	5	11	26	-7	-2	4	0	-21	34	74	15	13	19	30	0
35	0	-4	-1	1	12	26	33	22	10	5	41	38	38	15	14	7	-16	0
36	0	5	-4	2	7	12	17	-25	11	10	12	16	10	0	11	26	-9	0

TABLE A-30

Carrington rotation 1620, solution Type I, rms of fit, number of observations and A_{nm}, B_{nm} coefficients and unit weight standard deviations. All units are in Gauss.

1620 SIGMA = 3.320 NUMBER OF POINTS = 1056. CARRINGTON ROTATION = 1620

N	M	SCHMIDT NORMALIZED A,B		SIGMA A,B		N	M	FULLY NORMALIZED A,B		SIGMA A,B	
0	0	0.5146	0.0	0.0227	0.0	0	0	0.5146	0.0	0.0227	0.0
1	0	0.2074	0.0	0.0268	0.0	1	0	0.1198	0.0	0.0155	0.0
1	1	-0.0517	-0.3456	0.0303	0.0302	1	1	-0.0299	-0.1995	0.0175	0.0175
2	0	0.0421	0.0	0.0240	0.0	2	0	0.0188	0.0	0.0107	0.0
2	1	0.0337	0.0908	0.0271	0.0274	2	1	0.0151	0.0406	0.0121	0.0123
2	2	-0.0830	0.2717	0.0271	0.0271	2	2	-0.0371	0.1215	0.0121	0.0121
3	0	0.2444	0.0	0.0213	0.0	3	0	0.0924	0.0	0.0081	0.0
3	1	-0.0407	0.0786	0.0243	0.0251	3	1	-0.0154	0.0297	0.0092	0.0095
3	2	0.0268	-0.1727	0.0245	0.0244	3	2	0.0101	-0.0653	0.0093	0.0092
3	3	0.0333	0.0336	0.0237	0.0237	3	3	0.0126	0.0127	0.0089	0.0089
4	0	0.1269	0.0	0.0190	0.0	4	0	0.0423	0.0	0.0063	0.0
4	1	0.0018	-0.1203	0.0215	0.0230	4	1	0.0006	-0.0401	0.0072	0.0077
4	2	0.1760	-0.0056	0.0223	0.0222	4	2	0.0587	-0.0019	0.0074	0.0074
4	3	0.0590	-0.0666	0.0220	0.0220	4	3	0.0197	-0.0222	0.0073	0.0073
4	4	-0.0089	0.1299	0.0209	0.0210	4	4	-0.0030	0.0433	0.0070	0.0070
5	0	0.0711	0.0	0.0172	0.0	5	0	0.0214	0.0	0.0052	0.0
5	1	0.0558	-0.0008	0.0200	0.0217	5	1	0.0168	-0.0002	0.0060	0.0065
5	2	-0.0636	0.0620	0.0206	0.0204	5	2	-0.0192	0.0187	0.0062	0.0061
5	3	-0.0259	-0.0844	0.0206	0.0206	5	3	-0.0072	-0.0254	0.0062	0.0062
5	4	-0.0762	-0.0879	0.0199	0.0200	5	4	-0.0230	-0.0265	0.0060	0.0060
5	5	0.0602	-0.0607	0.0190	0.0190	5	5	0.0182	-0.0183	0.0057	0.0057
6	0	-0.0407	0.0	0.0158	0.0	6	0	-0.0113	0.0	0.0044	0.0
6	1	-0.0696	0.0189	0.0182	0.0198	6	1	-0.0193	0.0053	0.0050	0.0055
6	2	-0.0771	-0.0706	0.0191	0.0187	6	2	-0.0214	-0.0196	0.0053	0.0052
6	3	-0.0141	0.0019	0.0191	0.0191	6	3	-0.0039	0.0005	0.0053	0.0053
6	4	-0.0304	-0.0232	0.0189	0.0189	6	4	-0.0084	-0.0064	0.0052	0.0053
6	5	-0.0803	-0.0056	0.0182	0.0183	6	5	-0.0223	-0.0016	0.0050	0.0051
6	6	-0.0507	0.0080	0.0174	0.0175	6	6	-0.0141	0.0022	0.0048	0.0048
7	0	0.0754	0.0	0.0149	0.0	7	0	0.0195	0.0	0.0038	0.0
7	1	0.0389	0.0304	0.0171	0.0183	7	1	0.0100	0.0079	0.0044	0.0047
7	2	0.0711	-0.0381	0.0181	0.0175	7	2	0.0186	-0.0098	0.0047	0.0045
7	3	0.0009	0.0167	0.0180	0.0180	7	3	0.0002	0.0043	0.0046	0.0046
7	4	0.0303	0.1055	0.0179	0.0180	7	4	0.0078	0.0272	0.0046	0.0046
7	5	0.0063	0.0539	0.0175	0.0177	7	5	0.0016	0.0139	0.0045	0.0046
7	6	-0.0137	0.0356	0.0168	0.0171	7	6	-0.0035	0.0092	0.0043	0.0044
7	7	-0.1570	0.1310	0.0162	0.0163	7	7	-0.0405	0.0338	0.0042	0.0042
8	0	0.0542	0.0	0.0142	0.0	8	0	0.0131	0.0	0.0034	0.0
8	1	0.0260	-0.0160	0.0158	0.0165	8	1	0.0063	-0.0039	0.0038	0.0040
8	2	0.0173	0.0940	0.0166	0.0162	8	2	0.0042	0.0228	0.0040	0.0039
8	3	0.0184	0.0269	0.0165	0.0165	8	3	0.0045	0.0065	0.0040	0.0040
8	4	0.0014	-0.0429	0.0166	0.0166	8	4	0.0003	-0.0104	0.0040	0.0040
8	5	0.0480	0.0362	0.0164	0.0166	8	5	0.0117	0.0088	0.0040	0.0040
8	6	0.1079	0.0258	0.0161	0.0163	8	6	0.0262	0.0063	0.0039	0.0040
8	7	0.0448	-0.0016	0.0156	0.0158	8	7	0.0109	-0.0004	0.0038	0.0038
8	8	0.1477	0.0671	0.0151	0.0152	8	8	0.0358	0.0163	0.0037	0.0037
9	0	-0.0323	0.0	0.0136	0.0	9	0	-0.0074	0.0	0.0031	0.0
9	1	-0.0175	-0.0828	0.0149	0.0154	9	1	-0.0040	-0.0190	0.0036	0.0035
9	2	0.0271	-0.0367	0.0158	0.0154	9	2	0.0062	-0.0084	0.0036	0.0035
9	3	0.0140	-0.0807	0.0157	0.0158	9	3	0.0032	-0.0185	0.0036	0.0036
9	4	0.0627	-0.0464	0.0158	0.0159	9	4	0.0144	-0.0106	0.0036	0.0036
9	5	-0.0270	-0.0983	0.0157	0.0159	9	5	-0.0062	-0.0226	0.0036	0.0036
9	6	0.0296	-0.0107	0.0155	0.0157	9	6	0.0068	-0.0025	0.0036	0.0036
9	7	0.0791	-0.0473	0.0151	0.0154	9	7	0.0181	-0.0189	0.0035	0.0035
9	8	-0.0136	0.0302	0.0147	0.0149	9	8	-0.0031	0.0069	0.0034	0.0034
9	9	0.0332	-0.2094	0.0142	0.0144	9	9	0.0076	-0.0480	0.0033	0.0033

TABLE A-31

Carrington rotation 1625, solution Type I, rms of fit, number of observations and A_{nm}, B_{nm} coefficients and unit weight standard deviations. All units are in Gauss.

1625 SIGMA = .8169 NUMBER OF POINTS = 1053. CARRINGTON ROTATION = 1625

N	M	SCHMIDT NORMALIZED A,B		SIGMA A,B		N	M	FULLY NORMALIZED A,B		SIGMA A,B	
0	0	-0.0729	0.0	0.0226	0.0	0	0	-0.0729	0.0	0.0226	0.0
1	0	0.2069	0.0	0.0263	0.0	1	0	0.1195	0.0	0.0152	0.0
1	1	-0.0196	-0.2202	0.0302	0.0301	1	1	-0.0113	-0.1271	0.0174	0.0174
2	0	-0.1091	0.0	0.0235	0.0	2	0	-0.0488	0.0	0.0105	0.0
2	1	0.0249	0.0592	0.0270	0.0269	2	1	0.0111	0.0265	0.0121	0.0120
2	2	0.0710	0.0859	0.0271	0.0271	2	2	0.0317	0.0384	0.0121	0.0121
3	0	0.2864	0.0	0.0211	0.0	3	0	0.1082	0.0	0.0080	0.0
3	1	-0.0851	0.0263	0.0240	0.0240	3	1	-0.0322	0.0100	0.0091	0.0091
3	2	-0.0365	-0.0484	0.0244	0.0244	3	2	-0.0138	-0.0183	0.0092	0.0092
3	3	0.0217	0.0093	0.0237	0.0236	3	3	0.0082	0.0035	0.0089	0.0089
4	0	0.0254	0.0	0.0193	0.0	4	0	0.0085	0.0	0.0064	0.0
4	1	0.0133	0.0052	0.0213	0.0213	4	1	0.0044	0.0017	0.0071	0.0071
4	2	0.1352	-0.0056	0.0221	0.0221	4	2	0.0451	-0.0019	0.0074	0.0074
4	3	0.0225	-0.0115	0.0219	0.0219	4	3	0.0075	-0.0038	0.0073	0.0073
4	4	-0.0082	-0.1199	0.0210	0.0210	4	4	-0.0027	-0.0400	0.0070	0.0070
5	0	0.0989	0.0	0.0179	0.0	5	0	0.0298	0.0	0.0054	0.0
5	1	0.0395	0.0394	0.0197	0.0196	5	1	0.0119	0.0119	0.0059	0.0059
5	2	-0.0475	0.0443	0.0202	0.0202	5	2	-0.0143	0.0134	0.0061	0.0061
5	3	0.0733	-0.0192	0.0205	0.0205	5	3	0.0221	-0.0058	0.0062	0.0062
5	4	-0.0171	-0.0441	0.0199	0.0199	5	4	-0.0052	-0.0133	0.0060	0.0060
5	5	0.0538	0.0349	0.0190	0.0190	5	5	0.0162	0.0105	0.0057	0.0057
6	0	-0.0347	0.0	0.0167	0.0	6	0	-0.0096	0.0	0.0046	0.0
6	1	-0.0077	0.0034	0.0179	0.0179	6	1	-0.0021	0.0009	0.0050	0.0050
6	2	-0.0080	-0.0250	0.0185	0.0185	6	2	-0.0022	-0.0069	0.0051	0.0051
6	3	-0.0085	-0.0070	0.0189	0.0190	6	3	-0.0024	-0.0019	0.0053	0.0053
6	4	0.0481	-0.0389	0.0188	0.0188	6	4	0.0133	-0.0108	0.0052	0.0052
6	5	0.0482	0.0101	0.0182	0.0183	6	5	0.0134	0.0028	0.0050	0.0051
6	6	0.0253	-0.0717	0.0174	0.0175	6	6	0.0070	-0.0199	0.0048	0.0048
7	0	0.0756	0.0	0.0156	0.0	7	0	0.0195	0.0	0.0040	0.0
7	1	0.0083	-0.0485	0.0171	0.0170	7	1	0.0021	-0.0125	0.0044	0.0044
7	2	0.0411	0.0090	0.0171	0.0171	7	2	0.0106	0.0023	0.0044	0.0044
7	3	-0.0001	-0.0050	0.0178	0.0178	7	3	-0.0000	-0.0013	0.0046	0.0046
7	4	0.0086	0.0019	0.0178	0.0179	7	4	0.0022	0.0005	0.0046	0.0046
7	5	0.0689	-0.0302	0.0175	0.0175	7	5	0.0178	-0.0078	0.0045	0.0045
7	6	0.0101	0.0195	0.0169	0.0169	7	6	0.0026	0.0050	0.0044	0.0044
7	7	0.0533	0.0132	0.0162	0.0162	7	7	0.0138	0.0034	0.0042	0.0042
8	0	-0.0122	0.0	0.0147	0.0	8	0	-0.0030	0.0	0.0036	0.0
8	1	0.0130	0.0103	0.0159	0.0158	8	1	0.0032	0.0025	0.0038	0.0038
8	2	0.0219	0.0080	0.0158	0.0158	8	2	0.0053	0.0019	0.0038	0.0038
8	3	0.0195	0.0196	0.0163	0.0164	8	3	0.0047	0.0047	0.0040	0.0040
8	4	-0.0002	-0.0062	0.0166	0.0166	8	4	-0.0000	-0.0015	0.0040	0.0040
8	5	-0.0269	-0.0171	0.0164	0.0164	8	5	-0.0065	-0.0041	0.0040	0.0040
8	6	0.0076	0.0240	0.0161	0.0162	8	6	0.0018	0.0058	0.0039	0.0039
8	7	-0.0533	0.0379	0.0157	0.0157	8	7	-0.0129	0.0092	0.0038	0.0038
8	8	-0.0119	-0.0550	0.0151	0.0152	8	8	-0.0029	-0.0133	0.0037	0.0037
9	0	0.0312	0.0	0.0139	0.0	9	0	0.0072	0.0	0.0032	0.0
9	1	-0.0135	0.0042	0.0153	0.0152	9	1	-0.0031	0.0010	0.0035	0.0035
9	2	-0.0245	-0.0217	0.0150	0.0150	9	2	-0.0056	-0.0050	0.0034	0.0034
9	3	0.0283	0.0316	0.0154	0.0154	9	3	0.0065	0.0073	0.0035	0.0035
9	4	-0.0127	0.0026	0.0157	0.0157	9	4	-0.0029	0.0006	0.0036	0.0036
9	5	-0.0093	-0.0170	0.0157	0.0158	9	5	-0.0021	-0.0039	0.0036	0.0036
9	6	-0.0232	0.0088	0.0155	0.0156	9	6	-0.0053	0.0020	0.0036	0.0036
9	7	-0.0351	-0.0086	0.0153	0.0152	9	7	-0.0081	-0.0020	0.0035	0.0035
9	8	0.0166	-0.0533	0.0148	0.0148	9	8	0.0038	-0.0122	0.0034	0.0034
9	9	-0.0132	-0.0107	0.0143	0.0143	9	9	-0.0030	-0.0025	0.0033	0.0033

TABLE A-32

Carrington rotation 1663, solution Type I, rms of fit, number of observations and A_{nm}, B_{nm} coefficients and unit weight standard deviations. All units are in Gauss.

1663 SIGMA = 2.218 NUMBER OF POINTS = 745. CARRINGTON ROTATION = 1663

N	M	SCHMIDT NORMALIZED A,B		SIGMA A,B		N	M	FULLY NORMALIZED A,B		SIGMA A,B	
0	0	1.4848	0.0	1.3175	0.0	0	0	1.4848	0.0	1.3175	0.0
1	0	-2.8441	0.0	0.9643	0.0	1	0	-1.6420	0.0	0.5567	0.0
1	1	-2.1065	[illegible]6340	0.5893	3.1226	1	1	-1.2162	3.6754	0.3402	1.8029
2	0	-11.7499	[illegible].0	3.0107	0.0	2	0	-5.2547	0.0	1.3464	0.0
2	1	0.6442	7.3204	0.3765	1.9300	2	1	0.2881	3.2738	0.1684	0.8631
2	2	-5.2463	2.9228	3.0328	1.0145	2	2	-2.3462	1.3071	1.3563	0.4537
3	0	9.3495	0.0	1.8302	0.0	3	0	3.5338	0.0	0.6917	0.0
3	1	-0.6983	19.9861	0.4396	4.4521	3	1	-0.2639	7.5540	0.1662	1.6828
3	2	8.4164	-1.2941	1.9178	0.6727	3	2	3.1811	-0.4513	0.7249	0.2542
3	3	2.8910	4.2776	1.1276	2.5860	3	3	1.0927	1.6168	0.4262	0.9774
4	0	12.8827	0.0	2.8933	0.0	4	0	4.2942	0.0	0.9644	0.0
4	1	-0.3828	-14.4666	0.2543	2.6336	4	1	-0.1276	-4.8222	0.0848	0.8779
4	2	16.9616	1.2964	3.8435	0.7397	4	2	5.6539	0.4321	1.2812	0.2466
4	3	-1.3716	-7.4285	0.7675	1.5901	4	3	-0.4572	-2.4762	0.2558	0.5300
4	4	2.5306	-2.6015	2.0780	1.0142	4	4	0.8435	-0.8671	0.6927	0.3381
5	0	-9.4679	0.0	1.7213	0.0	5	0	-2.8547	0.0	0.5190	0.0
5	1	0.2884	-11.7437	0.2840	2.9396	5	1	0.0870	-3.5409	0.0856	0.8863
5	2	-12.3316	0.4660	2.1768	0.3734	5	2	-3.7181	0.1405	0.6563	0.1126
5	3	1.5040	-11.4729	0.8094	2.7775	5	3	0.4535	-3.4592	0.2441	0.8375
5	4	-5.6410	0.9474	1.1461	0.6820	5	4	-1.7008	0.2857	0.3456	0.2056
5	5	-1.8895	-0.9631	0.7790	1.5594	5	5	-0.5697	-0.2904	0.2349	0.4782
6	0	-4.3010	0.0	1.2234	0.0	6	0	-1.1929	0.0	0.3393	0.0
6	1	0.2551	9.2498	0.1377	1.6897	6	1	0.0708	2.5654	0.0382	0.4686
6	2	-5.9230	-0.1539	1.7173	0.3372	6	2	-1.6427	-0.0427	0.4763	0.0935
6	3	0.4156	8.4440	0.3653	1.4727	6	3	0.1153	2.3419	0.1013	0.4085
6	4	-6.2450	-1.4451	1.6841	0.6740	6	4	-1.7320	-0.4008	0.4671	0.1869
6	5	0.9557	3.4312	0.4962	0.7252	6	5	0.2651	0.9517	0.1376	0.2011
6	6	-0.0235	1.0980	1.0552	0.5181	6	6	-0.0065	0.3045	0.2926	0.1437
7	0	3.1839	0.0	0.6454	0.0	7	0	0.8221	0.0	0.1666	0.0
7	1	-0.0996	2.6801	0.0834	0.8300	7	1	-0.0257	0.6920	0.0215	0.2143
7	2	4.6956	-0.2858	0.8969	0.1504	7	2	1.2124	-0.0738	0.2316	0.0388
7	3	0.0178	2.2313	0.2526	0.8238	7	3	0.0046	0.5761	0.0652	0.2127
7	4	4.6553	-0.3382	0.8057	0.2713	7	4	1.2020	-0.0873	0.2086	0.0700
7	5	-1.0349	2.5653	0.4413	0.8416	7	5	-0.2672	0.6624	0.1140	0.2173
7	6	1.7893	-0.4299	0.4001	0.2964	7	6	0.4620	-0.1110	0.1033	0.0765
7	7	0.6937	-0.3353	0.2976	0.6131	7	7	0.1791	-0.0866	0.0768	0.1583
8	0	0.7951	0.0	0.2253	0.0	8	0	0.1928	0.0	0.0546	0.0
8	1	-0.0705	-1.4601	0.0357	0.3453	8	1	-0.0171	-0.3541	0.0087	0.0838
8	2	0.9500	0.0727	0.3171	0.0710	8	2	0.2304	0.0176	0.0769	0.0172
8	3	-0.3027	-1.7763	0.0992	0.3520	8	3	-0.0734	-0.4308	0.0241	0.0854
8	4	0.5112	0.0181	0.3113	0.1371	8	4	0.1240	0.0044	0.0755	0.0333
8	5	-0.0861	-2.0449	0.1530	0.3392	8	5	-0.0209	-0.4960	0.0371	0.0823
8	6	0.4630	0.3739	0.3288	0.2209	8	6	0.1123	0.0907	0.0797	0.0536
8	7	-0.1390	-0.6801	0.1418	0.1863	8	7	-0.0337	-0.1650	0.0344	0.0452
8	8	-0.4351	-0.2186	0.2842	0.1446	8	8	-0.1055	-0.0530	0.0689	0.0351
9	0	-0.1590	0.0	0.0589	0.0	9	0	-0.0365	0.0	0.0135	0.0
9	1	-0.0461	-0.2586	0.0206	0.0805	9	1	-0.0106	-0.0593	0.0047	0.0185
9	2	-0.2077	0.0492	0.0824	0.0270	9	2	-0.0477	0.0113	0.0189	0.0062
9	3	0.0239	-0.2309	0.0368	0.0820	9	3	0.0055	-0.0530	0.0085	0.0188
9	4	-0.6150	0.2465	0.0886	0.0440	9	4	-0.0952	0.0566	0.0203	0.0101
9	5	-0.0409	0.0190	0.0526	0.0219	9	5	-0.0094	0.0044	0.0121	0.0088
9	6	-0.5852	0.1063	0.0958	0.0603	9	6	-0.1342	0.0244	0.0220	0.0138
9	7	0.3671	0.1054	0.0758	0.0887	9	7	0.0842	0.0242	0.0174	0.0203
9	8	0.0404	0.1015	0.0659	0.0516	9	8	0.0093	0.0233	0.0151	0.0118
9	9	-0.0208	0.2036	0.0552	0.0903	9	9	-0.0048	0.0467	0.0127	0.0207

TABLE A-33

Carrington rotation 1620, solution Type II (iteration 5), rms of fit, number of observations and A_{nm}, B_{nm} coefficients and unit weight standard deviations. All units are in Gauss.

1620 SIGMA = .9594 ITER = 5 NUMBER OF POINTS = 1026. CARRINGTON ROTATION = 1620

N	M	SCHMIDT NORMALIZED A,B		SIGMA A,B		FULLY NORMALIZED A,B		SIGMA A,B	
0	0	0.5541	0.0	0.0236	0.0	0.5541	0.0	0.0236	0.0
1	0	0.2173	0.0	0.0270	0.0	0.1254	0.0	0.0156	0.0
1	1	-0.0175	-0.3832	0.0307	0.0324	-0.0101	-0.2212	0.0177	0.0187
2	0	0.0291	0.0	0.0245	0.0	0.0130	0.0	0.0109	0.0
2	1	0.0207	0.0582	0.0272	0.0279	0.0093	0.0260	0.0122	0.0125
2	2	-0.0732	0.2554	0.0295	0.0275	-0.0327	0.1142	0.0132	0.0123
3	0	0.2159	0.0	0.0217	0.0	0.0316	0.0	0.0082	0.0
3	1	-0.0498	0.0795	0.0244	0.0256	-0.0188	0.0301	0.0092	0.0097
3	2	-0.0229	-0.1687	0.0252	0.0246	-0.0087	-0.0638	0.0095	0.0093
3	3	0.0527	0.0105	0.0243	0.0255	0.0199	0.0040	0.0092	0.0097
4	0	0.1166	0.0	0.0193	0.0	0.0389	0.0	0.0064	0.0
4	1	-0.0130	-0.0867	0.0216	0.0236	-0.0043	-0.0289	0.0072	0.0079
4	2	0.1347	-0.0096	0.0227	0.0222	0.0449	-0.0032	0.0076	0.0074
4	3	0.0431	-0.0188	0.0222	0.0228	0.0144	-0.0063	0.0074	0.0076
4	4	-0.0398	0.1141	0.0226	0.0217	-0.0133	0.0380	0.0075	0.0072
5	0	0.0977	0.0	0.0176	0.0	0.0294	0.0	0.0053	0.0
5	1	0.0553	0.0490	0.0201	0.0220	0.0167	0.0148	0.0060	0.0066
5	2	-0.0442	0.0746	0.0213	0.0205	-0.0133	0.0225	0.0064	0.0062
5	3	-0.0390	-0.0415	0.0207	0.0209	-0.0118	-0.0125	0.0062	0.0063
5	4	-0.0414	-0.0629	0.0207	0.0203	-0.0125	-0.0190	0.0062	0.0061
5	5	0.0486	0.0213	0.0197	0.0204	0.0146	0.0064	0.0059	0.0061
6	0	-0.0007	0.0	0.0160	0.0	-0.0002	0.0	0.0044	0.0
6	1	-0.0587	-0.0154	0.0183	0.0203	-0.0163	-0.0043	0.0051	0.0056
6	2	-0.0377	-0.0616	0.0193	0.0188	-0.0105	-0.0171	0.0054	0.0052
6	3	-0.0069	-0.0209	0.0192	0.0195	-0.0019	-0.0058	0.0053	0.0054
6	4	-0.0010	-0.0192	0.0191	0.0191	-0.0003	-0.0053	0.0053	0.0053
6	5	-0.0537	-0.0259	0.0185	0.0190	-0.0149	-0.0072	0.0051	0.0053
6	6	0.0618	0.0707	0.0186	0.0182	0.0171	0.0196	0.0051	0.0051
7	0	0.0459	0.0	0.0152	0.0	0.0119	0.0	0.0039	0.0
7	1	0.0460	-0.0168	0.0172	0.0185	0.0119	-0.0043	0.0044	0.0048
7	2	0.0570	-0.0538	0.0185	0.0176	0.0147	-0.0139	0.0048	0.0045
7	3	0.0094	-0.0223	0.0180	0.0181	0.0024	-0.0058	0.0047	0.0047
7	4	0.0110	0.0927	0.0184	0.0181	0.0028	0.0239	0.0047	0.0047
7	5	-0.0010	-0.0056	0.0176	0.0179	-0.0003	-0.0014	0.0045	0.0046
7	6	-0.0187	0.0151	0.0174	0.0174	-0.0048	0.0039	0.0045	0.0045
7	7	-0.0679	0.0529	0.0169	0.0173	-0.0175	0.0137	0.0044	0.0045
8	0	0.0088	0.0	0.0143	0.0	0.0021	0.0	0.0035	0.0
8	1	-0.0009	0.0022	0.0159	0.0170	-0.0002	0.0005	0.0039	0.0041
8	2	-0.0529	0.0886	0.0168	0.0163	-0.0128	0.0215	0.0041	0.0039
8	3	0.0045	0.0247	0.0167	0.0171	0.0011	0.0060	0.0041	0.0042
8	4	-0.0628	-0.0414	0.0168	0.0168	-0.0152	-0.0100	0.0041	0.0041
8	5	0.0283	0.0351	0.0167	0.0171	0.0069	0.0085	0.0041	0.0042
8	6	0.0041	0.0079	0.0163	0.0165	0.0010	0.0019	0.0040	0.0040
8	7	0.0420	-0.0121	0.0161	0.0166	0.0102	-0.0029	0.0039	0.0040
8	8	0.0703	0.0174	0.0160	0.0160	0.0171	0.0042	0.0039	0.0039
9	0	-0.0116	0.0	0.0139	0.0	-0.0027	0.0	0.0032	0.0
9	1	-0.0201	-0.0062	0.0150	0.0156	-0.0046	-0.0014	0.0034	0.0036
9	2	0.0159	-0.0146	0.0163	0.0155	0.0036	-0.0034	0.0037	0.0036
9	3	0.0092	-0.0066	0.0158	0.0160	0.0021	-0.0015	0.0036	0.0037
9	4	0.0493	-0.0374	0.0163	0.0161	0.0113	-0.0086	0.0037	0.0037
9	5	-0.0233	-0.0154	0.0158	0.0161	-0.0053	-0.0035	0.0036	0.0037
9	6	0.0064	0.0018	0.0159	0.0161	0.0015	0.0004	0.0037	0.0037
9	7	0.0377	0.0357	0.0153	0.0157	0.0087	0.0082	0.0035	0.0036
9	8	-0.0115	0.0137	0.0154	0.0154	-0.0026	0.0031	0.0035	0.0035
9	9	-0.0066	-0.0719	0.0149	0.0152	-0.0015	-0.0165	0.0034	0.0035

TABLE A-34

Carrington rotation 1625, solution Type II (iteration 5), rms of fit, number of observations and A_{nm}, B_{nm} coefficients and unit weight standard deviations. All units are in Gauss.

1625 SIGMA = .7999 ITER = 5 NUMBER OF POINTS = 1052. CARRINGTON ROTATION = 1625

N	M	SCHMIDT NORMALIZED A,B		SIGMA A,B		N	M	FULLY NORMALIZED A,B		SIGMA A,B	
0	0	-0.0776	0.0	0.0226	0.0	0	0	-0.0776	0.0	0.0226	0.0
1	0	0.2054	0.0	0.0263	0.0	1	0	0.1186	0.0	0.0152	0.0
1	1	-0.0144	-0.2291	0.0302	0.0302	1	1	-0.0083	-0.1323	0.0174	0.0174
2	0	-0.1049	0.0	0.0236	0.0	2	0	-0.0469	0.0	0.0105	0.0
2	1	0.0260	0.0574	0.0270	0.0269	2	1	0.0116	0.0257	0.0121	0.0120
2	2	0.0759	0.0941	0.0271	0.0271	2	2	0.0339	0.0421	0.0121	0.0121
3	0	0.2879	0.0	0.0211	0.0	3	0	0.1088	0.0	0.0080	0.0
3	1	-0.0874	0.0303	0.0240	0.0240	3	1	-0.0330	0.0114	0.0091	0.0091
3	2	-0.0356	-0.0461	0.0244	0.0244	3	2	-0.0134	-0.0174	0.0092	0.0092
3	3	0.0128	0.0094	0.0237	0.0236	3	3	0.0049	0.0036	0.0090	0.0089
4	0	0.0219	0.0	0.0193	0.0	4	0	0.0073	0.0	0.0064	0.0
4	1	0.0118	0.0079	0.0213	0.0213	4	1	0.0039	0.0026	0.0071	0.0071
4	2	0.1328	-0.0097	0.0221	0.0221	4	2	0.0443	-0.0032	0.0074	0.0074
4	3	0.0194	-0.0116	0.0219	0.0219	4	3	0.0065	-0.0039	0.0073	0.0073
4	4	-0.0041	-0.1271	0.0210	0.0210	4	4	-0.0014	-0.0424	0.0070	0.0070
5	0	0.0966	0.0	0.0179	0.0	5	0	0.0291	0.0	0.0054	0.0
5	1	0.0418	0.0355	0.0197	0.0196	5	1	0.0126	0.0107	0.0059	0.0059
5	2	-0.0491	0.0416	0.0202	0.0202	5	2	-0.0148	0.0125	0.0061	0.0061
5	3	0.0778	-0.0191	0.0205	0.0205	5	3	0.0234	-0.0058	0.0062	0.0062
5	4	-0.0155	-0.0468	0.0199	0.0199	5	4	-0.0047	-0.0141	0.0060	0.0060
5	5	0.0578	0.0416	0.0190	0.0190	5	5	0.0174	0.0126	0.0057	0.0057
6	0	-0.0327	0.0	0.0167	0.0	6	0	-0.0091	0.0	0.0046	0.0
6	1	-0.0064	0.0011	0.0179	0.0179	6	1	-0.0018	0.0003	0.0050	0.0050
6	2	-0.0063	-0.0220	0.0185	0.0185	6	2	-0.0017	-0.0061	0.0051	0.0051
6	3	-0.0060	-0.0070	0.0190	0.0190	6	3	-0.0017	-0.0019	0.0053	0.0053
6	4	0.0461	-0.0356	0.0188	0.0188	6	4	0.0128	-0.0099	0.0052	0.0052
6	5	0.0495	0.0125	0.0182	0.0183	6	5	0.0137	0.0035	0.0050	0.0051
6	6	0.0180	-0.0717	0.0174	0.0175	6	6	0.0050	-0.0199	0.0048	0.0048
7	0	0.0776	0.0	0.0156	0.0	7	0	0.0200	0.0	0.0040	0.0
7	1	0.0071	-0.0464	0.0171	0.0171	7	1	0.0018	-0.0120	0.0044	0.0044
7	2	0.0424	0.0114	0.0171	0.0171	7	2	0.0110	0.0029	0.0044	0.0044
7	3	-0.0033	-0.0049	0.0178	0.0178	7	3	-0.0008	-0.0013	0.0046	0.0046
7	4	0.0073	0.0042	0.0178	0.0179	7	4	0.0019	0.0011	0.0046	0.0046
7	5	0.0671	-0.0335	0.0175	0.0175	7	5	0.0173	-0.0087	0.0045	0.0045
7	6	0.0073	0.0194	0.0169	0.0169	7	6	0.0019	0.0050	0.0044	0.0044
7	7	0.0567	0.0072	0.0162	0.0162	7	7	0.0147	0.0019	0.0042	0.0042
8	0	-0.0142	0.0	0.0147	0.0	8	0	-0.0034	0.0	0.0036	0.0
8	1	0.0112	0.0134	0.0159	0.0159	8	1	0.0027	0.0032	0.0039	0.0038
8	2	0.0206	0.0057	0.0158	0.0158	8	2	0.0050	0.0014	0.0038	0.0038
8	3	0.0157	0.0196	0.0163	0.0164	8	3	0.0038	0.0047	0.0040	0.0040
8	4	0.0015	-0.0091	0.0166	0.0166	8	4	0.0004	-0.0022	0.0040	0.0040
8	5	-0.0287	-0.0203	0.0164	0.0164	8	5	-0.0070	-0.0049	0.0040	0.0040
8	6	0.0117	0.0240	0.0162	0.0162	8	6	0.0028	0.0058	0.0039	0.0039
8	7	-0.0513	0.0349	0.0157	0.0157	8	7	-0.0125	0.0085	0.0038	0.0038
8	8	-0.0084	-0.0490	0.0151	0.0153	8	8	-0.0020	-0.0119	0.0037	0.0037
9	0	0.0287	0.0	0.0139	0.0	9	0	0.0066	0.0	0.0032	0.0
9	1	-0.0124	0.0022	0.0153	0.0152	9	1	-0.0029	0.0005	0.0035	0.0035
9	2	-0.0264	-0.0248	0.0150	0.0150	9	2	-0.0060	-0.0057	0.0034	0.0034
9	3	0.0305	0.0317	0.0154	0.0154	9	3	0.0070	0.0073	0.0035	0.0035
9	4	-0.0107	-0.0007	0.0157	0.0158	9	4	-0.0025	-0.0002	0.0036	0.0036
9	5	-0.0078	-0.0144	0.0157	0.0158	9	5	-0.0018	-0.0033	0.0036	0.0036
9	6	-0.0194	0.0088	0.0156	0.0156	9	6	-0.0045	0.0020	0.0036	0.0036
9	7	-0.0371	-0.0052	0.0153	0.0153	9	7	-0.0085	-0.0012	0.0035	0.0035
9	8	0.0183	-0.0503	0.0148	0.0148	9	8	0.0042	-0.0115	0.0034	0.0034
9	9	-0.0199	-0.0107	0.0144	0.0143	9	9	-0.0046	-0.0024	0.0033	0.0033

TABLE A-35

Carrington rotation 1663, solution Type II (iteration 5), rms of fit, number of observations and A_{nm}, B_{nm} coefficients and unit weight standard deviations. All units are in Gauss.

1663 SIGMA = 1.192 ITER = 5 NUMBER OF POINTS = 722. CARRINGTON ROTATION = 1663

N	M	SCHMIDT NORMALIZED A,B		SIGMA A,B		N	M	FULLY NORMALIZED A,B		SIGMA A,B	
0	0	0.6512	0.0	1.3562	0.0	0	0	0.6512	0.0	1.3562	0.0
1	0	-4.4378	0.0	1.0232	0.0	1	0	-2.5622	0.0	0.5907	0.0
1	1	-2.6175	-1.0853	0.6334	3.2183	1	1	-1.5112	-0.6266	0.3657	1.8581
2	0	-3.5548	0.0	3.1384	0.0	2	0	-1.5897	0.0	1.4035	0.0
2	1	-1.2976	8.5045	0.4203	2.0187	2	1	-0.5803	3.8033	0.1880	0.9028
2	2	-0.9238	4.1055	3.1264	1.0846	2	2	-0.4132	1.8360	1.3982	0.4851
3	0	7.2439	0.0	1.8635	0.0	3	0	2.7379	0.0	0.7043	0.0
3	1	0.6686	5.8312	0.4428	4.6601	3	1	0.2527	2.2040	0.1696	1.7613
3	2	7.7346	2.1551	1.9858	0.7477	3	2	2.9234	0.8146	0.7505	0.2326
3	3	4.2652	0.3783	1.1999	2.6617	3	3	1.6121	0.1430	0.4535	1.0060
4	0	2.9873	0.0	3.0236	0.0	4	0	0.9958	0.0	1.0079	0.0
4	1	0.1777	-9.2496	0.2707	2.6624	4	1	0.0592	-3.0832	0.0902	0.8875
4	2	4.5237	-1.0829	4.0255	0.7537	4	2	1.5079	-0.3610	1.3418	0.2512
4	3	2.2734	-5.4781	0.8489	1.6359	4	3	0.7578	-1.8260	0.2830	0.5453
4	4	-0.2452	-3.6838	2.1326	1.0748	4	4	-0.0817	-1.2279	0.7109	0.3585
5	0	-5.8343	0.0	1.7370	0.0	5	0	-1.7591	0.0	0.5237	0.0
5	1	-0.5104	-1.7538	0.2895	3.0583	5	1	-0.1539	-0.5288	0.0873	0.9221
5	2	-7.1916	0.0149	2.1970	0.3909	5	2	-2.1684	0.0045	0.6624	0.1179
5	3	-1.0927	-2.7485	0.8245	2.9889	5	3	-0.3295	-0.8287	0.2486	0.8771
5	4	-3.1657	-2.2500	1.1755	0.7515	5	4	-0.9545	-0.6784	0.3544	0.2266
5	5	-2.6484	0.5936	0.8226	1.5948	5	5	-0.7985	0.1790	0.2480	0.4809
6	0	-0.0756	0.0	1.2636	0.0	6	0	-0.0210	0.0	0.3505	0.0
6	1	0.1591	6.0065	0.1427	1.7050	6	1	0.0441	1.6654	0.0396	0.4729
6	2	-0.1695	0.0243	1.7783	0.3435	6	2	-0.0470	0.1732	0.4932	0.0953
6	3	0.2446	4.6331	0.3783	1.4855	6	3	0.0679	1.2850	0.1049	0.4120
6	4	-1.3757	0.7712	1.7636	0.6869	6	4	-0.3815	0.2139	0.4891	0.1905
6	5	-1.5283	1.2359	0.5438	0.7440	6	5	-0.4239	0.3428	0.1508	0.2064
6	6	0.6730	1.4625	1.0753	0.5446	6	6	0.1866	0.4056	0.2982	0.1511
7	0	2.2249	0.0	0.6514	0.0	7	0	0.5745	0.0	0.1682	0.0
7	1	0.0974	-0.2884	0.0847	0.8524	7	1	0.0251	-0.0745	0.0219	0.2201
7	2	3.1548	-0.1862	0.9046	0.1555	7	2	0.8146	-0.0481	0.2336	0.0401
7	3	0.4421	-0.3937	0.2571	0.8483	7	3	0.1142	-0.1017	0.0664	0.2190
7	4	2.3927	-0.3558	0.8124	0.2789	7	4	0.6178	-0.0919	0.2098	0.0720
7	5	0.4570	0.4893	0.4498	0.8812	7	5	0.1180	0.1263	0.1161	0.2275
7	6	0.2737	1.0452	0.4115	0.3225	7	6	0.0707	0.2699	0.1063	0.0833
7	7	0.7342	-0.4087	0.3107	0.6232	7	7	0.1896	-0.1055	0.0802	0.1609
8	0	-0.0438	0.0	0.2303	0.0	8	0	-0.0106	0.0	0.0559	0.0
8	1	-0.0847	-1.0396	0.0364	0.3483	8	1	-0.0205	-0.2521	0.0088	0.0845
8	2	-0.1712	0.0146	0.3243	0.0721	8	2	-0.0415	0.0036	0.0786	0.0175
8	3	-0.1836	-1.2267	0.1019	0.3549	8	3	-0.0445	-0.2975	0.0247	0.0861
8	4	-0.4077	-0.1796	0.3186	0.1397	8	4	-0.0989	-0.0436	0.0773	0.0339
8	5	-0.1610	-0.9974	0.1565	0.3420	8	5	-0.0390	-0.2419	0.0380	0.0829
8	6	0.0298	-0.3698	0.3449	0.2251	8	6	0.0072	-0.0897	0.0837	0.0546
8	7	0.6257	0.1071	0.1534	0.1924	8	7	0.1518	0.0260	0.0372	0.0467
8	8	-0.2633	-0.2169	0.2685	0.1496	8	8	-0.0639	-0.0526	0.0700	0.0363
9	0	-0.0764	0.0	0.0593	0.0	9	0	-0.0175	0.0	0.0136	0.0
9	1	-0.0624	0.0122	0.0209	0.0819	9	1	-0.0143	0.0028	0.0048	0.0188
9	2	-0.1404	0.0998	0.0829	0.0273	9	2	-0.0322	0.0229	0.0190	0.0063
9	3	-0.0012	0.0080	0.0374	0.0836	9	3	-0.0003	0.0018	0.0086	0.0192
9	4	-0.3174	0.1527	0.0893	0.0449	9	4	-0.0728	0.0350	0.0205	0.0103
9	5	-0.0153	0.2190	0.0535	0.0830	9	5	-0.0035	0.0502	0.0123	0.0190
9	6	-0.2769	0.1327	0.0968	0.0615	9	6	-0.0635	0.0304	0.0222	0.0141
9	7	0.0046	0.0735	0.0776	0.0931	9	7	0.0010	0.0169	0.0178	0.0213
9	8	0.1900	-0.2085	0.0682	0.0547	9	8	0.0436	-0.0478	0.0157	0.0125
9	9	-0.0137	0.0969	0.0562	0.0915	9	9	-0.0031	0.0222	0.0129	0.0210

TABLE A-36